Kontturi, Eero; Laaksonen, Päivi; Linder, Markus B.; Nonappa; Gröschel, André H.; Rojas, Orlando J.; Ikkala, Olli

Advanced Materials through Assembly of Nanocelluloses

Published in:
Advanced Materials

DOI:
10.1002/adma.201703779

Published: 01/06/2018

Document Version
Peer reviewed version

Please cite the original version:
Kontturi, E., Laaksonen, P., Linder, M. B., Nonappa, Gröschel, A. H., Rojas, O. J., & Ikkala, O. (2018). Advanced Materials through Assembly of Nanocelluloses. *Advanced Materials*, *30*(24), [1703779]. https://doi.org/10.1002/adma.201703779

DOI: 10.1002/((please add manuscript number))
Article type: Review

Novel materials through assembly of nanocelluloses

*Eero Kontturi, Päivi Laaksonen, Markus Linder, Nonappa, André H. Gröschel, Orlando J. Rojas, Olli Ikkala**

Prof. E. Kontturi, Prof. P. Laaksonen, Prof. M. Linder, Dr. Nonappa, Prof. O. J. Rojas, Prof. O. Ikkala
Department of Bioproducts and Biosystems, Aalto University, Espoo FI-00076, Finland

Dr. Nonappa, Prof. O. J. Rojas, Prof. O. Ikkala
Department of Applied Physics, Aalto University, Espoo FI-00076, Finland

Prof. A. Gröschel
University of Duisburg-Essen, Physical Chemistry and Centre for Nanointegration (CENIDE), DE-45127 Essen, Germany

Prof. P. Laaksonen, Prof. M. Linder, Dr. Nonappa, Prof. O. J. Rojas, Prof. O. Ikkala
Center of Excellence Molecular Engineering of Biosynthetic Hybrid Materials Research, Aalto University and VTT, Espoo, Finland

E-mail: olli.ikkala@aalto.fi

Keywords: Nanocellulose, cellulose nanofiber, nanofibrillated cellulose, cellulose nanocrystal, functional

Abstract

There is an emerging quest for lightweight materials with excellent mechanical properties and economic production, still being sustainable and functionalizable. They could form the basis of the future bioeconomy for energy and material efficiency. Therein, cellulose has long been recognized as an abundant polymer. Modified celluloses were, in fact, among the first polymers used in technical applications, however, later replaced by petroleum-based synthetic polymers. Currently, however, there is a resurgence in the interest to utilize renewable resources, where cellulose is foreseen to make again a major impact, this time in the development of advanced materials. This is because of its availability and properties as well as, in the future, its economic and sustainable production. Among the cellulose-based structures, cellulose nanofibrils and nanocrystals display nanoscale lateral dimensions and

lengths ranging from nanometers to micrometers. Their excellent mechanical properties are, in part, due to their crystalline assembly via hydrogen bonds. Owing to their abundant surface hydroxyl groups, they can be easily functionalized with nanoparticles, (bio)polymers, inorganics or nanocarbons to form functional fibers, films, bulk matter and porous aerogels and foams. Here, we review some of the recent progress in the development of advanced materials within this rapidly growing field.

1. Introduction

Cellulose is the polysaccharide responsible for the structural scaffold of all cells in all green plants. In wood and plant cell walls, cellulose resides in microfibrils with crystalline and disordered domains. Within their crystals cellulose chains align in tightly packed assemblies owing to inter- and intra-chain hydrogen bonding, facilitated by the abundant hydroxyl groups of cellulose (**Figure 1**a). At the molecular level, this is closely related to the rigidity of the polymer chain and the nature of the β-1,4 glycosidic bonds between the repeating units. The resultant structures span different dimensions and hierarchies, as can be observed in the cell walls of fibers in plants, including those in trees (Figure 1a). Deconstruction of fibers from wood or other structures formed by plants can result in cellulose nanofibrils (CNF) and/or cellulose nanocrystals (CNC).[1–8] The latter ones are high-aspect "whiskers" that are produced from fibers and fibrils after removal of the disordered cellulose domains by acid hydrolysis. Consequently, highly crystalline nano-objects are obtained at different yields, depending on the conditions used (Figure 1b). Upon dispersion in aqueous media, CNCs form characteristic chiral assemblies that, upon drying, reproduce such structuring except for tighter packing in the absence of water and owing to strong hydrogen bonding (see a scanning electron, SEM, micrograph of a cross section of such films in Figure 1c).

By contrast, the longer and less crystalline CNFs are most typically produced by strong mechanical shearing of fibers, resulting in micro and nanofibrils with dimensions that vary depending on the source, pre-treatment and specific process used for deconstruction (Figure 1d). Therefore, characteristically CNFs form highly percolative structures in water, with a high tendency to form hydrogels, even at low concentrations. They can display a strong shear thinning behavior (Figure 1e), which is useful in applications where injectability is needed.

In addition to plants, some bacteria are able to directly extrude cellulose microfibrils without the hierarchical order found in plant cell walls. Such nanocellulose species are termed bacterial cellulose (BC).[4] CNF, CNC, BC, as well as rod-like tunicates[4] are here generically referred to as "nanocelluloses". They possess different morphologies and sizes depending on the sources and processes, and are excellently suited for the fabrication of advanced materials, taking advantage of their remarkable physical, mechanical and chemical features. Associated topics have become widely discussed in the scientific literature in the recent years, and full coverage of all progress would be a grand challenge. This review focuses on self-assembled, biomimetic, and directed assembled materials based on nanocelluloses, their interactions with water, the possibilities for functionalization and fabrication of nano-objects, nanoparticles, filaments, films and 3D structures, as well as tribology. Such systems facilitate a number of functional properties and materials, for example, biomimetic toughening, plasmonics, fluorescence, mechanosensing, actuation, motility, membranes, biosensors and bioactive systems, flexible piezoelectric, magnetic, and conducting materials, among many others. Even if we present the state of the art broadly, this review emphasizes the role of nanocelluloses within such emerging advanced materials concepts, in the view of the present thematic issue on Finnish research and related collaborations. Therefore, some of the main applications of nanocelluloses will not be discussed here, such as fiber-reinforced composites, viscosity modifiers, barrier properties for food packaging, electronics templating, and drug delivery,

some of which are already maturing towards technical applications. They have been recently reviewed in a comprehensive manner.[9]

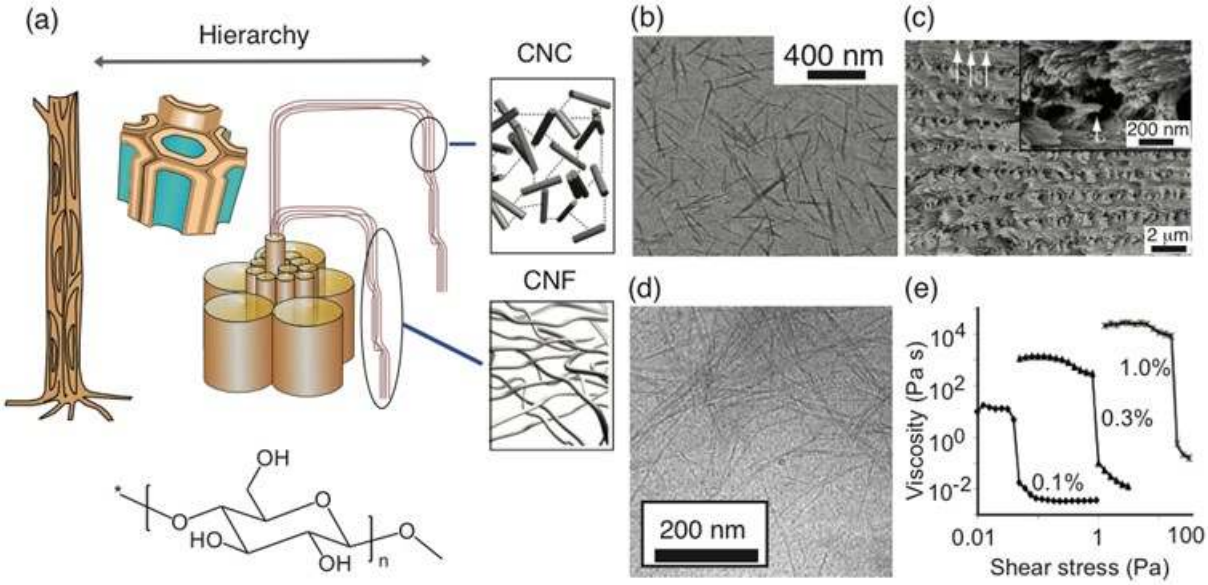

Figure 1. Disintegration of wood and plant cell wall material to form nanocelluloses and some of their most characteristic properties. a) Schematics to disintegrate cellulose nanocrystals (CNC) and cellulose nanofibers (CNF) from wood and plant cell walls and chemical formula of cellulose. Modified with permission.[10] Copyright 2004, Wiley-VCH. b) Transmission electron micrograph of CNC nanorods. Reproduced with permission.[11] Copyright 2001, Wiley-VCH. c) CNCs typically form chiral assemblies, as shown in a scanning electron micrograph. Reproduced with permission.[12] Copyright 2012, Springer. d) By contrast, the longer CNFs typically form percolative structures, such as hydrogels. Reproduced with permission.[13] Copyright 2007, American Chemical Society. e) They can be strongly shear thinning, promoting injection. Reproduced with permission.[14] Copyright 2012, Elsevier.

2. Nanocelluloses as colloidal level structural units

2.1 Advanced preparation techniques, fundamental interactions, and modification

Sulfuric acid hydrolysis is overwhelmingly the most widely used preparation technique for CNCs. It is executed within a fairly small reaction window that efficiently cleaves the disordered segments in a native microfibril (Figure 1a, b), leaving behind just the crystallites (i.e., CNCs) and simultaneously introducing sulfate esters on their surface to enhance the colloidal stability.[1,15,16] CNFs, in turn, are generally isolated from the fiber matrix by high mechanical shear coupled with suitable pretreatments.[4,17] A notable case of pretreatment is the oxidation catalyzed by 2,2,6,6-tetramethylpiperidine-1-oxyl radical (TEMPO) which

greatly reduces the energy consumption of CNF preparation and results in CNFs of nearly monodisperse width and high charge density.[18]

New methods have emerged within the past few years particularly in CNC preparation.[15,16] Esterification[19] and oxidation[20–24] routes to CNCs as well as uses of alternative acids[25,26] vs. sulfuric acid have been reported. In addition, a completely new approach utilizing HCl vapor was introduced.[27] This method is able to tackle several issues in CNC preparation, like the laborious purification steps and the difficulties in acid recycling. Furthermore, the CNC yields are superior at over 97%, aided partially by simultaneous crystallization of cellulose upon its degradation with HCl vapor (**Figure 2**a). The difficulty here lies in the dispersion step after the hydrolysis. More practical methods to the initial proof-of-concept system[27] have been put forward, including dispersion with polysaccharides and modified proteins[28] as well as TEMPO-oxidation,[29] all of which can end up with ~60% yield at the highest (Figure 2b).

Both CNFs and CNCs are based on the native microfibril structure which bears an amphiphilic character as cellulose I crystal possesses both hydrophilic planes, exposing the equatorial OH groups, and hydrophobic planes, exposing the axial C-H functionalities (Figure 2c).[30,31] This amphiphilicity of the crystal can be used both in CNFs and CNCs after their preparation for exfoliation of the hydrophobic planes to yield entirely distinct nano-objects (Figure 2c).[32,33] Overall, the amphiphilic nature of nanocelluloses is beneficial for their use as emulsion stabilizers. Analogous to Janus particles, exploitation of CNFs or CNCs leads to enhanced stability of Pickering emulsions in contrast to homogeneous colloidal particles.[6]

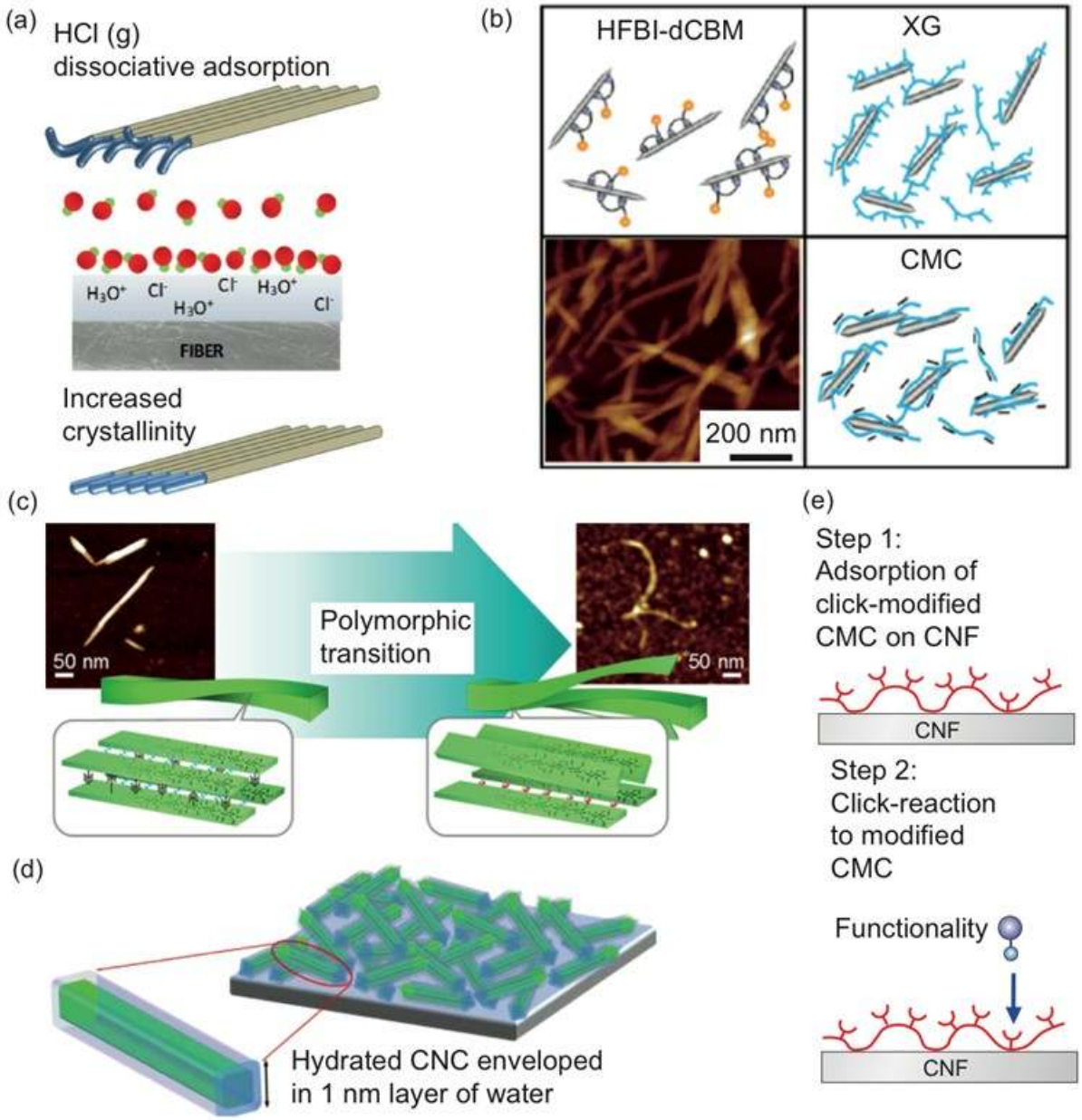

Figure 2. a) Simultaneous degradation and crystallization by adsorption of HCl vapor for high-yield preparation of CNCs. Reproduced with permission.[27] Copyright 2016, Wiley-VCH. b) Dispersion of CNCs prepared by HCl vapor (lower left) is feasible with cellulose binding modules combined with cellulose binding motif adduct with hydrophobin (dCBM-HFBI), xyloglucan (XG), and carboxymethyl cellulose (CMC). Reproduced with permission.[28] Copyright 2017, American Chemical Society. c) In a cellulose I crystal, hydrogen bonded sheets which are stacked on top of each other with van der Waals bonding can be exfoliated in a polymorphic transition. Reproduced with permission.[33] Copyright 2017, American Chemical Society. d) Cellulose nanocrystals are enveloped in 1 nm layer of water under high humidity. Reproduced with permission.[34] Copyright 2015, American Chemical Society. e) Adsorption of an azide-click modified dissolved polysaccharide (such as modified carboxylmethyl cellulose) on a cellulose surface enables further aqueous modular modification with a large number of molecules and functional groups. Reproduced with permission.[35] Copyright 2012, American Chemical Society.

It is often claimed that cellulose and particularly nanocelluloses are "highly hydrophilic" but in fact, the theoretical contact angle of water even on the OH-exposing (110) plane of cellulose I crystal is 43°,[36] thus certainly hydrophilic but not excessively so. However, cellulose is unambiguously hygroscopic[37] and this defines much of the relationship of dry nanocellulose networks with water. Although water never penetrates inside the cellulose crystal,[37] CNCs under high humidity are enveloped with 1 nm layer of water on their surface (Figure 2d).[34] When exposed to liquid water, CNC and CNF networks generally swell, forming a hydrogel.[38] In excess water, dry CNCs without added charge just aggregate and precipitate.[27] Under high mechanical forces and suitable surface charges, dried CNCs can be re-dispersed in water but this not self-evident in every case and can often be incomplete.[39] The dried networks are strongly held together in water presumably by van der Waals forces between the hydrophobic planes in the cellulose crystals.[34] Orientation of the surface hydroxyls has been proposed as another or a complementary reason behind the irreversible association of nanocelluloses upon drying.[40]

The tendency of cellulose to stick together is not confined to the dried state. Both CNCs and CNFs form gels,[13,14,41–68] CNFs at very low concentrations (ca. 0.5-1.0 w-%) because of the interfibrillar junctions enabled by the flexible fibrillary structure in contrast to the rigid CNCs.[38] It is impossible to have dilute running aqueous dispersions of CNCs or CNFs without added chemical modifications on the surface, usually in the form of charges.[1,4,29] Furthermore, virtually no common organic solvent is able to disperse nanocellulose.[29,69] However, with added charge, generally as sulfate groups stemming from the hydrolysis, CNCs are stable in water well into the 20 w-% regime, forming liquid crystals beyond a certain threshold at 5-10 w-%.[1] Good dispersion properties are among the major reasons why CNCs have been subjected to targeted self-assembly and more sophisticated modification techniques more than CNFs which tend to gel already at low concentrations.

Chemical modification of all nanocellulosic species is challenging because (i) cellulose as a structural component is relatively inert or its hydroxyl groups are generally less reactive than other corresponding alcohols and (ii) proper dispersion is usually feasible only in water, thus defying or at least complicating the use of most organic solvents. Yet a substantial body of literature exists on modifying the hydroxyl groups on both CNF and CNC surfaces, generally by esterification and etherification reactions.[1,4,70,71] Some of these modifications have been performed in organic solvents whereupon the degree substitution is often fairly low due to reduced accessibility. Polymer grafting on nanocellulose surfaces has also received significant attention,[70–75] being particularly important for guiding self-assembly and tuning the compatibility of nanocelluloses with other materials. Therein, we emphasize two-step chemistry, first making aerogels of CNC or CNFs, next exposing them to chemical vapor deposition of initiators for surface-initiated atom transfer radical polymerization (SI-ATRP), which allows organic solvent dispersibility. In the second step, the surface concentration of the initiator can even be increased in the organic solvent phase, leading to a high concentration of initiation sites for polymerization and subsequently to high-density polymer brushes.[75–79] This process is elaborated later on in this review in chapter 2.6.

Besides covalent modification, supramolecular interactions are available for modifying the nanocellulose surface. Modified cellulose binding modules (CBMs), alternatively denoted as cellulose-binding domains (CBDs),[80–82] i.e., the binding sites in cellulose-specific enzymes, can be utilized to attach various functionalities on the (nano)cellulose surface.[83] Many water-soluble polysaccharides also possess high affinity on cellulose surfaces and can be used in a modular fashion for surface modification via further utilization of, e.g., click chemistry (Figure 2e).[35,84] More recently, aprotic systems have been applied to directly attach hydrophobic polymers by adsorption on nanocellulose surfaces.[85]

2.2 Assembly of nanocelluloses at the air/water and oil/water interfaces

Amphiphilic CNC were achieved by introducing lipophilic groups to the reducing end of the cellulose nanocrystal *via* consequent regioselective periodate oxidation and reductive amination (**Figure 3**a).[21] The modification resulted in individual CNCs that did not show any sign of clustering upon drying when investigated by TEM (Figure 3b). However, in soybean oil/water emulsions, a clear effect of the lipophilic groups was observed as the emulsion droplet sizes decreased by a decade when compared to a system where the unmodified CNC was employed as the stabilizer. Nanocellulose, especially CNC, can act as a stabilizer in a Pickering emulsion where solid particles at the liquid/liquid interface provide stabilization against coalescence of the liquid droplets.[86] It has been approximated, that a significantly smaller number of rod-like particles can provide the same emulsion stabilization as spherical particles. However, it is good to notice that the Pickering emulsification does not rely on amphiphilicity or self-assembly of the particles but the Gibbs energy gain depends merely on the dimensions of the particle, contact angle of the particle and surface tension of the media.

Several attempts to facilitate the assembly of nanocellulose at air/water and oil/water interfaces have been taken by coupling the nanocellulose with an amphiphilic molecule or by coupling the nanocellulose to a readily assembled monolayer of the amphiphilic molecule at the interface.[87,88] In a typical experiment, the surfactant layer is first spontaneously formed at the air/water interface in a Langmuir trough and the cellulose is added from the sub phase and then assembled to the near vicinity of the surfactant layer. The assembly is enabled if there is a strong long-range interaction, such as electrostatic interaction, between the surfactant and the cellulose, guiding towards a sandwich structure where the nanocellulose forms a layer below the surface-active molecules.

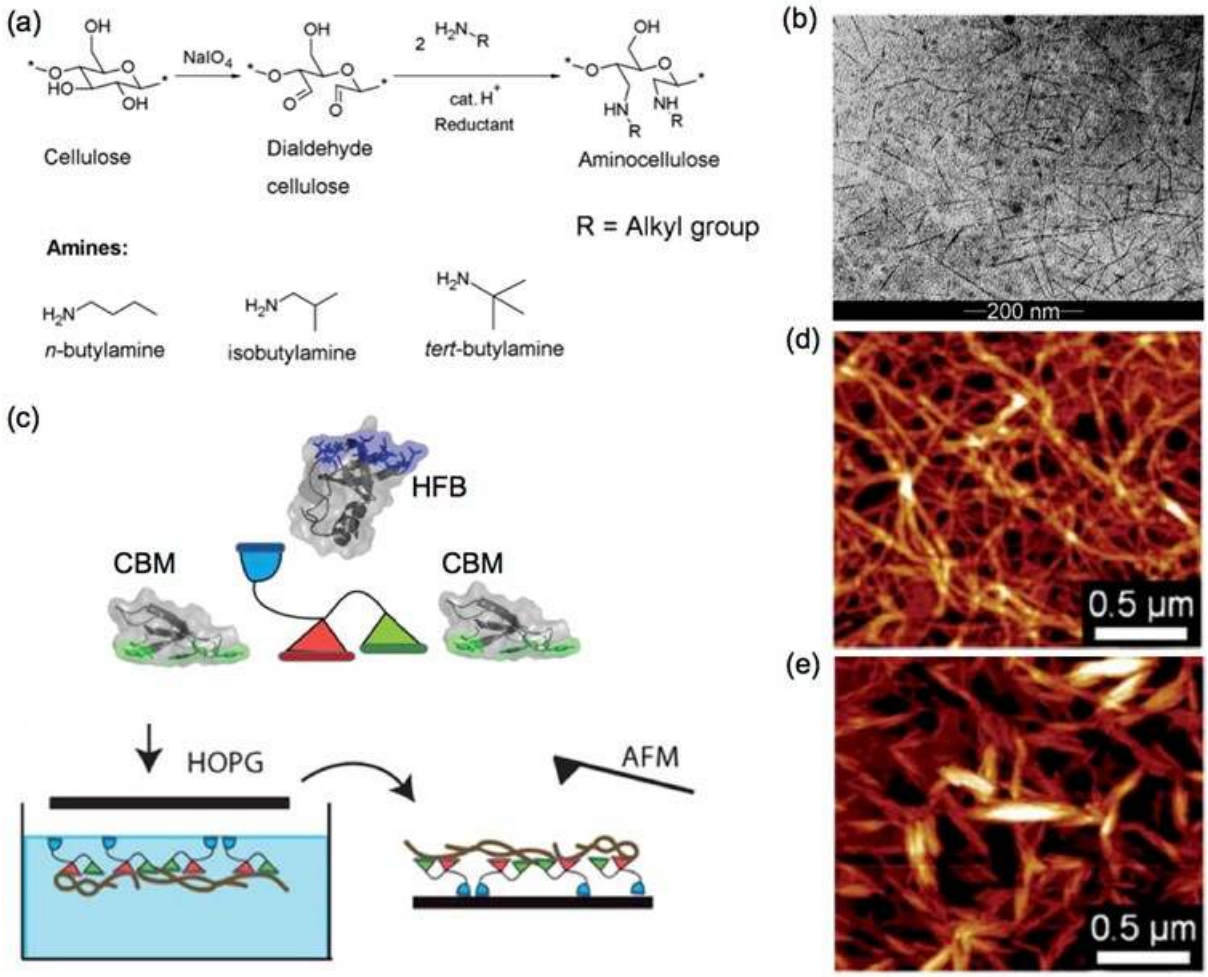

Figure 3. a) Periodate oxidation and reductive amination of cellulose, and (b) TEM-image of *n*-butylamino-functionalized CNCs. Reproduced with permission.[21] Copyright 2014, American Chemical Society. c) Facilitated assembly of CNF at air/water interface via amphiphilic biomolecules and film transfer on a hydrophobic surface, d) AFM topography image of a self-assembled protein CNF film picked up from air/water interface, and e) AFM topography image of a self-assembled protein CNC film picked up from air/water interface. Reproduced with permission.[87] Copyright 2011, Royal Society of Chemistry.

Block copolymer-like fusion protein consisting of an amphiphilic domain called hydrophobin (HFB)[89] and CBM were applied for attracting nanocellulose crystals and cellulose nanofibrils at the air/water and oil/water interfaces.[87,88] The cellulosic structures at the interface were studied *ex-situ* by AFM from hydrophobic solid surfaces, where the interfacial films were picked up by Langmuir–Schaefer technique (Figure 3c). The resulting layers consisted of randomly organized nanocellulose layers showing a separate condensed protein layer facing the hydrophobic surface as presented in Figure 3d and e. The shear rheological properties of the different interfaces showed large variation for the different systems studied.

Comparison of the pure cellulose nanofibrils to the mixed protein/CNF films at air/water interface clearly demonstrated that CNF alone could not significantly assemble at the interface. By contrast, together with the protein, there was more than a decade larger rheological moduli observed for the interface. However, at the oil/water interface the CNF alone had comparably higher rigidity than the protein/CNF film, but the values were overall much lower than at air/water interface. CNF combined with the same protein also showed good capability to stabilize emulsions and could also stabilize certain hydrophobic drug nanoparticles.[87,90]

By studying the interfacial behavior, we can understand the fundamentals of stabilization of emulsions and foams by nanocelluloses and state that this is a potential application for them. However, other feasible bio-polymer based materials for stabilizing interfaces exist, including regenerated amorphous cellulose that performs well and can be produced by lower manufacturing costs[91] and any other anionic polyelectrolyte that is attracted to the interface via counter charges.[92] Employing CNF or CNC at the interfaces of two-phase systems will thus be motivated only when the precise nanocrystalline or fibrillary structure can bring a benefit.

2.3 Binding of polymers on nanocelluloses

The plant cell wall serves as a model for biomimetic self-assembly of cellulose, and can provide inspiration for this.[93] Mostly, reports of nanocellulose with components of hemicellulose or lignin - the other two major polymers in plant cells - suggest advantages in dispersibility, stability, and enhanced fibril-interactions. Using a core-shell model for CNF with a surface coating of hemicellulose, a comparison to a high surface charge CNF was made.[94] The use of hemicellulose led to a lower sensitivity to electrolytes, resulting in lower flocculation tendencies at high salt concentrations (**Figure 4**a). Enzymatic removal of hemicellulose significantly affected the flocculation and entanglement properties.[47] Addition

of arabinoxylan to CNF, in turn, led to an increase of tensile strength of a CNF film. The strength increase was proportional to the length of hemicellulose chains demonstrating this as a route for controlled film production.[95] Xylan was also shown to function as an electrostatic stabilizer on CNF, with additional properties leading to functions such as reduced gas permeability and increased moisture uptake.[96] Similarly, lignin has been studied as a cementing material between CNF fibrils (Figure 4b),[97] where it also reduced surface hydrophilicity. An approach to make CNC from holocellulose, led to residues of lignosulfonate and other non-cellulose molecules on the CNC,[98] resulting in increasingly amphiphilic particles with properties for diverse interfacial assembly. CNF from holocellulose displayed advantageous mechanical properties due to adhesion, mediated by the hemicellulose matrix.[99] In conclusion, the current literature on hemicellulose and lignin modifications of nanocellulose suggests that benefits towards processability in self-assembly is found but a detailed understanding allowing advanced cell wall mimicking mechanisms is yet to be achieved.

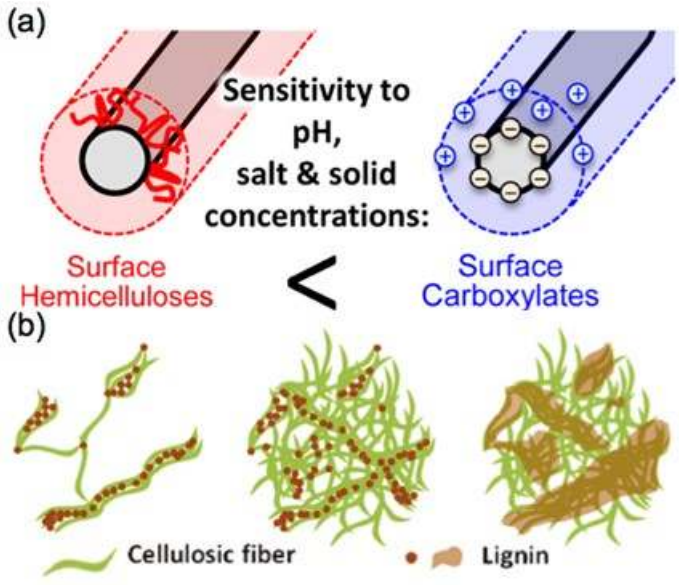

Figure 4. Hemicellulose and lignin-based interactions to CNF. a) CNFs with hemicellulose surface layers remain softer in films than the carboxylate-rich CNF films. Reproduced with permission.[94] Copyright 2016, American Chemical Society. b) Lignin acts as a connecting material within the CNF films. Reproduced under the terms of the CC-BY-X license.[97] Copyright 2015, Royal Society of Chemistry.

A major challenge in the use of nanocelluloses is their typically low wet strength. Different approaches have been proposed in the literature to overcome this issue, mainly by adsorption of surface active moieties, covalent crosslinking, and surface hydrophobization. Chemical functionalization strategies for cellulose and, especially nanocelluloses, have been covered extensively in recent reviews.[71,100] Here, we are interested in a simple alternative that facilitates processing. Chitosan is an interesting biobased option. Indeed, films were produced from hydrogels comprising mixtures of CNF and chitosan, which resulted in materials with high mechanical strength in the wet state, while maintaining a high level of transparency (~ 70 – 90 % in the 400 – 800 nm wavelength).[101] This was allegedly a result of complexation or physical crosslinking, triggered by a simple shift in pH during processing in order to reduce the hydration of chitosan and to promote multivalent physical interactions. Films containing 80% CNF presented a dry strength of 200 MPa (maximum strain of 8% at 50% air relative humidity) while the wet strength was largely preserved, at 100 MPa (strain of 28%). This is remarkable, considering that the pure CNF films loose, for all purposes, the strength under wet conditions.[101] The proposed mechanism of crosslinking in the CNF network is illustrated in **Figure 5**a (thick red fibers or fibril network) in the presence of chitosan chains (narrow green fibers) in the wet state. If chitosan is charged at low pH, electrostatic repulsion and large hydration layers between chitosan segments are expected, resulting in low wet strength. However, in the case of neutral chitosan at high pH, crosslinking is effective in increasing significantly the wet strength, Figure 5a.[101] This approach is of interest since the physical crosslinks are weaker compared to covalent ones, but can possibly rearrange upon stress, potentially serving as sacrificial bonds for dissipating energy during deformation. In several applications, the interactions to the surrounding, often hydrophobic, media need to be tuned, suggesting the use of amphiphiles. The adsorption of surfactants and, especially, polymeric amphiphiles, has been widely addressed, and recently also reviewed for nanocelluloses.[102] Therein, non-ionic block copolymers allow a wide range

of tunability based on different block lengths and architectures to enhance the interactions between hydrophilic nanocelluloses and hydrophobic solvent or polymeric medium. One example, illustrated in Figure 5b, is that of polyethyleneoxide-*b*-polypropyleneoxide-*b*-polyethyleneoxide block copolymer (Pluronic) surfactants,[103] which can be adjusted to produce different levels of interactions, aggregation and binding with nanocelluloses in hydrophobic media.

Among the hemicelluloses, especially xyloglucans are known to bind particularly efficiently on celluloses.[104,105] One could hypothesize that its structure with xylose side-groups, potentially also containing galactose residues,[106,107] improves sugar-sugar binding to cellulose due to the steric availability of the side chain repeat units. A platform for tunable sugar-sugar interactions could also be provided by dendrons or dendronized polymers with sugar peripheral groups.[108] Indeed, maltose-decorated dendrimer-functionalized polymers (Figure 5c) show generation dependent binding on CNCs.[109] Due to the high molecular weight and large colloidal scale diameter of the third generation dendrimer-decorated polymer, its wrapping around CNCs could be directly visualized using cryogenic HR-TEM and electron tomography (Figure 5c).[109]

Conceptually similar wrapping was recently suggested between methyl cellulose onto CNC.[110] Specifically, by mixing CNC and methylcellulose, the hydrogel properties were significantly enhanced and the gels were useful in stabilizing aqueous foams. It was hypothesized that CNCs bind to large MC coils both in solution and at the air/water interface. In sum, physical crosslinking, adsorption, complexation and binding are phenomena that bear great potential for practical purposes, for example in fiber spinning of nanocelluloses, as will be covered in further sections of this review. In conclusion, it has been demonstrated that especially hemicellulose and chitin carbohydrate polymers can be used as versatile tools to modify interactions and colloidal properties of nanocellulose. These modifications utilize naturally occurring interactions yielding potentially large benefits in specificity. The use of

enzymes to tailor their functions has still not been studied widely, but we expect that this line of research will increase due to the mild conditions that can be used and the specificity and selectivity of the modifications.

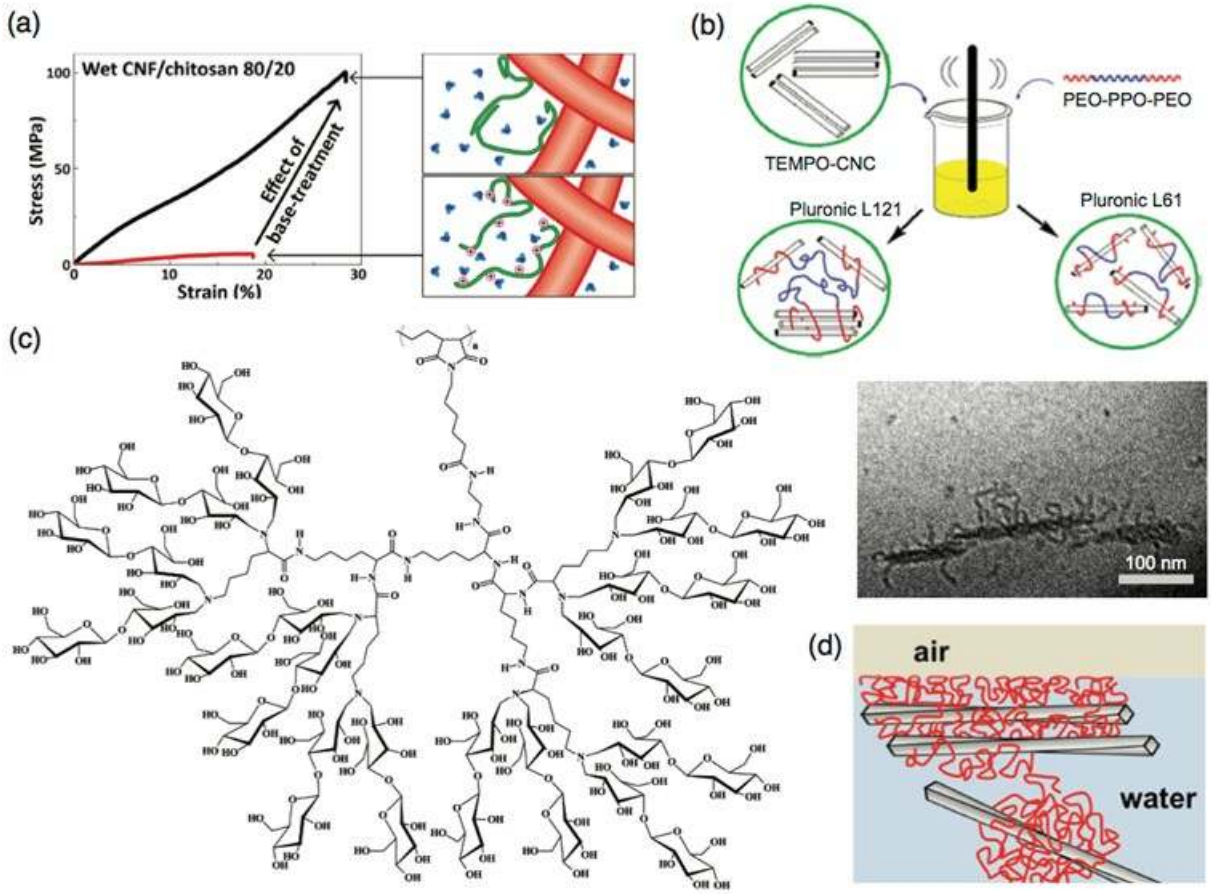

Figure 5. Binding of polymers on nanocelluloses. a) Electrostatic binding of cationic chitosan on CNF with residual adsorbed polysaccharides to stabilize the material under wet conditions. Reproduced with permission.[101] Copyright 2015, American Chemical Society. b) Schematics of interactions of TEMPO-oxidized CNC with block copolymer (Pluronic) surfactants for the interaction tuning for hydrophobic media. Reproduced with permission.[103] Copyright 2015, Springer. c) Maltose-decorated 3rd generation dendronized polymers allow multivalent binding and consequent wrapping around CNCs as illustrated using cryo-TEM. Reproduced with permission.[109] Copyright 2014, American Chemical Society. d) Proposed wrapping of methyl cellulose on CNC to stabilize aqueous foams. Reproduced with permission.[110] Copyright 2016, American Chemical Society.

2.4 Protein-mediated interactions on nanocelluloses

Due to their well-defined structures and supramolecular interactions, it is logical to explore how proteins can be used to drive self-assembly and interactions of nanocellulose. There are several different approaches that one can take toward this topic, broadly categorized

as either specific molecular recognition or non-specific in the interactions with cellulose. In the specific approaches a biological molecule whose natural function is to bind to cellulose is used in a new context, and in the non-specific ones, molecules interact by either charge interactions or other weak interactions, such as hydrogen bonding, π-stacking, or van der Waals interactions.

One approach utilizing specific interactions is to take advantage of CBMs (**Figure 6**a).[80–82] The CBMs are a very diverse type of proteins found widely in different organisms, also showing convergent evolution, i.e., there are evolutionarily distinct proteins fulfilling the same function, but achieved by clearly different routes. In their original context CBMs are often found in enzymes that degrade cellulose, and therefore have developed to interact specifically.[111] The potential advantage is that adsorption of CBMs will be spontaneous, specific and fast, as it relies on a molecular recognition event. As the interaction with cellulose is dependent on very precisely defined interactions, their use to modify CNC can sometimes be complicated as charged groups introduced on the cellulose surface can prevent CBM docking, but on the other hand non-specific electrostatic interactions may be enhanced.[112] An attractive approach is to combine functions of structural proteins such as resilin within a scaffold of nanocellulose in order to achieve an elastic interconnection between the cellulose components. Resilin is a protein found in insects and has been reported as the most resilient material known, i.e., it can release stored energy by elastic deformation very efficiently.[113] If resilin is placed between two CBMs, its function is retained and it can efficiently increase the elastic modulus of suspensions of CNF.[114] In dry films, cross-linking was evident and showed a commonly observed behavior in cross-linking that stiffness was increased but overall strain was reduced, leading to a stiffer but more brittle material (Figure 6b). In another use of resilin-CBM fusions it was found that the protein could be used as a primer that binds to CNC, and to which epoxy resin could react.[115] Thereby, the protein could serve as a surface modifier that allows incorporation of aqueous CNC into the epoxy

resin without solvent exchange. The incorporation of resilin through CBM interactions also led to enhancing the plasticizing effect of glycerol in CNC films.[116]

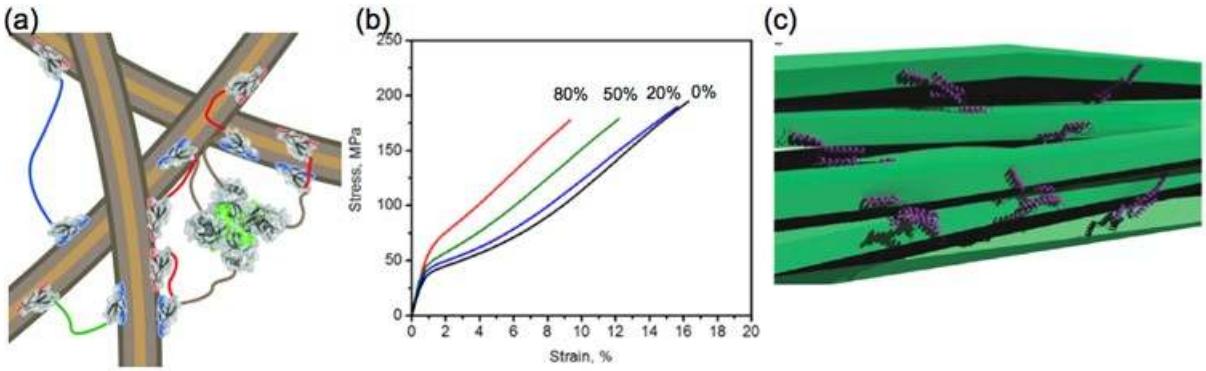

Figure 6. Protein-mediated binding on nanocelluloses to mediate supramolecular interactions. a) Physical crosslinking based difunctional proteins that bind on CNFs by cellulose binding modules and mutually based on hydrophobins. Reproduced with permission.[80] Copyright 2015, Wiley-VCH. b) Stress-strain curves for CNFs interconnected by resilins which are telechelically modified with cellulose binding modules for different protein weight fractions. Reproduced under the terms of the CC-BY-X license.[114] Copyright 2017, American Chemical Society. c) Combining CNF and silk proteins leads to ultra-strong fibers. Reproduced under the terms of the CC-BY-X license.[117] Copyright 2017, American Chemical Society.

Nanocellulose has also been combined with proteins by interactions that do not rely on molecular recognition, but on general electrostatic or weak interactions.[118] The use of materials properties of proteins in combination with cellulose is motivated by the interface compatibility or due to exploring the promising mechanical properties of proteins.[119] Collagen is an example of a mechanically functional protein that has been combined with charged CNC. By an isoelectric focusing technique, aligned fibers were formed that were stiffened by 5% CNC and showed enhancement in wet mechanical properties.[120] Other proteins that are typically not associated with mechanical properties, such as plant storage proteins (prolamins), have been explored for mechanical functions through processing by electrospinning.[121] In these fibers a 3% addition of CNC gave a 4-fold increase in strength. Overall these studies suggest that a stable interface is formed between different as well as unrelated proteins and cellulose, even though these proteins have no natural function of interacting with cellulose. It should be kept in mind that the CNCs used are surface modified

with charged groups and therefore potentially interact with the proteins simply by electrostatic interactions. The concept of compatibility was taken further and even non-modified CNFs, coated with soy protein and casein were found to create a compatibility layer between the cellulose and a PLA polymer.[122] A widely studied case of combining nanocellulose and a protein not naturally occurring with cellulose is the combination with silk. Especially spider silk is attractive because of its mechanical properties, such as toughness.[123] There are extensive attempts to produce spider silks, i.e., spidroin proteins, by recombinant means (in bacteria),[124,125] and it was suggested that CNF would be used to mix with low amounts of spidroin in order to provide material on the bulk scale, as spidroin production levels tend to be low. This led to composite fibers (Figure 6c) that had surprising properties at a low spidroin content of 10%.[117] The spidroin led to a significantly increased strain in the material while stiffness, and slope during plastic extension remained unaltered. Consequently, a remarkable ultimate strength was achieved, exceeding 1 GPa. This is noteworthy since the behavior is unlike in other studies where crosslinking was achieved, which typically leads to increased stiffness (Figure 6b).[114] Instead the effect of increased strain was more similar to other studies where fiber length had been increased.[126] Silkworm silk is more abundant and can be dissolved readily into the constituent fibroin proteins with for example lithium salts. Reassembling fibers by extrusion of fibroin into an anti-solvent leads to fibers with reduced properties. Addition of 5% CNC into the fibroin melt, resulted in a doubling of stiffness of fibers mimicking the function of crystallized protein domains in the native fiber.[127] A similar approach as was taken with films, combining dissolved fibroins with extracted CNFs by using aq. lithium bromide.[128] Combining again lithium dissolved fibroin with bacterial cellulose resulted in lamellar self-assembled structures, suggested to be used as a bone repair material.[129]

The potential benefit of using biomolecular CBM interactions for modifying cellulose is the high specificity that can be achieved in the assembly. Spontaneous, selective, and quick

interactions in combination with virtually endless possibilities to functionalize forms a great advantage that surely is worth pursuing. On the other hand, the approach is currently too expensive at a larger scale, and protein interactions may be too sensitive to denaturation to be practical in many applications. These are not inherent problems to proteins and we may expect these problems to be resolved in the future. We are likely to see applications combining nanocellulose and bulk proteins such as soy or silk in a closer future, as this approach in terms of price competitiveness for added benefit is more promising.

2.5 Nanoparticle binding on nanocelluloses

The high aspect ratio, tunable surface functionalities, low density, as well as colloidal stability makes nanocelluloses promising candidates for hybrid nanostructures. Furthermore, the one dimensional (1D) fibrillar CNFs with their high length and the rod-like CNCs with their helical twisting provide attractive opportunities to prepare nanocellulose-nanoparticle hybrids and composite materials for chiral plasmonics, optoelectronics, and catalytic applications. The nanoparticle binding to the nanocellulose surface has been demonstrated using i) electrostatic binding of cationic nanoparticles to anionic nanocellulose or anionic nanoparticles to surface modified cationic nanocellulose, with some unavoidable aggregations; ii) covalent attachment of surface functionalized nanoparticles; iii) direct synthesis of nanoparticles on nanocellulose surface; and iv) selective end functionalization of CNCs with thiol units to bind nanoparticles topochemically at one end of CNC. The synthetic and characterization approaches for gold nanoparticle-nanocellulose hybrid materials,[130] and their generic application potential of certain metal nanoparticle bound CNCs have recently been reviewed.[131] By contrast, the focus here will be to highlight some of the representative examples. The interaction and adsorption characteristics have recently been studied between negatively charged CNFs with cationic nanosized precipitated calcium carbonate particles (nanoPCC, *d*~50 nm) and anionic nanoclay particles (thickness ~1 nm width and length ~150-

200 nm) by using quartz crystal microbalance dissipation (QCM-D) and AFM measurements.[132,133] Addition of carboxymethyl cellulose (CMC) to CNF increased the surface negative charge of CNF, thus resulting in a strong affinity for cationic nanoPCC particles. However, the complexation led to flocculation or aggregation of large clusters indicating unstable colloidal dispersion. On the other hand, due to the anionic nature of nanoclay, the addition of CMCs had the opposite effect compared to that of nanoPCC-CNF interaction, yielding a stable nanoclay-CNF dispersion. With this method, composite papers/films could be prepared with tailored surface properties.

Gold nanoparticles (AuNPs) can be either electrostatically deposited onto the nanocellulose surface or covalently linked by modifying the CNF surface functional groups with quaternary ammonium, azido-, propargyl or amino groups (**Figure 7**a).[134] Negatively charged gold nanoparticles with an average diameter of *d*~15 nm were found to bind more efficiently (electrostatically) compared to those of smaller size (*d*~5 nm) by using a covalent click-chemistry approach. Similarly, sulfuric acid hydrolyzed CNCs were used to prepare optically transparent and strong hybrid materials by using amorphous calcium carbonate nanoparticles (*d*~11.3 ± 0.5 nm).[135] In order to obtain a homogeneous dispersion, CNCs were complexed with $CaCl_2$ and solvent exchanged to ethanol in the presence of sodium carbonate to generate amorphous $CaCO_3$ nanoparticles-CNC hybrid material. A systematic study was carried out on the direct synthesis of silver nanoparticles (AgNPs) on sulfuric acid hydrolyzed CNCs using sodium borohydride reduction.[136] The size of resulting AgNPs can be controlled by tuning the amount of sulfate groups using aqueous sodium hydroxide. The size of the AgNPs decreased upon increasing the concentration of CNCs, along with improved stability and narrow size dispersion. Similarly, upon decreasing the number of surface sulfate esters, a similar trend on size and stability was observed. However, below a certain threshold, the nanoparticles tended to aggregate.

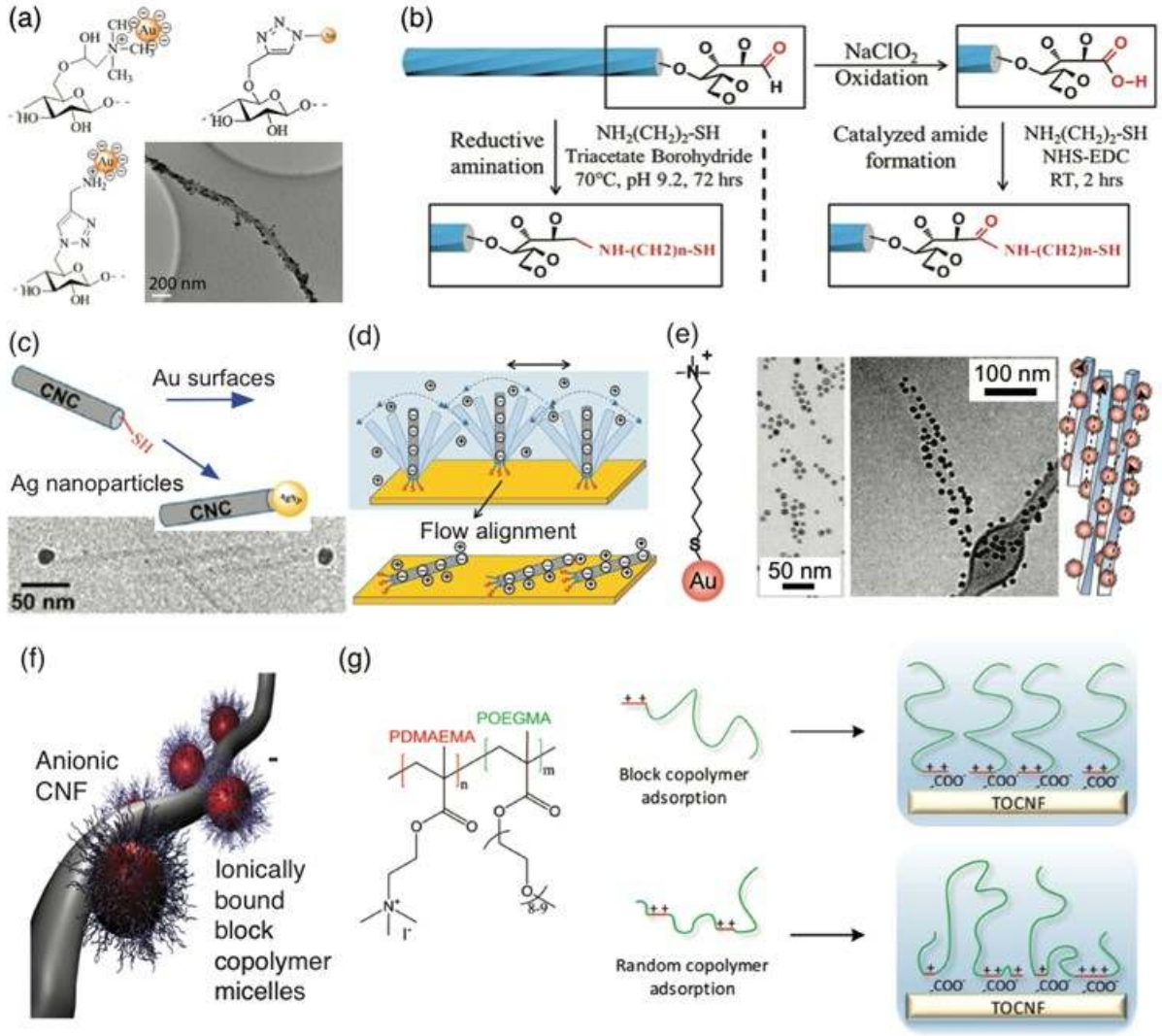

Figure 7. Nanoparticle binding on nanocelluloses. a) Click-chemistry approach towards surface functionalized CNFs for electrostatic and covalent binding of AuNPs as shown by a TEM micrograph. Reproduced with permission.[134] Copyright 2016, Springer. b) Synthetic routes for selective end functionalization of CNCs. Reproduced with permission.[137] Copyright 2014, Springer. c) Schematic representation of asymmetric thiol functionalized CNC and TEM micrograph depicting Janus-like rod-sphere adduct due to selective binding of Ag nanoparticles to one end of CNC, and d) schematic illustration of cilia-like alignment of asymmetrically functionalized CNCs on gold surface. Reproduced with permission.[138] Copyright 2013, American Chemical Society. e) TEM micrographs of 8.5 nm cationic gold nanoparticles, electrostatically bound to form nanofibrillar adducts. Reproduced with permission.[139] Copyright 2016, Wiley-VCH. f) Schematic of colloidal co-assembly through ionic complexation of anionic CNFs and cationic polybutadiene-*b*-poly[2-(dimethylamino)ethyl methacrylate] micelles. Reproduced with permission.[140] Copyright 2015, American Chemical Society. g) The architecture of the polymer decoration on CNCs can be tuned by selecting block copolymers or random polymers. Reproduced with permission.[141] Copyright 2015, American Chemical Society.

The specific feature of all native cellulose species is the possibility to selectively functionalize one end (i.e., reducing end) using, for example, reductive amination or *N*,*N*-

(dimethyl amino)propyl-*N*′ -ethylcarbodiimide hydrochloride/*N*-hydroxysuccinimide (EDC/NHS) coupling chemistry to furnish asymmetrically functionalized CNCs (Figure 7b). This approach has been utilized to prepare CNCs containing silver nanoparticles at one end resulting in an asymmetric Janus-like rod-sphere colloidal particle (Figure 7c).[137] Similarly, the affinity of thiol to gold surfaces has been exploited to prepare cilia like structures on a gold surface. Due to asymmetric thiolation and significant coulombic repulsion, the end-tethered CNC rods, which are preferentially oriented upright in aqueous media, are reminiscent of biological cilia like structures (Figure 7d). The alignment of CNCs was achieved using convective shear of an evaporating drop of water, which indicated that the interaction between the surface and CNCs is chemisorption and the presence of flexible linkers allowed realignment as evidenced by QCMD measurements.[138]

Mixing of CNCs involving anionic charges and cationically charged gold nanoparticles would be expected to form uncontrolled aggregates. However, by slowly adding cationic nanoparticles to aqueous dispersion of CNCs and tuning the nanoparticle sizes, mesoscale fibrillar adducts can be achieved instead of uncontrolled aggregates (Figure 7e).[139] Three different sizes of nanoparticles were examined, i.e., 8.5 nm, 11.7 nm and 2.6 nm metal core diameters, capped with (*11*-mercaptoundecyl)-*N, N, N*-trimethylammonium bromide ligands and *23*-mercapto-*N, N, N*-trimethyl-3,6,9,12-tetraoxatricosan-1-aminium bromide ligands. Later in this review it will be shown that using a 8.5 nm metal core, i.e., particle size balanced with the lateral size of the CNCs (7 nm), results in mesoscale fibrillar adducts with chiral plasmonic signal.

By contrast, instead of the CNC directed self-assemblies, space filling self-assemblies were reported by ionic complexation of CNFs and block copolymers upon solvent removal. An example is provided based on anionic CNF and a diblock copolymer consisting of cationic block and polybutadiene (PB) (Figure 7f).[140] In aqueous medium, the diblock copolymer forms micelles with cationic surfaces, and mixing with anionic CNFs leads to ionic self-

assemblies. Although well-defined order is not obtained, there is evidence that the block copolymer micelles intercalate domains of CNF.[140] An optimum concentration was identified where the work-of-fracture, i.e. the area below the stress-strain curve, becomes large, indirectly indicating toughening of CNF films.[141,142]

All the above methods used to bind various nanoparticles appear to be generic and have the potential for applications e.g. in surface enhanced Raman scattering (SERS) imaging, separation, catalysis and transducer enhancers for biomolecular delivery.

2.6 Polymer-Grafted Nanocellulose

The modification of cellulose has a long tradition, also affected by a large variety of diverse strategies to change the surface chemistry of nanocelluloses. Among those, modification for surface-initiated polymerization is a convenient tool to implement virtually any function or chemistry by polymerizing the respective monomers as polymer brushes. Several types of brushes on nanocellulose have been demonstrated using various surface-initiated polymerization techniques including cerium(IV)-initiated free-radical polymerization, RAFT or ATRP.[70,74,143–150] In most cases, the respective initiating site is anchored to the surface by wet chemical reactions or chemical vapor deposition. The polymer brushes then grow from the surface with convenient control over the brush size by tuning the polymerization conditions (see schematic of a CNC-*g*-brush in **Figure 8**a). With this method, polymer shells have been grown from the CNC surface that are permanently ionic,[78] respond to temperature[73,151] or pH[76] (or both),[152] or that are intrinsic hydrophobicity for compatibilization and processing with polymer matrices.[153] Such polymer-grafted CNCs were then utilized in diverse applications. For instance, poly(*tert*-butyl methacrylate)s have been polymerized using SI-ATRP giving access to well-controlled polyacrylic acid (PAA) brushes as visualized in TEM and AFM.[76] Polycationic CNC-*g*-poly(4-vinylpyridine) brushers were reported as flocculants with reversible precipitation/redispersion

capabilities.[154] Upon changing the pH, the polarity of the polymer brush changes from a protonated hydrophilic to deprotonated hydrophobic state. Since the polymer brush is covalently grafted to the CNC, the pH responsive behavior is thereby transferred from the polymer to the CNC as well, and both precipitate at high pH values. Other polycationic brushes such as poly(*N*-(2-aminoethylmethacrylamide) and poly(2-aminoethylmethacrylate) have been investigated for their cytotoxicity in mouse cells and human breast cancer cells.[155] In this regard, pH- and thermo-responsive poly[2-(dimethylamino)ethyl methacrylate] (PDMAEMA) brushes were also grafted from CNCs and studied for their ability to complex genes for enhanced gene transfection.[152] The dual responsiveness of CNC-*g*-PDMAEMA and other polymers has further been used to tune the stabilizing effect of colloidal surfactants in Pickering emulsions.[156,157] Colloidal particles are particularly effective to stabilize interfaces and polymer-grafted CNCs may find application as emulsifiers in emulsion polymerization or as compatibilizers in polymer blends.[158–161] Also more advanced copolymer brushes have been presented with host guest functionalities[55] and supramolecular bonding motifs[77] in order to generate sophisticated fracture behavior, which will be discussed in more detail in Chapter 3.2.

Polymer-brushes around CNCs can also be utilized for a tunable and dense set of interaction sites to direct self-assemblies. For instance, interpolyelectrolyte complexation[162,163] of diblock copolymers involving a polycationic block and a nonionic polyethylene glycol block leads to self-assemblies directed on the CNC surface decorated with well-controlled PAA brushes in aqueous dispersion.[79] More precisely, Figure 8b illustrates that using a diblock copolymer poly[2-(methacryloyloxy)-ethyl trimethylammoniumiodide]-*block*-poly(ethylene oxide) and PAA-brushes with a length of 870 repeat units, lamellar morphologies are observed around the CNCs. The alternating lamellae consist of the interpolyelectrolyte complex and the nonionic PEG blocks. Curiously, however, the lamellae seem to twist to form helically winding lamellae instead of lamellar

disks. This is logical, as packing frustrations can be relieved by winding the separate disks to helical arrangements. Interestingly, using slightly shorter PAA brushes, and consequently smaller amount of the block copolymer upon complete charge neutralization, cylindrical self-assemblies are observed on CNCs. This is in accordance with the classic diblock copolymer concepts where the relative volume fractions of the repulsive units drive to the self-assemblies.

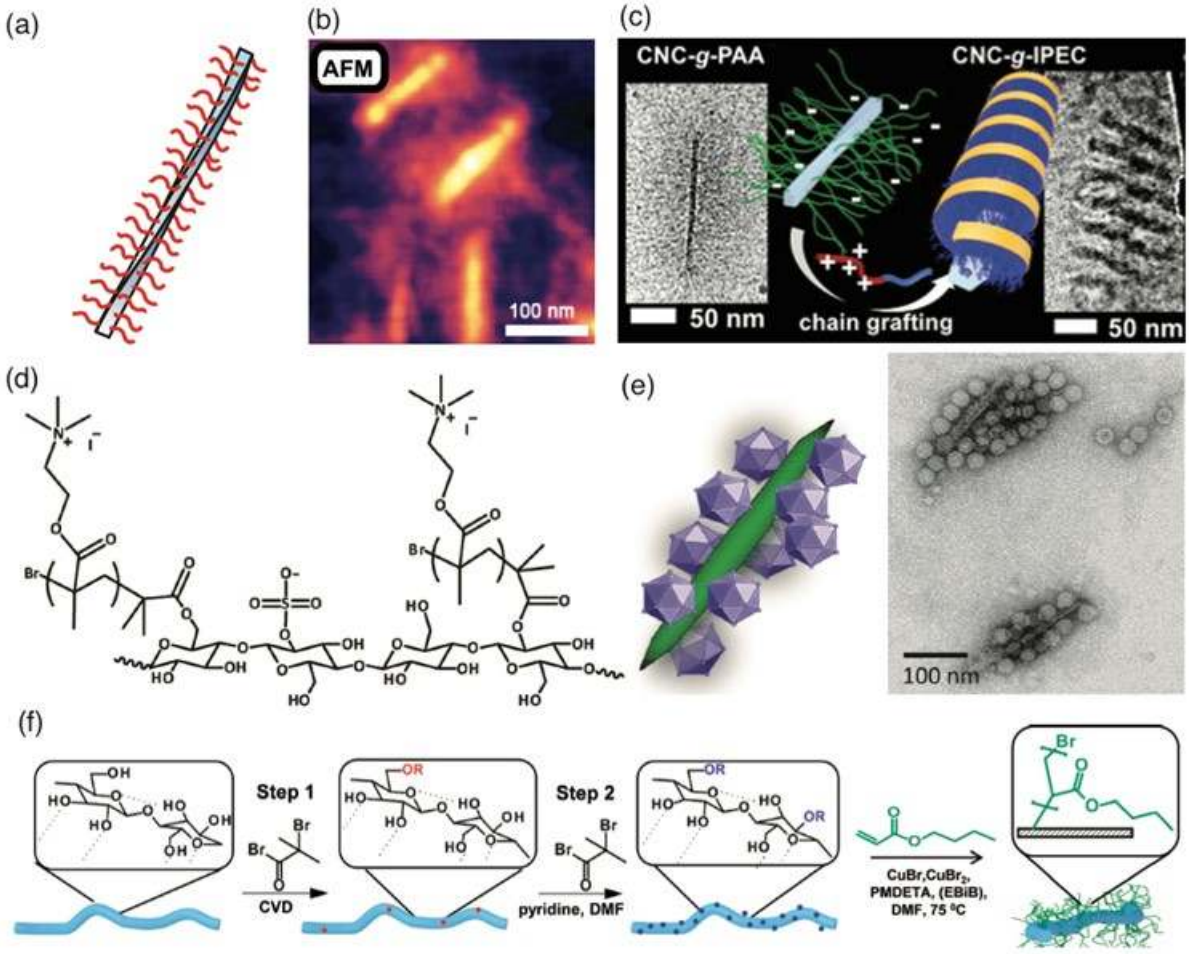

Figure 8. Nanocellulose-directed self-assemblies. a) Scheme for a CNC-based brushes for a high density of supramolecular binding sites along the colloidal rod. b) Polyacrylic acid brush modified CNC, as resolved using AFM. Reproduced with permission.[76] Copyright 2011, American Chemical Society. c) Poly(acrylic acid)-decorated CNC-brushes direct self-assembly of nanostructures on CNCs in aqueous media, upon interpolyelectrolyte complexation of cationic-nonionic diblock copolymers. Reproduced with permission.[79] Copyright 2016, American Chemical Society. d) Chemical structure of cationic CNC-*g*-PQDMAEMA. e) The cationic CNC-*g*-PQDMAEMA electrostatically bind to negatively charged viruses, like cowpea chlorotic mottle virus (CCMV), as shown by a TEM micrograph. Reproduced with permission.[78] Copyright 2014, Royal Society of Chemistry. f) Two-step surface modification of CNF followed by SI-ATRP of hydrophobic poly(*n*-

butylacrylate) (P*n*BA). Reproduced with permission.[75] Copyright 2011, American Chemical Society.

In an example of colloidal level ionic complexation, cationic CNCs were first synthesized by modifying the intrinsically negative CNC surface with cationic poly[2-(dimethylamino)ethyl methacrylate] (CNC-*g*-PDMAEMA) to form polymer brushes via SI-ATRP to study CNC-virus particle interaction (Figure 8d).[78] The polymer brushes were quaternized using methyl iodide leading to CNC-*g*-PQDMAEMA with permanent positive charges along the nanocrystal surface. By adjusting the electrolyte concentration, cowpea chlorotic mottle virus (CCMV) and norovirus-like particles (NoV-VLPs) bind efficiently to produce micron-sized superstructures allowing easy separation (Figure 8e).[78] This suggests a toolbox for concentration of viruses and other anionic materials in biomedical analysis.

The surface modification of colloidal CNCs is well established by now. The situation is different for CNFs, where only few protocols exist. The fundamentally different physical characteristics of long entangled fibers and partially disordered CNFs as compared to well-separated freely diffusing fully crystalline CNCs plays a crucial role in purification (e.g. from trace water), redispersion, and accessibility to the surface.[164] One way for successful surface modification by polymerization is a combination of TEMPO-oxidation[18] to generate carboxylic groups followed by modification with an ATRP initiator and subsequent polymerization of polystyrene.[165] The dual-modified CNFs were then used as advanced filtering materials that bind metal pollutants (e.g. Cu^{2+}).

One of the main aims of cellulose modification is to aim for components that could partially replace petroleum-based synthetic polymers in disposable consumer goods, first and foremost packaging (e.g., plastic shopping bags). Currently it is challenging to create waterproof materials purely made from hydrophilic nanocellulose. Proper surface modification with hydrophobic polymers would enhance compatibility of cellulose with hydrophobic matrices to form stable fiber-reinforced nanocomposites. In recent works, the

peculiarities of CNF surface modification for SI-ATRP were overcome by either esterification of 2-bromoisobutyryl bromide in 1 wt.-% CNF gels in DMSO[166] or by using an excess of initiator in dilute DMSO dispersions.[75] In the latter case, a successful surface modification of CNF was demonstrated by carefully adjusting excess of surface initiator and the overall reaction volume. Thereby, two largely different grafting densities were achieved, whereas a high grafting density gave first evidence of degradation processes resulting in small CNF fragments. Potentially, attachment of an ATRP initiator preferentially occurs in the disordered domains of the CNFs that might be more available for reagents for chemical modification (as compared to fully crystalline domains). Subsequent grafting of polymer chains may cause swelling of the amorphous domains during brush growth in turn destabilizing the CNF backbone followed by CNF degradation into small fragments. This suggested that preferential modification of amorphous domains might have implications for a wide range of surface modifications strategies.

2.7 Atomic layer deposition on nanocelluloses

Atomic layer deposition (ALD) has become one of the indispensable approaches towards precisely controlled oxide layers in industry, especially in electronics.[167] Originally invented in Finland,[168] the concept is based on sequential deposition of mutually chemically reacting chemical vapors. At each step, a monolayer coverage is pursued towards complete chemical conversion, followed by purging of the chemically unreacted reagents. Related to nanocelluloses, the natural platform is based on nanocellulose aerogels, which have amply been studied during recent years.[169–218] Their nanoscopic skeletons are functionalized with different inorganic oxides, such as Al_2O_3, ZnO, or TiO_2, see **Figure 9**.[178,179,219,220] They provide different functionalities, to be discussed later, ranging from mechanically strengthened coatings to semiconductors, switchable adsorption, selective organic spill

recovery, and optically active coatings. After the ALD-coatings, the templated CNF can be degraded, leading to aerogels of hollow inorganic nanotubes, Figure 9.[179]

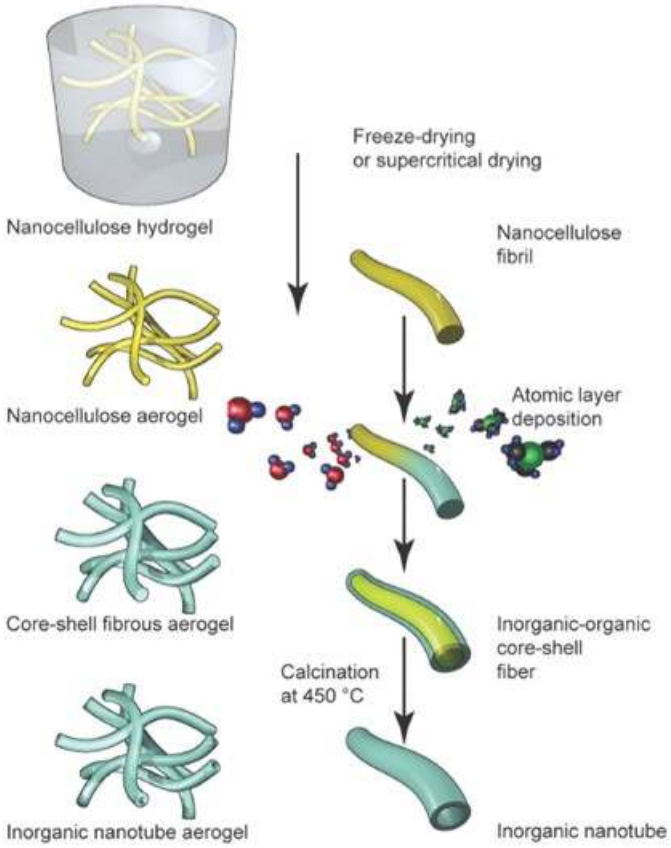

Figure 9. Atomic layer deposition (ALD) allows well defined oxide layers on CNF aerogels and optionally a concept for hollow tube aerogels by thermally degrading the CNF template. Reproduced with permission.[179] Copyright 2011, American Chemical Society.

2.8 Fibers

2.8.1 Electrospun fibers

Nonwoven mats formed by ultra-thin fibers with diameters in the micron and nano-scales have considerable high surface area-to-volume ratio, superior mechanical properties and they are very versatile in terms of surface functionality. The electrospinning technique[221,222] has opened several opportunities for the manufacture of these materials from nanocellulose, which are finding applications in the fields of medicine, pharmacy, tissue engineering and nanocomposites. Highly competitive compared to typical inorganic fillers such as carbon nanotubes, hydroxyapatite, gold, silver, clay, or silica, nanocelluloses are

strong and resistant to wear and erosion. Their aspect ratio strongly influences the structuring and thus the properties of their composite systems. A key issue in order to gain the benefits of the extraordinary properties of nanocelluloses in nanocomposites is to gain control of the alignment and distribution of nanocellulose within the matrix. This aspect is usually a challenge since nanocelluloses tend to agglomerate in non-polar matrices, thus, leading to low interfacial compatibility between the phases and poor mechanical properties. Many efforts have been devoted to mimic bio-composites by blending nanocelluloses from different sources with polymer matrices such as polyamides, polyesters, polyurethanes, polypeptides, and polysaccharides. In the case of incorporation of hydrophilic nanocelluloses to non-polar matrices, several surface chemical modification techniques have been applied. Here, CNCs have been used to reinforce electrospun fibers produced upon application of electrostatic fields to the respective viscoelastic suspension. Under the effect of electric fields, free charges are generated in the solution, which respond to the electrical potential by migrating from the tip of the capillary to the collector, in opposite polarity direction. With increasing intensity of the electrical field the drop stretches forming a Taylor cone. At a critical applied voltage value, composite mats of micro- or nano-fibers are formed. In this way, composite microfibers from polystyrene and CNCs were produced by electrospinning.[223] Surface porosity, unique ribbon-shapes, and the presence of twists along the fiber axis were observed in such composite microfibers. The reinforcing effect of CNCs was confirmed as the glassy modulus of electrospun microfibers increased with CNC load. Similar results have been observed for biodegradable poly(ε-caprolactone) (PCL)[224] as well as hydrophilic matrices, such as polyvinyl alcohol (PVA)[225] (**Figure 10**a). In the latter case, it was interesting to observe the stabilizing effect of the CNCs in the matrix, which could be otherwise compromised by water absorption, disrupting the hydrogen bonding within the structure. As they were conditioned from low (10% RH) to high relative humidity (70% RH), the reduction in tensile strength of neat polyvinyl alcohol (PVA) fiber mats was found to be about 80%,

from 1.5 to 0.4 MPa. When the structure was reinforced with CNCs, the reduction in strength was minimized drastically. More importantly, the CNC-loaded PVA fiber mats showed a reversible recovery in mechanical strength after cycling the relative humidity and induced significant enhancement of their strength as a result of the adhesion between the continuous matrix and the CNCs.[226] Additionally, all-cellulose composite fibers were produced by electrospinning dispersions containing cellulose acetate (CA) and CNCs. The obtained fibers had typical widths in the nano- and micro-scale and presented a glass transition temperature of 145 °C. The CA component was converted to cellulose by using alkaline hydrolysis to yield all-cellulose composite fibers that preserved the original morphology of the precursor system. Noticeable changes in the thermal, surface and chemical properties were observed upon deacetylation. Not only the thermal transitions of cellulose acetate disappeared but the initial water contact angle of the web was reduced drastically.[227] Finally, lignin-based fibers were produced by electrospinning aqueous dispersions of lignin, PVA and CNCs[228–230] (see Figure 10b). Defect-free nanofibers with up to 90 wt % lignin and 15% CNCs were achieved. The thermal stability of the system was observed to increase with the addition of CNCs owing to a strong interaction of the lignin−PVA matrix with the dispersed CNCs, mainly via hydrogen bonding.[228] Importantly, the size of the phase separated (lignin-PVA) domains was reduced by the addition of CNCs. Here, the importance of molecular interactions and phase separation on the surface properties of fibers from lignin and CNCs for the fabrication of new functional materials can be highlighted.

2.8.2 Filaments from wet and dry spinning of nanocelluloses

Spinning of nanocelluloses offers the opportunity to produce a renewable filament without the need for cellulose dissolution and regeneration.[64,193,231–239] Provided that the energy consumption is limited during CNF preparation, the absence of dissolution chemicals signifies a reduced environmental impact. Current results suggest that nanocellulose-based

filaments with competitive mechanical performance can be produced. Different approaches have been recently reviewed for wet and modifiable (Figure 10c), dry, as well as melt and electrospun CNFs and CNF-polymer combinations.[240,241] CNFs isolated from both softwoods[193,236,242] and hardwoods[64,243,244] have been used to produce filaments by spinning. CNFs from banana rachis have been dry-spun into filaments with remarkable mechanical properties (Young's modulus up to 12.6 GPa and tensile strength up to 222 MPa) that are comparable to those of cotton fibers.[245] Filaments wet-spun from dopes of tunicate-derived CNF hydrogels were produced by taking advantage of the higher aspect ratio, which results in higher toughness as compared to those of wood-derived nanocelluloses. Filaments from the former displayed a more regular, circular cross-section and grooved surfaces.[233] Apparently, the extension of the long, entangled fibrils dissipates energy efficiently. Furthermore, the high degree of crystallinity of tunicate CNF can also positively contribute to the mechanical performance. TEMPO-oxidation and carboxymethylation of nanocellullose affects its spinnabilty and filament properties. TEMPO-oxidation was found to enhance fibril orientation during wet-spinning because of the elevated fibril aspect ratio and surface charge, which causes both entanglement and osmotic repulsion between the fibrils.[232,243]

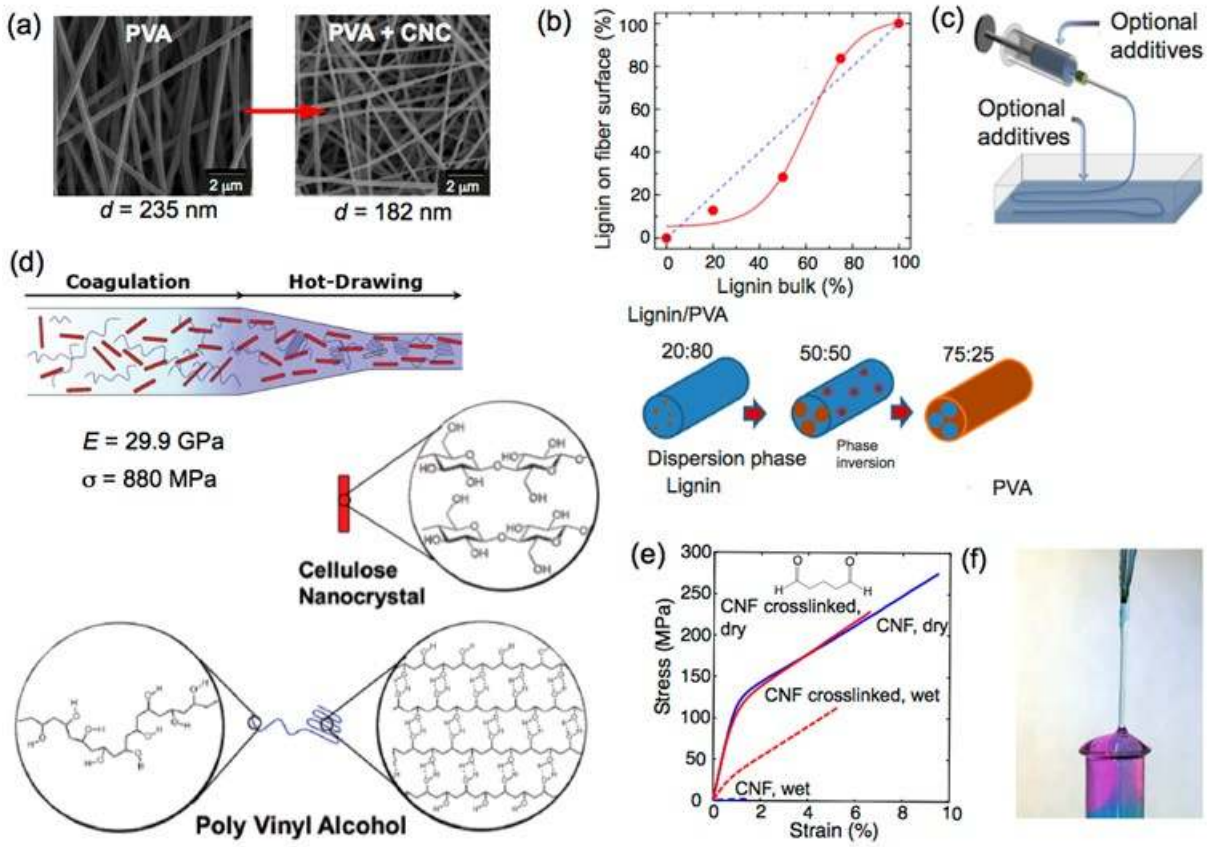

Figure 10. Fibers based on nanocelluloses. a) Composite electrospun PVA fibers in the absence (left) or in the presence of reinforcing CNC (right).[225] Reproduced with permission. Copyright 2010, American Chemical Society. b) CNC-reinforced lignin electrospun hybrid fibers. Reproduced with permission.[230] Copyright 2013, American Chemical Society. c) CNF can be spun by injecting the CNF aqueous dope in a coagulant. Reproduced with permission.[232,243] Copyright 2011, Wiley-VCH and reproduced under the terms of the CC-BY-X license 2016, Nature Group. d) Nanocomposite CNC/polyvinyl alcohol fibers with high strength fibers reaching strength of 880 MPa. Reproduced with permission.[246] reproduced under the terms of the CC-BY-X license Copyright 2016, American Chemical Society. e) Glutaraldehyde promotes wet strength for CNF fibers for surgery threads. The threads support stem cell growth for improved wound healing. Reproduced with permission.[64] Copyright 2016, Elsevier. f) Interfacial polyelectrolyte complex spinning render multicomponent CNF fibers that allow crimping. Reproduced with permission.[247] Copyright 2017, American Chemical Society.

To summarize, filaments spun from nanocellulose have shown promising mechanical properties, depending on the aspect ratio of the materials, charge and other factors not discussed here for brevity. They include processing variables such as solids content in the dope, shear rate in the spinneret, addition of drawing and the coagulation and drying conditions. The option of adding additives, co-adjutants and chemicals for crosslinking is worth mentioning. The most recent results in this respect include the use of polyvinyl alcohol

to spin CNC-loaded fibers, which yielded a remarkable high strength (880 MPa) (Figure 10d).[246] Moreover, crosslinking with glutaraldehyde promoted sufficient wet strength for CNF fibers to generate surgery threads or to support stem cell growth for improved wound healing (Figure 10e).[64] Finally, interfacial polyelectrolyte complex spinning with chitosan toward multicomponent CNF fibers has been demonstrated, producing fibers that can allow crimping (Figure 10f).[247,248]

Nanocelluloses can also be put in the perspective of polymeric fibers. Cellulose fibers can be spun by dissolution and regeneration, in which case the native crystal structure is not recovered.[249–251] The technology of such fibers is well-developed and the resulting fibers have very good properties, showing strengths of even up to ca. 1.7 GPa. However, they typically require aggressive solvents and processes, and there have been considerable efforts to find more benign alternatives. Ionic liquids have recently been extensively pursued as "green solvents" with suppressed emission, taken that the solvent can be re-circulated. Such fibers render tensile strength ca. 0.9 GPa.[252] The fibers spun from CNF from aqueous solvent have so far had relatively modest properties in relation to the regenerated cellulose fibers, reaching typically strengths of 0.3-0.6 GPa.[232,233,236,242,253] A probable reason is that so far, the processes have not allowed sufficient alignment of the colloidal CNF fibrils. Various processes have been suggested and explored (discussed in Chapter 2.8). Note that even if it is often claimed that CNFs with their nanometric lateral dimension and micrometer length have a high aspect ratio, it is, in fact, only a few hundreds, at maximum. Such a value is not high in comparison to some polymers used for high strength fibers, such as that of ultrahigh molecular weight polyethylene (UHMWPE) allowing gel spinning.[254] Such diameters enable the long polymers to undergo gelation and a sufficient number of entanglements leads to stretching and alignment of the chains. By contrast, even if the CNFs form gels, they are not similarly entangled due to the fibrillary rigidity and the physics of spinning would be different from that of UHMWPE. Finally, a comparison can also be made to solution spinning of rigid

rod liquid crystalline aromatic or heteroaromatic polymers.[255] Therein, solution spinning and post-drawing result in fibers with very high mechanical properties where the strength can be even several GPa. Moreover, related to such fibers, the so far performance of CNF spun fibers remains poor. We finally point out a similarity between CNF colloidal fibrils and the above-mentioned rigid rod polymers, as neither of them melts due to rigidity. However, in both cases fusible materials can be obtained by furnishing side chains to make a comb-shape or bottle-brush architecture. In conclusion, the mechanical properties achieved so far for nanocelluloses are very modest in comparison to the state of the art of the best spun fibers. Therefore, new concepts have still to be developed to align the nanocellulose colloidal fibers. On the other hand, in some applications the present lower mechanical properties may suffice, taken that the facile functionalizability of nanocelluloses allows design benefits over the more classic fibers.

3. Functional materials based on nanocelluloses

Here we review some approaches towards functional advanced material based on nanocelluloses. For compactness, we emphasize emerging fields while leaving out cases of specific applications, such as classic composites, layer-by-layer deposition, and drug release, where good reviews can already be found.[9]

3.1 Advanced hydrogels

Nanocelluloses have been used to create a wealth of hydrogels types.[13,14,41–68] The simplest case is offered by pristine CNFs, which spontaneously form hydrogels, probably promoted by their length and interacting entanglements. Naturally, different physical and chemical interactions can be used to crosslink nanocelluloses. Nontrivial combinations of properties of hydrogels can be obtained when specific supramolecular cross-linking motifs are used. Cucurbiturils (CBs)[256] are ring-like units that can host different guests depending on the number of its repeat units. In particular, CB[8] (**Figure 11**a), consisting of 8 repeat units, can host two guests, the primary guest (here viologen) and the secondary guest (here

naphthyl). Characteristic for such bonding is that the bond exchange rate is very high, and that the bonding is selective due to the three participant units. This supramolecular bonding motif can be exploited to self-assemble CNC-reinforced hybrid hydrogels (Figure 11b).[55] For this, CNCs with poly(methyl methacrylate) brushes were synthesized, incorporating a fraction of repeat units containing naphthyl pendant groups. Correspondingly, polyvinyl alcohol polymer with methyl viologen decorations was synthesized. By mixing them with CB[8] molecules, approximately fulfilling the stoichiometric relation between CB[8], naphthyls, and methylviologens, hydrogels are formed. Due to the reinforcement by CNCs, high stiffness is achieved with the storage modulus > 10 kPa. On the other hand, due to the rapid exchange rate of CB[8] driven host-guest interactions, rapid reversible sol-gel transition in a few seconds is inferred. And due to the selectivity of the CB[8] supramolecular bonding motif, the gel self-heals quickly without being passivated even after one year of storage time.

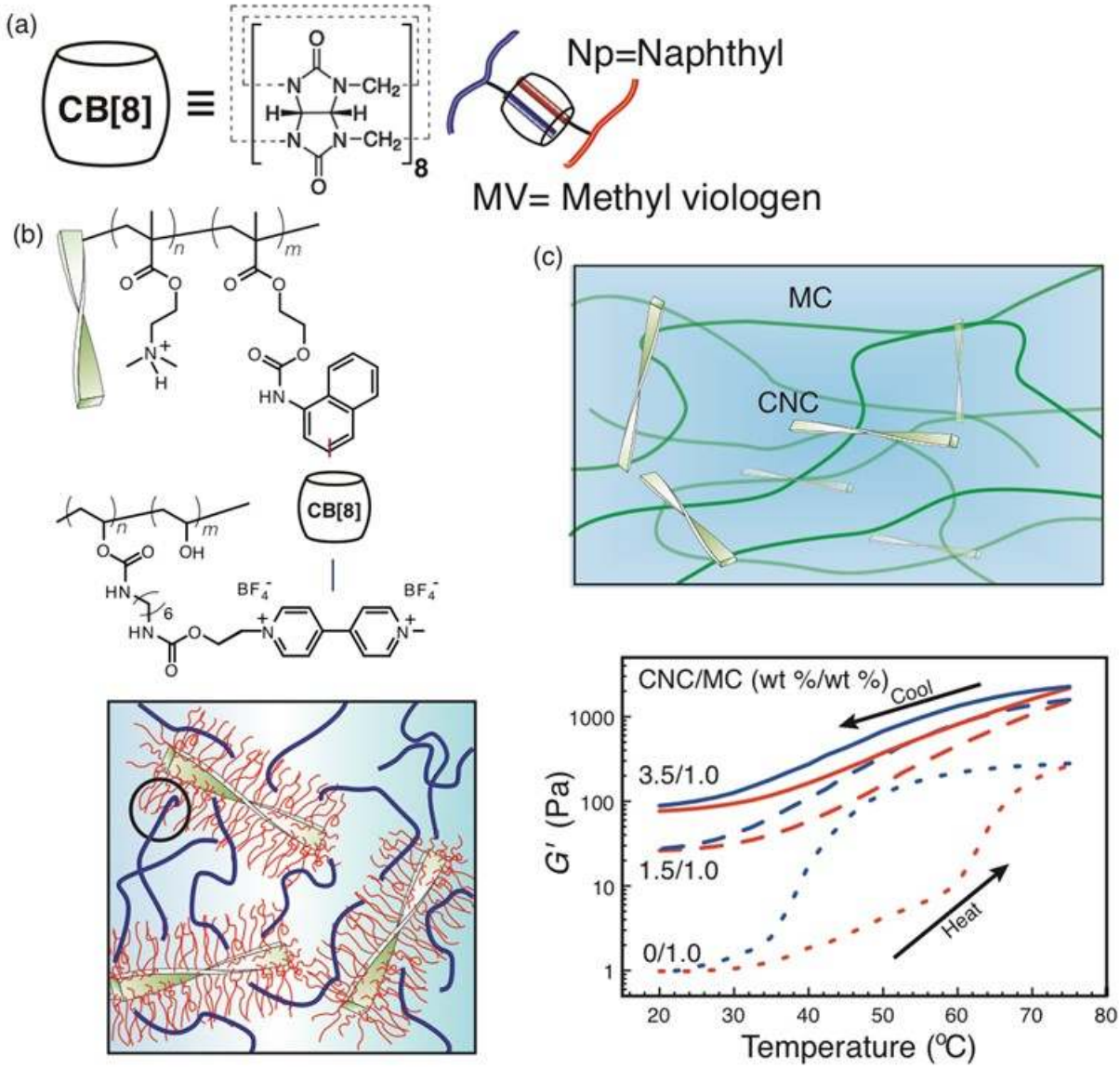

Figure 11. CNC-reinforced hybrid hydrogels. a) Cucurbit[8]uril shows relatively strong simultaneous binding of methyl viologens and naphthyl groups, still sustaining rapid exchanges, generating a stiff hydrogel of naphthyl modified CNC and viologen modified polyvinyl alcohol. Reproduced with permission.[55] Copyright 2014, Wiley-VCH. c) Methyl cellulose gel reinforced with CNC allows reversibly increased gel stiffness upon heating. Reproduced with permission.[53] Copyright 2014, American Chemical Society.

Another example deals with methyl cellulose/CNC hybrid hydrogels (Figure 11c).[53] The pristine water soluble methyl cellulose (MC) is known to undergo gelation upon heating.[257] The CNC reinforces the gel thereby creating widely tunable and thermoresponsive dispersions and hydrogels. This can be interesting for biological scaffolding as both components are biocompatible.

3.2 Biomimetic composites

Nature offers fascinating examples for structural materials that combine stiffness, strength, and toughness, which are typically considered to be conflicting properties.[258] Classic examples include pearl of nacre, bone, antler, silk, and insect exoskeletons.[259–263] Such materials are also light-weight and consist solely of sustainable components.[264,265] Therefore, combination of all of these properties have raised considerable interest among materials scientists toward future post-oil sustainable, non-metallic, and mechanically excellent materials.[266] Such natural structural materials are typically, however, expensive to grow and they lack scalability. This has encouraged efforts for biomimetic composites, trying to learn the essential features of biological materials, but using technically more viable components and processes.[267,268] The biological structural materials are characteristically self-assembled composite materials, with a high volume fraction of reinforcing domains (often aligned to promote stiffness), combined with a low volume fraction matrix that dissipates fracture energy (to promote toughness).[269–272] In more detail, the latter domains involve reversible physical bonds (sacrificial bonds) and hidden lengths to dissipate fracture energy, thus providing toughness.[273] In addition, the typically intrinsic hierarchical architecture of biocomposites offer a number of mechanics that work against crack initiation, crack propagation, and catastrophic failure of the material.[274–276] In biomimetic composites, some or all of these concepts are mimicked.[277]

Probably the most well-known biological composite is the pearl of nacre,[278,279] which is composed of ca. 95 w-% of 400 nm stacked and aligned $CaCO_3$ plates, as bonded by proteins,[280] able to dissipate fracture energy. Nacre has offered models for several types of biomimetic composites with aligned sheet-like inorganic reinforcement within fracture energy dissipating medium.[281–283] A particular difficulty therein is to reach defect-free space-filling of the platelets with no stacking defects without the need of the slow in-situ biomineralization.[284] Several approaches have been presented to approach the structural

features and mechanical properties of nacre.[285–288] Thereby the so-called freeze casting or ice-templating has not only created structural materials with exceptional mechanical properties,[289–291] but very recently also replicated the structural and chemical composition or real nacre.[292] Evaporation-induced self-assembly is another process that has rendered films containing a high volume fraction of nanoclays where the lateral packing defects are minimized by the flexibility of the 1 nm thick nanosheets, separated by thin polymer layers.[293,294] Subsequent lamination of such films allow bulk materials with flexural strength of 220 MPa, bending modulus of 25 GPa, and K_{IC} = 3.4 MPa $m^{1/2}$, i.e., the fracture properties approaching that of real red abalone nacre (**Figure 12**a,b).[295] Such materials are additionally property fireproof, i.e. intumescent.[217,294,296–298] A closer look at nacre reveals that the soft matrix consists of nanofibrillar chitosan as well as bifunctional proteins, binding on chitosan on one and $CaCO_3$ on the other hand.[299,300] Therefore, oversimplified biomimetic composites were foreseen by combining essentially neutral CNF and 2D components including talc,[301] graphene,[302] graphene oxide[303] and clays (Figure 12b).[296] In this case, the interaction can be tuned to be quite small, suggesting sacrificial bonds in deformations. Fascinating mechanical properties are indeed achieved. On the other hand, if cationic CNFs and anionic nanoclays are combined, aggregated and nonaligned structures are expected (Figure 12c).[304] But such structures show clear yielding under compression of a 3D specimen. One could ask whether the replacement of clay nanosheets with intrinsically stronger nanosheets would be beneficial for biomimetic composites. Therein, graphene is a natural selection. Interestingly, CNF allows to cleave graphene sheets from KISH graphite (Figure 12d).[305] But perhaps a better mimic of nacre can be obtained by a concept where the aragonite sheets, the chitosan nanofibrillar skeleton, and the protein mediating their mutual interactions are replaced by graphene, CNF, and a difunctional synthetic protein involving graphene binding domains and cellulose binding domains (Figure 12e).[83] Such materials reach the strength of 300 MPa. The

conceptual difference, though, is that the reinforcing graphene concentration is just 1% in contrast to the 95% in nacre.

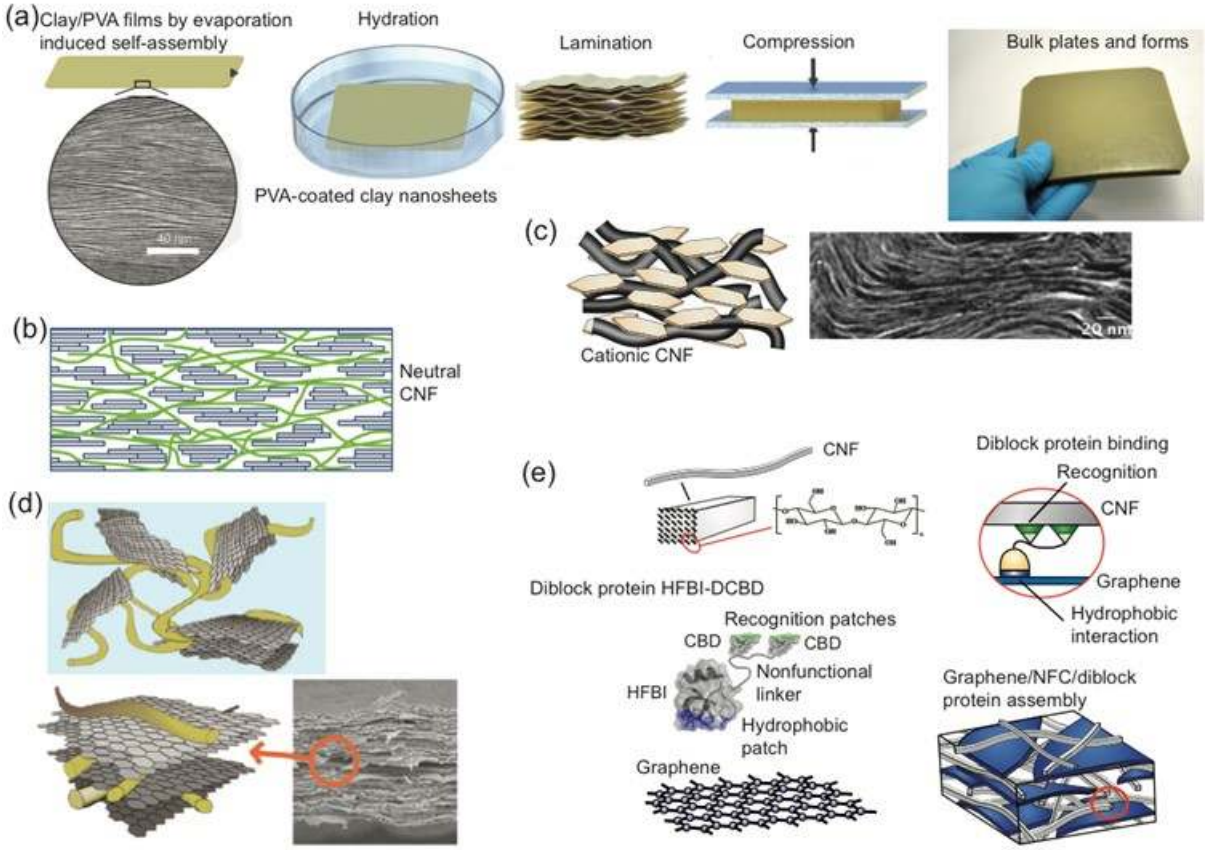

Figure 12. Biomimetic nanocomposites by colloidal self-assembly. a) Biomimetic nanocomposite by evaporation-induced self-assembly of nanoclay and polyvinyl alcohol to films. Subsequent lamination produces thick bulk samples enabling the characterization of fracture toughness in 3-point bending. Reproduced with permission.[295] Copyright 2017, Wiley-VCH. b) Scheme for CNF/nanoclay biomimetic nanocomposite films with high tensile mechanical properties and fireproof properties. Reproduced with permission.[296] Copyright 2011, American Chemical Society. c) Oppositely charged CNFs and nanoclays assemble into tough composites in compression. Reproduced with permission.[304] Copyright 2013, Royal Society of Chemistry. d) CNFs exfoliating graphene. Reproduced with permission.[305] Copyright 2012, American Chemical Society. e) Biomimetic nanocomposites based on graphene and CNFs, as bound together by bifunctional proteins, thus mimicking the protein bonding motifs in nacre between the aragonite and chitin nanofibers. Reproduced with permission.[83] Copyright 2011, Wiley-VCH.

Toughening of biological composites is a complex phenomenon, where sacrificial supramolecular bonds trap loopings, i.e. hidden lengths of macromolecules, connecting structural units and reinforcements.[273] Thus upon deformations, the sacrificial bonds open, revealing the hidden lengths, whereupon the stress values become stepwise reduced.[306] The phenomena also depend on the deformation rate, and thus completely mimicking biological

toughening is a grand challenge. In an oversimplified approach, one could use the classic entropic coiling of polymers to mimic hidden lengths in combination with supramolecular bonds to mimic sacrificial bonds. Therein the supramolecular bond strength and reversibility should play an important role. In the colloidal nanocellulose systems, biomimetic toughening is intensely studied[307] but not understood in its entirety. As CNFs are relatively long, their potential entanglements may hamper their structural relaxations in deformation. In a potentially simpler approach, rod-like CNCs were used as reinforcements, as decorated by poly(*n*-butyl methacrylate-*rnd*-methyl methacrylate) brushes.[77] Due to their high length 357 kg/mol, there should be coiling at the periphery. Such brush-decorated CNCs behave totally elastically in tensile tests, leading to brittle fracture, i.e. no fracture energy dissipation was observed. By contrast, upon adding a small fraction of supramolecular units, pronounced yielding was observed, the catastrophic propagation of cracks was suppressed, and energy dissipating voids were observed (**Figure 13**a).[77] Mechanistic insight was suggested due to birefringence that was observed in polarized optical microscopy near the crack tips. This suggests that upon deformations, the CNCs slide past each other and become aligned leading to optical anisotropy, which indirectly suggests that the supramolecular bonds are reformed, working as sacrificial bonds.

As indicated by several studies, sliding of components facilitated by nanolubrication could contribute to toughness. The frictional forces and adhesion between pure CNF interfaces were determined by colloidal probe AFM and compared to values obtained for CNFs coated with soft lubricating polyethyleneglycol-grafted carboxymethyl cellulose (CMC-*g*-PEO) (Figure 13b)[308]. The CNF/CNF interface experiences considerable friction likely cause by entanglements of fibers and strong hydrogen bonding. Adding the nanolubricant significantly reduced that friction while maintaining good adhesion between interfaces. Based on these results, a nanocomposite was designed containing 99 wt.-% of reinforcing CNFs impregnated with only 1 wt.-% of CMC-*g*-PEO. The resulting

nanocomposite showed higher fracture strain and enhanced toughness promoted by a complex interplay of a considerable number of weak hydrogen bonds and reduced friction. Graphene is also used as a highly durable lubricant[309] and has also been used to enhance the mechanical properties of CNF materials. Here, CNFs and reduced graphene oxide were mixed with a 1:1 ratio of PAA and 1,6-hexanediol diglycidyl ether (Figure 13c)[310] and kept at 90 °C to induce esterification and reduce the volume into viscous suspensions. The suspensions were extruded *via* syringe into filaments and dried at 120 °C for 10 min. The produced fibers displayed enhanced moduli and strength provided by the reinforcing effect of the CNFs while maintaining a high fracture strain promoted by nanolubrication of the added reduced graphene oxide.

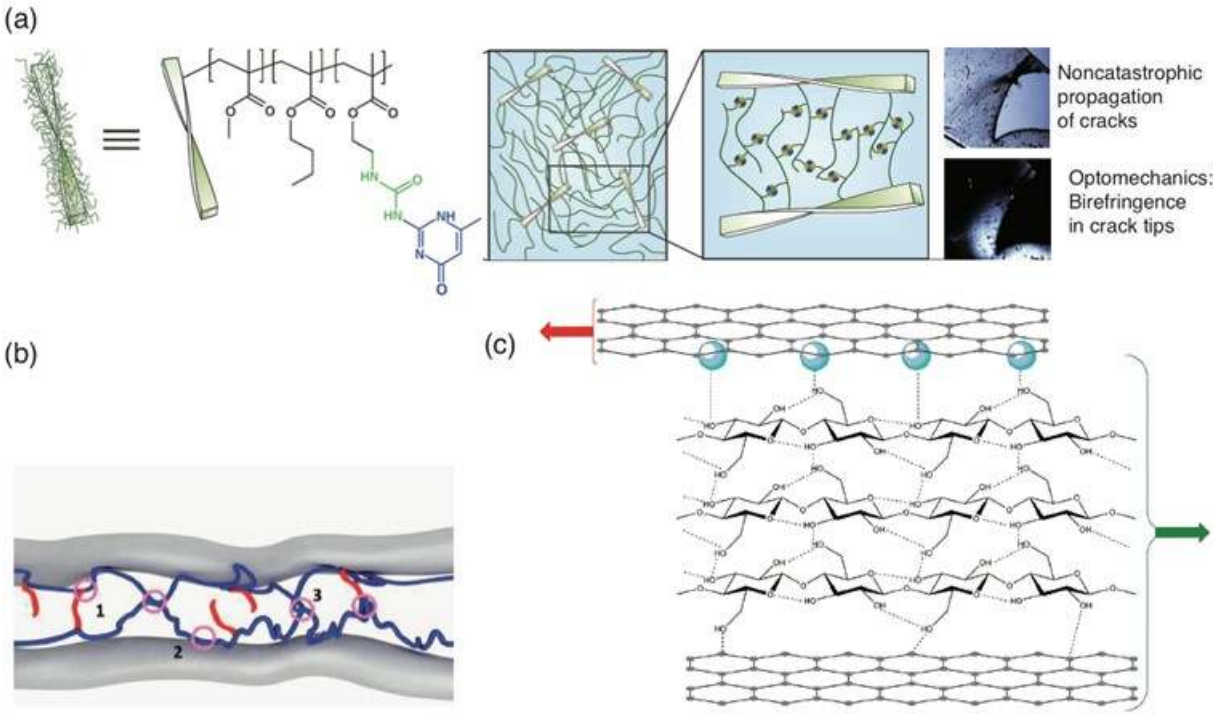

Figure 13. Synthetic sacrificial bond mimics. a) CNCs decorated with long acrylate brushes with a small fraction of UPy lead to suppressed catastrophic crack growth. Reproduced with permission.[77] Copyright 2014, Wiley-VCH. b) Suggested hydrogen bonds and van der Waals attraction between CNF and carboxymethyl cellulose-*graft*-polyethylene glycol hanhancing structural rearrangements in deformations. Reproduced with permission.[308] Copyright 2013, Royal Society of Chemistry. c) Poly(acrylic acid) crosslinked with 1,6-hexanediol diglycidyl ether, reinforced with CNF, and dispersed with reduced graphene oxide result in tough and high strain filaments. Reproduced with permission.[310] Copyright 2015, Royal Society of Chemistry.

3.3 Magnetic materials

Nanocelluloses can be functionalized to be magnetic by equipping them with magnetic nanoparticles. **Figure 14**a describes bacterial cellulose aerogels which have been decorated with cobalt ferrite nanoparticles[175] This leads to porous magnetic materials, which interestingly are also flexible and thus can be actuated by magnetic fields. In addition, they can absorb water, and release it again upon compression, thus suggesting a platform for multifunctional materials. Similar cobalt ferrite nanoparticles can be loaded into CNF fibers, which have been extruded in a coagulation bath.[232] CNCs can also be decorated with cobalt iron oxide nanoparticles leading to magnetically responsive aqueous dispersions films and composite fibers.[311] The hybrid material shows saturation magnetization of ca. 20 emu g^{-1} and allows magnetic manipulation using small fields (Figure 14b, c). The magnetically functionalized CNCs open possibilities to magnetically driven protein purification taken the CNC are additionally decorated with protein binding sites (Figure 14d).

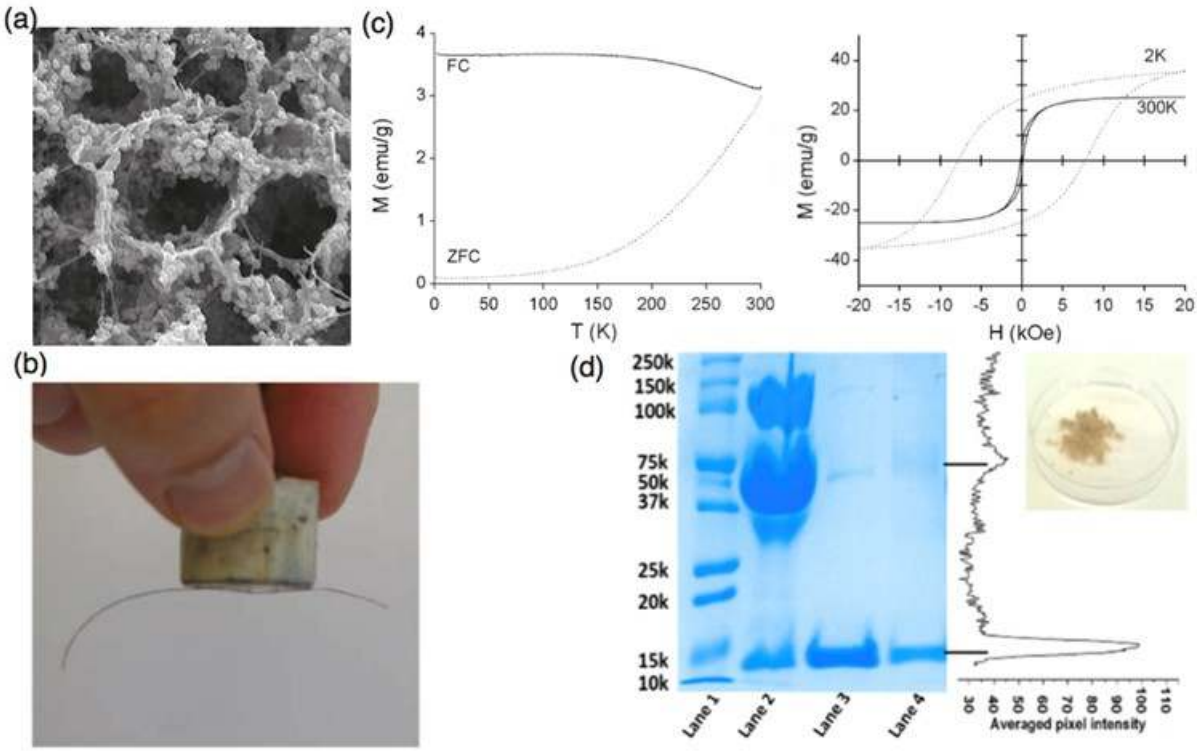

Figure 14. Magnetic materials based on nanocelluloses. a) SEM micrographs of a flexible bacterial cellulose aerogel decorated with cobalt ferrite nanoparticles, allowing magnetic actuation. Reproduced with permission.[175] Copyright 2010, Nature Publishing Group. b)

Cobalt ferrite nanoparticle render magnetic CNF threads. Reproduced with permission.[232] Copyright 2011, Wiley-VCH. c) Magnetic behavior of CNCs decorated with cobalt iron oxide nanoparticles. Reproduced with permission.[311] Copyright 2014, Springer. d) Magnetic nanoparticle-decorated CNCs facilitates protein purification, as shown based on lysozyme separation from egg white. Reproduced with permission.[312] Copyright 2017, American Chemical Society.

3.4 Electrically conducting materials

Electrical functionalization of nanocelluloses can be accomplished in several ways by dispersing electrically conducting components. In typical multicomponent materials, electrical percolation of the conducting component is pursued. In gels and aerogels, the mechanical percolation is inherent, and can lead to electrical percolation at low volume fraction due to double percolation. Therefore, it becomes particularly interesting to strive to embed an electrically conducting component to e.g. an aerogel skeleton. Electrical conductivity was shown using CNF aerogels,[171] which were dipped in polyaniline-dodecylbenzene sulphonate solution in toluene to coat the aerogel skeleton with a layer of conjugated polymer. This led to conducting aerogels with a very low geometric volume fraction of conjugated polymer due to the low density of the aerogels. Polyaniline can also be polymerized directly on TEMPO-oxidized CNF templates, catalyzed by laccase, thus leading to prepare electrically conducting films.[313] Higher conductivity values in polyaniline films were obtained using oxidative polymerization of aniline using ammonium persulfate in the presence of aqueous dispersed CNF (**Figure 15a**).[314] This leads to relatively high conductivity 1.8 S/cm for 80 wt% polyaniline loading and still moderate conductivity 2.9 x 10^{-5} S/cm at the 5 wt% loading, where the mechanical properties are essentially the same as for the pristine CNF. Reduced graphene oxide offers interaction sites that are compatible with CNFs. Subsequent chemical reduction transfers graphene into the conducting state. Figure 15b displays the electrical percolation of reduced graphene oxide within a CNF host.[315] Reasonably high conductivity of 0.1 S/cm is achieved using loading of 10 % of graphene oxide. Larger conductivity of 3 S/cm in films is achieved by mixing 10 % ultrasonically dispersed single wall CNTs in CNF whereas in spun

fibers high conductivity of 207 S/cm is achieved at CNT loading 43 %.[193] Also silver nanowires within CNF nanopaper are useful, resulting in high conductivity of ca. 500 S/cm allowing also transparency of 86 %.[316] There are considerable efforts to replace the brittle indium tin oxide (ITO) by non-brittle materials for flexible devices. Figure 15c shows an approach using CNF and aerosol processed carbon nanotubes (CNT). Inspired by related approaches for silica gels, first a sequential solvent exchange is performed for a CNF hydrogel from water to octanol,[317] followed by the organic solvent evaporation into transparent aerogels.[216] Such porous aerogels are strong in tension (tensile strength 100 MPa), while still flexible in bending, and their porosity allows aerosol deposition of carbon nanotubes. This leads to highly transparent and conducting films, where the properties compete favorably with those of indium tin oxide, but are in addition flexible with high tensile strength. Finally, Figure 15d deals with hybrid aerogels, consisting of CNF and CNT both of which are 1D nanoscale components. The composite aerogel exhibits pressure dependent resistance, obviously as under compression the CNTs achieve an improved percolation.[187] The materials show stable mechanical and electrical properties under repeated cycles.[318] One could foresee applications in pressure sensing.

On a more general note, electrically conducting aerogels and foams have been extensively pursued during the recent years using different carbon allotropes, especially graphene and carbon nanotubes.[319–324] They can have remarkable properties. For example, pure graphene aerogels show relatively high conductivity up to ca. 50 S/cm, which easily outperforms the available conductivities of nanocellulose-based hybrid aerogels. However, we still foresee that the nanocellulose hybrid aerogels with advanced carbons can allow synergistic design benefits as the nanocellulose component allows easy functionalization while the carbons lead to conductivity. Furthermore, hybrid aerogels may open routes for the economics optimization.

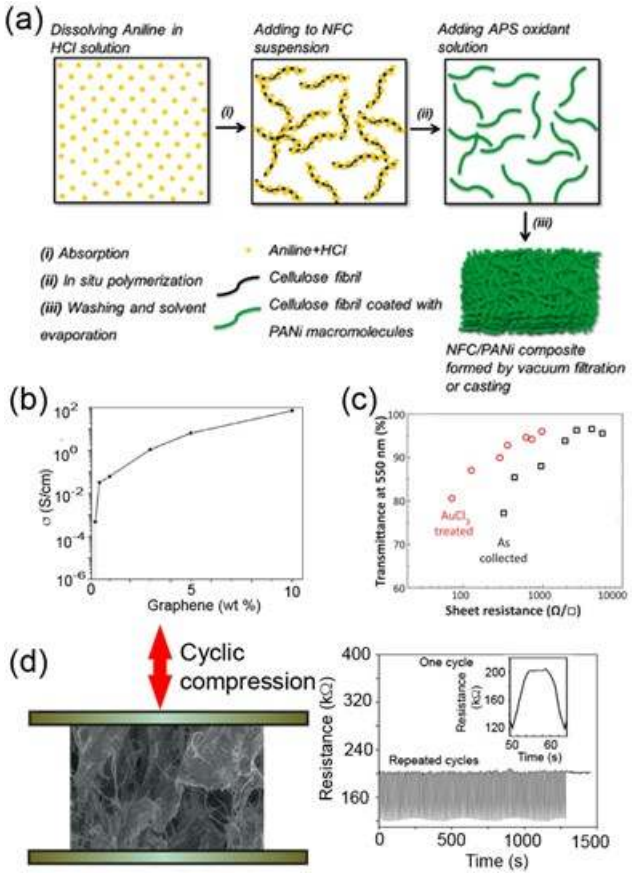

Figure 15. Nanocellulose hybrids with conducting organic matter. a) Schematics for in-situ polymerization of polyaniline in CNF aqueous suspensions. Reproduced with permission.[314] Copyright 2013, Elsevier. b) Electrical conductivity of reduced graphene oxide/aminated CNF hybrid films. Reproduced with permission.[315] Copyright 2011, Royal Society of Chemistry. c) CNF film with CNT coating, leading to high transparency, conductivity, flexibility, and still high tensile strength. Reproduced with permission.[216] Copyright 2015, Wiley-VCH. d) Hybrid CNF/CNT aerogels allow reversible compressional strain-dependent conductivity in repeated cycles. Reproduced with permission.[187,318] Copyright 2013, Wiley-VCH, and reproduced under the terms of the CC-BY-X license 2016, Royal Society of Chemistry.

3.5 Optical functions

Various optical functions can be achieved using nanocelluloses. Probably the most widely reported deals with cholesteric liquid crystallinity of CNCs, which causes tunable iridescence, i.e. structural colors,[325–329] and allows transferring such properties into other materials upon templating. [330–334] Also some berries show structural colors due to chiral twisting of native cellulosic components.[335] The formation of chiral nematic phases of CNCs was also studied in spherical confinement in emulsions to follow tactoid formation[336] or in case of microfluidic droplets demonstrating radial symmetric orientation of the CNC layers

with angle independent photonic properties.[337,338] On the other hand, one of the main efforts related to nanocellulosics has been to achieve transparency in films.[216,339–342] Instead, we deal here with tunable optical and photonic functionalities by decorating nanocelluloses with luminescent or plasmonic nanoparticles or optically active coatings.

Carbon dots are roughly 1 nm fluorescent nanoparticles which were found upon purification of single wall carbon nanotubes.[343] As they are nontoxic, they have application potential for biosensors, biomedical imaging, marker development, and anticounterfeiting. As also CNFs are biocompatible, a natural question is to combine CNFs and carbon dots for example for biosensing. Cationic amine-coated carbon dots have been connected to carboxymethylated CNFs using *N*,*N*'-(dimethyl amino)propyl-*N*′-ethylcarbodiimide hydrochloride/*N*-hydroxysuccinimide (EDC/NHS) coupling chemistry (**Figure 16**a).[344] In a follow-up research, TEMPO-CNF was decorated with amine-coated carbon dots again using carbodiimide-assisted coupling chemistry. Fluorescent adducts were observed (Figure 16b). Cell viability tests suggest that the TEMPO-CNF decoration with amine-coated carbon dots improves the cytocompatibility and also enhances their cellular association and internalization for both HeLa and RAW 264.7 cells after 4 and 24 h incubation.[345]

Metallic nanoparticles can exhibit plasmonic properties, which are known to be tunable by the particle sizes and assemblies.[346–350] Embedding Au or Ag nanoparticles in CNC cholesteric liquid crystals gives access to chiral plasmonic films by the interplay of the left-handed liquid crystalline twisting of the CNCs and the plasmonics of the constituent nanoparticles in films.[333,351] On the other hand, a driving force to the left-handed liquid crystalline CNC assemblies is expected to be the right handed twisting of individual CNCs.[11] The latter twisting can be harnessed to plasmonics by bonding Au-nanoparticles on aqueous dispersed CNC (Figure 16c),[139] using concepts already discussed in relation to Figure 7e. In that case, even if no clear helical twisting of the nanoparticles is resolved in electron tomograms, the handedness of their assembly around the CNCs shows a broken symmetry,

leading to a distinct right handed plasmonic signal, see Figure 16c. More generally, the templated chiral twisting around aqueous dispersed CNCs can be exploited also in chiral catalysis.[352]

Beyond using nanoparticles, optically active coatings can be used. A classic coating is based on TiO_2, where UV radiation creates radical cations and the material changes from relatively hydrophobic to hydrophilic.[353] Such properties can be used in systems containing nanocellulosics for different functionalities. First, optically switchable water absorption can be obtained using CNF aerogels. The first step to prepare such materials is freeze-drying of CNF from the corresponding hydrogels to form the porous aerogels. Thereafter, classic atomic layer deposition (ALD) by sequential exposition to trimethyl aluminium and water vapors and consequent purging was applied. In the non-illuminated state, water does not penetrate the aerogel porous interior, instead a relative high contact angle of 140°C is observed at the aerogel surface (Figure 16d). Upon UV illumination, the water droplet becomes quickly absorbed. If the TiO_2 coated CNF aerogel is kept in the non-illuminated condition for ca. 2 weeks, the water repellency is restored. The TiO_2-coated CNF aerogels can be applied in photocatalytic degradation, as demonstrated on methylene blue dye (Figure 16e), as well as for the selective recovery of organic solvents or oil spills from water (useful for water remediation).[178]

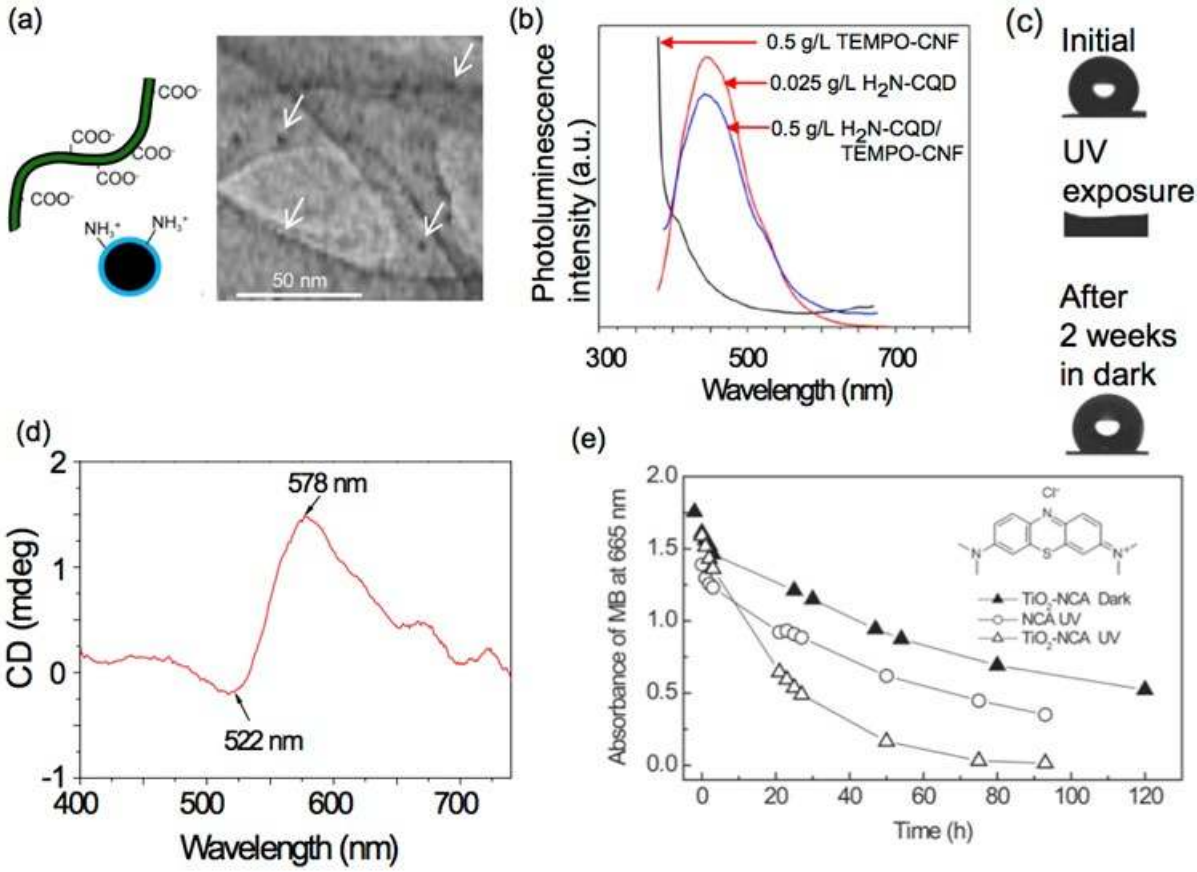

Figure 16. Optical functionalities based on nanocelluloses. a) CNF can be decorated with fluorescent carbon dots. Reproduced with permission.[344] Copyright 2014, American Chemical Society. b) They can be used for biological imaging due to the fluorescence. Reproduced with permission.[312] Copyright 2017, American Chemical Society. c) CNF aerogels upon atomic layer deposition (ALD) coating with TiO_2 layers show photo-triggered reversible water repulsion/absorption. Reproduced with permission.[219] Copyright 2011, Wiley-VCH. d) Au-nanoparticles can be electrostatically bound on CNCs undergoing right-handed twist for chiral plasmonics. Reproduced with permission.[139] Copyright 2016, Wiley-VCH. e) CNF aerogels coated with TiO_2 layers through ALD for photocatalysis, demonstrated by light-driven decomposition of methylene blue dye. Reproduced with permission.[219] Copyright 2011, Wiley-VCH.

3.6 Piezoelectric materials.

Asymmetric crystalline structures display a piezoelectric response under an electric field. Therein, cellulose nanocrystals are distinctive since they exhibit a permanent electric dipole that has been described as “giant”, after measurements in rectangular reversing pulse experiments (a permanent dipole of about 4400 Debye along CNC long axis was reported).[354] The occurrence of permanent dipole, which leads to a polarization density, has been explained from the parallel arrangement of cellulose chains in CNC, in a non-

centrosymmetric crystallographic lattice, coupled with the inherent dipole moment of the repeating unit of cellulose. Indeed, the effective piezoelectric coefficient d25 of films comprising oriented CNC, as obtained by combining shear and electric fields,[355] were measured for the first time recently.[356] The piezoelectric response depended on the degree of CNC alignment in the film and a value of up to 2.10 Å/V was determined (see also **Figure 17**a).[356] Remarkably, the large piezoelectric response was not exclusive to CNC: Self-standing films of CNF were used as functional sensing layers in piezoelectric sensors for which sensitivities from 4.7 to 6.4 pC/N were measured, indicating that despite the randomly aligned crystalline regions in CNF, their films still display a piezoelectric behavior.[357] The capacitance was dominant in the measurements at electric fields from 5 to 15 V/µm, implying that the CNF film had no significant ferroelectric hysteresis at low or moderate electric fields (Figure 17b, left). However, between 40 to 50 V/µm electric fields (Figure 17b, right) a nonlinear behavior was detected, suggesting that the CNF film had some level of ferroelectric properties at high electric fields. The evidence of nanocellulose acting as an incipient organic ferroelectric material under high electric fields points to the piezoelectric effect displayed by CNF in films, owing to a permanent dipole moment of fibrils with some level of orientation.

In recent developments, it was found that free-standing films comprising chitosan mixed with either CNCs or CNFs, were suitable in sensing and actuation applications. For instance, Figure 17c illustrates the measured sensitivities for different sample types. Thus, a simple solvent casting method was suitable for preparing films with given piezoelectric properties.[358] Overall, it can be suggested that nanocellulose is a suitable precursor for disposable piezoelectric sensors. The electromechanical actuation and strain can be changed as a function of CNC (or CNF) alignment. Related structures can result in high mechano-electrical energy transfer. Such electromechanical or flexoelectric behavior of ultra-thin films of CNC (and CNF) can be considered for potential applications in the fields of electronics, sensors and biomedical diagnostics.

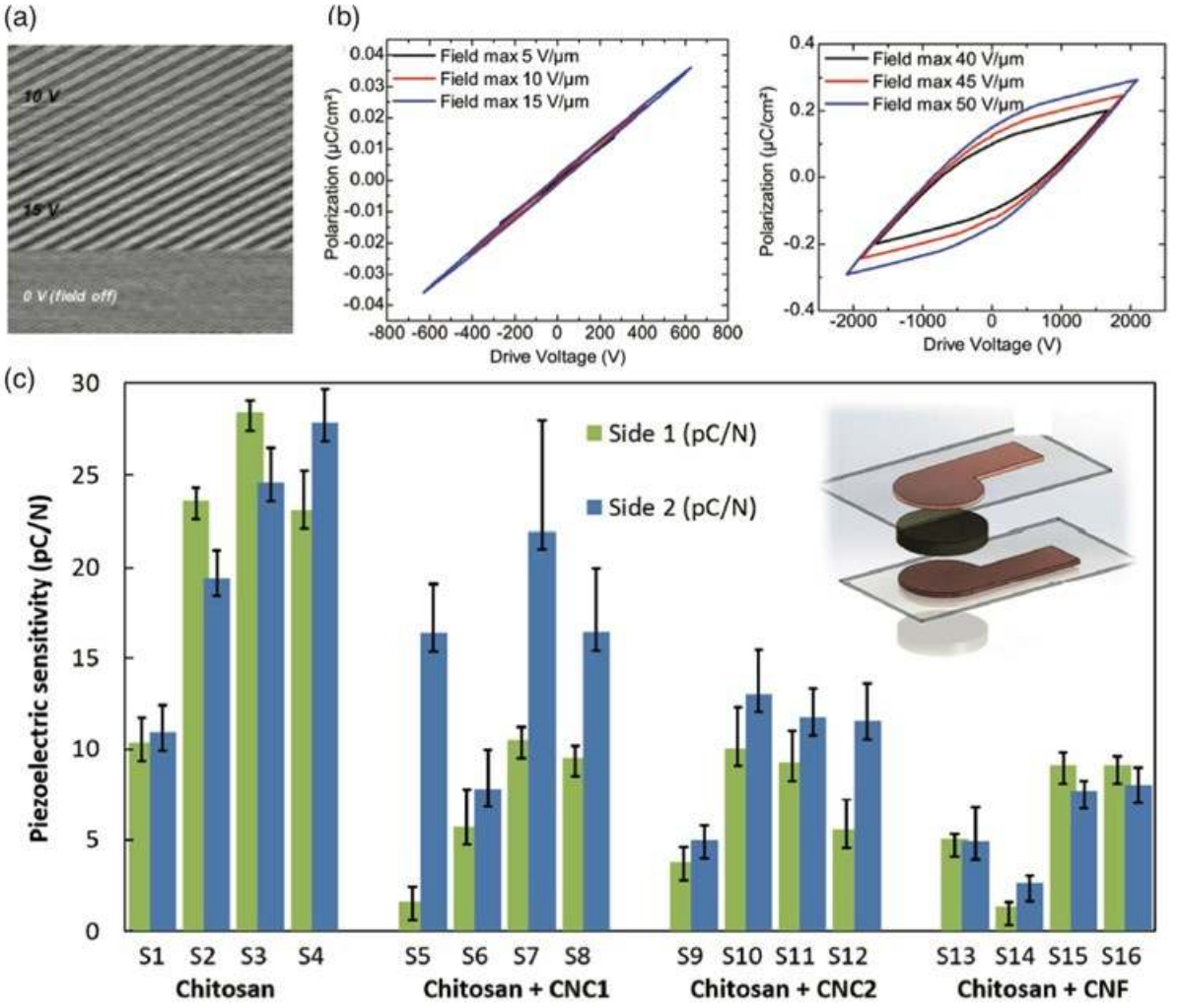

Figure 17. Piezoelectric properties of nanocelluloses. a) AFM height map showing the extent of CNC film displacement (z direction) as a result of their piezoelectric effect. The extent of displacement is indicated by lighter or darker fields as monitored by an AFM tip in contact with the film. A single point was monitored under given intermittent electric fields (10, 15 and 0 V). The deflection measured was used to calculate the piezoelectric constant of the films. The x and z scales in the image are dimensionless but indicate film deflection evolution with time as the voltage is turned on and off. Reproduced with permission.[356] Copyright 2012, American Chemical Society. b) Polarization hysteresis of CNF at low and high voltages. Reproduced with permission.[357] Copyright 2016, American Chemical Society. c) Piezoelectric sensitivity measured in units of pC/N of four parallel samples of films containing either CNC or CNF in the presence of chitosan. The schematic piezoelectric sensor elements are in the inset. Reproduced with permission.[358] Copyright 2016, Elsevier.

3.7 Nanocellulose as a biointerface in sensing

As nanoscale organization and molecular level architectures are important for biomolecular sensors and interactions with living matter, there has been significant interest to adopt nanocellulose for these applications. One aspect of these studies has been on how

bioactive molecules can be immobilized, but perhaps more significantly, it has been important to understand what advantages nanocellulose brings to biointerface and biosensing applications. One advantage of immobilizing enzymes on CNF has been that CNFs can easily be used to create surface layers with an open structure, for example by spin-coating. Thus, the immobilization reactions of biomolecules to cellulose can be made using dispersed cellulose, which involve reactions that typically can be performed with a good yield. Then the cellulose is fixed or physisorbed to the surface. This route of creating a bioactive surface is easier to scale-up than direct surface coupling and proceeds typically with a better yield.[359] The relative stabilities of proteins immobilized to cellulose films compared to those in solution or immobilized to other substrates have also been studied, concluding that immobilization through nanocellulose in fact can have a stabilizing effect on proteins.[359–361] Another important aspect of biosensors is the non-specific binding of molecules to sensor surfaces, giving false positive signals or disturbing measurements. Also in this context there are encouraging results from using nanocellulose, either as TEMPO-modified,[362] or together with surface passivating polymers.[141]

A successful approach for covalent immobilization has been to use a combination of 1-ethyl-3-[3-dimethylaminopropyl]carbodiimide hydrochloride and *N*-hydroxysulfosuccinimide (EDC/NHS) to couple carboxyl groups of TEMPO-oxidized cellulose to amine groups, either on proteins or on tags that mediate further conjugation.[141,359,360,362,363] Other methods have relied on the oxidation of cellulose C-6 hydroxyls to reactive aldehydes[364] or the use of aldehyde-based cross-linkers. [360,361] Immobilization has also been facilitated and made more generic by first immobilizing a protein such as avidin[363] or sortase[364] that then readily can be used as an affinity docking link to other biomolecules.

Specific examples are discussed next. **Figure 18**a shows one route to bind antibodies. Mechanically disintegrated CNF films were first TEMPO-oxidized to provide carboxylic acid

groups, followed by surface activation by EDH/NHS coupling chemistry to conjugate antibodies.[365] In another route, CNF films were first grafted with poly(2-aminoethyl methacrylate hydrochloride-*co*-2-hydroxyethyl methacrylate), i.e., poly(AMA-*co*-HEMA), copolymer brushes to provide a dense set of cationizable pendant groups, shown in Figure 18b. They, in turn, were electrostatically complexed with acetylated oligopeptide His-Trp-Arg-Gly-Trp-Val-Ala, i.e. Ac-HWRGWVA, which has high affinity to human immunoglobulin (hIgG). Indeed, a selective binding is achieved, as quartz crystal microbalance measurement show that hIgG is bound whereas bovine serum albumin (BSA) is not bound, as a reference.[366] Another CNF-based immunosensor is targeted to sense C-reactive protein (CRP), which is an important clinical marker for infections, by immobilizing anti C-reactive proteins using the EDC/NHS coupling chemistry. The amount of adsorbed CRP was quantified with the aid of time-resolved quartz crystal microbalance.[367] Finally, an avidin-biotin approach is illustrated in Figure 18b, where avidins are first coupled to the CNF films with coupling chemistries already described above, to further facilitate modular binding of biofunctional groups (Figure 18c).[363]

Despite the piezoelectric properties, nanocellulose bears no intrinsic sensing mechanism for detection of analytes, meaning that the chemical or biochemical conjugation of the sensory molecules is an unavoidable process step and the detection can only be monitored indirectly. With respect to an emerging group of biosensors based on field effect transistors of carbon nanomaterials, the lack of intrinsic response clearly distinguishes nanocellulose from carbon nanomaterials in biosensing and therefore, their comparison is not straightforward. Among the greatest benefits of employing nanocellulose in biosensing is the built-in ability to block non-specific binding whereas in graphene or carbon nanotube sensors this problem can be overcome only via a precise design of the surface architecture.[368]

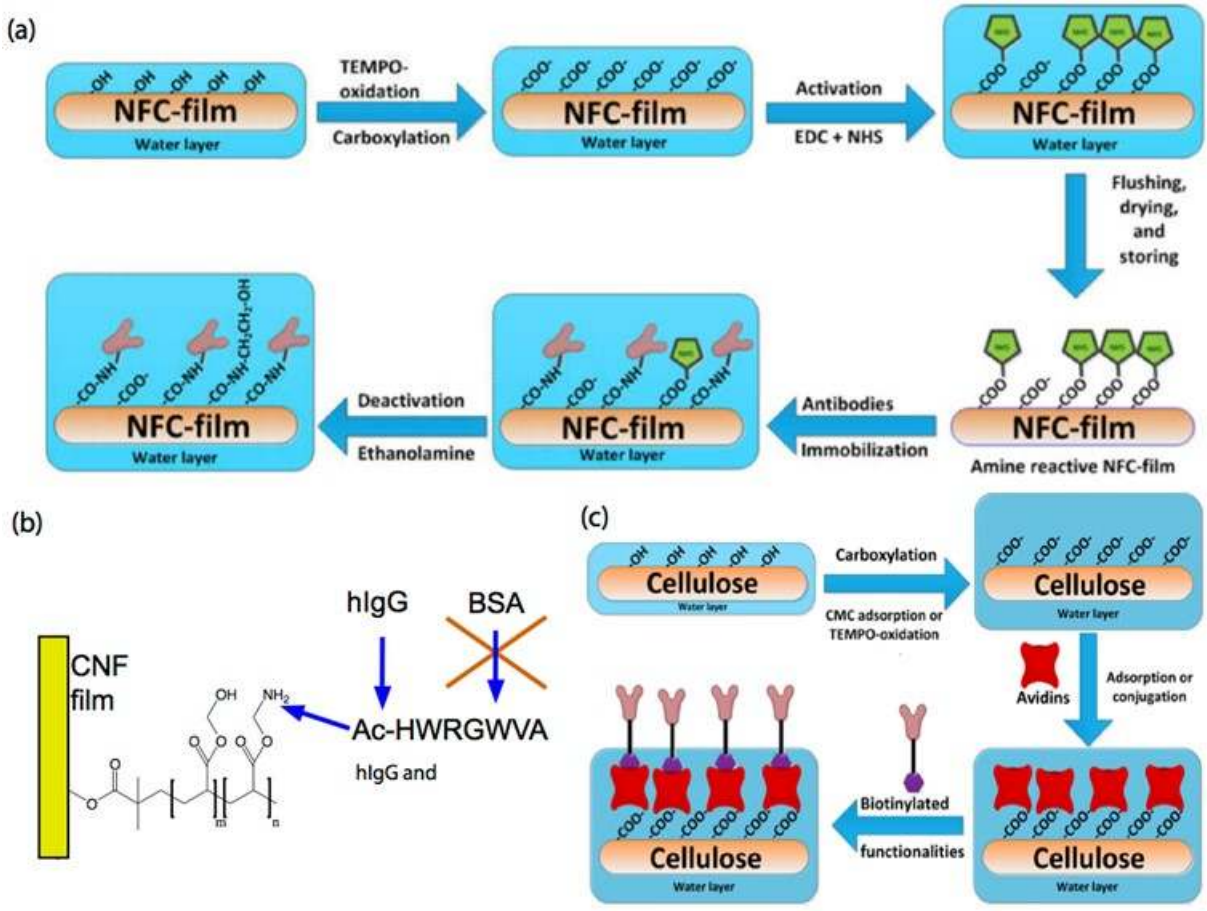

Figure 18. Nanocelluloses for biosensing. a) Schematics for antibody immobilization on CNF films using EDC/NHS coupling chemistry. Reproduced under the terms of the CC-BY-X license.[365] Copyright 2012, Springer. c) CNF with poly(AMA-*co*-HEMA) brushes electrostatically bind oligopeptide acetylated-HWRGWVA, which has specific affinity with human immunoglobulin G (hIgG) but reduced binding on bovine serum albumin. Reproduced with permission.[366] Copyright 2013, American Chemical Society. c) Scheme to exploit avidin/biotin complexation for biofunctionalized CNF films. Reproduced with permission.[363] Copyright 2012, American Chemical Society.

3.8 Biological scaffolds

In the past several years, a tremendous effort has been made to design three-dimensional (3D) hydrogel-based scaffolds and adopting them in cell culture, tissue culture, organoid culture, drug discovery and stem cell studies. This is attributed to the fact that, unlike traditional 2D culture systems, the 3D scaffolds, display an increased degree of complexity, which resemble the native cellular microenvironment, thereby, offering a predictable and reliable data for in vivo experiments. In a conventional cell culture system, the cells adhere to a flat 2D substrate, which induce the flattening and stretching of the cells.

Therefore, the cells attain unusual morphology, which eventually affects the cellular process such as proliferation, differentiation, apoptosis and expression of genes and proteins. This is particularly important in pharmaceutical drug discovery as majority of the drugs fails at the most expensive phase of clinical trials, due to a lack of reliable and predictive culture systems. This has spurred extensive efforts to develop 3D hydrogel culturing media to mimic extracellular environments.[369–372] The 3D culture matrices influence both the spatial organization as well as physical constraints to the cells or tissues under investigation. Therefore, in 3D cultures the signal transduction occurs from outside to inside the cells, which affects the cellular process and behavior similarly to that of cells in the *in vivo* extracellular matrix. Considerable progress has been made in hydrogel cell culture matrix development, and probably the most widely used growing medium is commercial Matrigel®, which is extracted from the Engelbreth-Holm-Swarm (EHS) mouse sarcoma. Its origin and batch-to-batch variation (heterogeneity), however, are major drawbacks. A wide range of other hydrogel scaffolds have been explored, such as collagen, peptides, alginates, chitosan, silk, hyaluronic acid, polyacrylamide, PEG, as well several synthetic polymers such as poly(isocyanates), which have been decorated with biocompatible side groups.[372–374] They cover a wide range of physical and chemical properties. However, recently it has been emphasized that extracellular matrices are typically strain stiffening, where the stiffness increases upon imposed strain or loading of the gel.[375–380] Towards that, proper mimicking of extracellular matrix may require detailed tuning of the network skeleton persistence length, network mesh size, and interactions with cells. Proper mimicking is a grand challenge as the biological environment interacts with cells using a complex combination of chemical, physical and mechanical cues. In this context, nanocellulose hydrogels at physiological conditions provide a tunable platform technology for biomedical scaffolding, due to their unique mechanical and chemical properties, biocompatibility, low toxicity and functionalities.

Related to nanocelluloses, bacterial cellulose has extensively been used as a scaffold to grow cells and organs.[381–383] More recently, wood-based CNF has been developed for cell culture as a response to the need of xeno-free medium, i.e. being free of human- or animal-based constituents. CNF hydrogels mimic the 3D in vivo stem cell niche to culture human pluripotent stem cells keeping the pluripotency for 26 days, as evidenced in immunofluorescence studies and formation of noncancerous tumors, i.e. teratomas, which are characteristic for cultures of embryonic stem cells, see Figure 19a.[384] This was based on a recently commercialized CNF-based culture medium GrowDex™ which has been introduced by UPM-Kymmene Corporation suggesting a promising platform for cell therapy, drug research and tissue engineering. Another application of CNF is a 3D growth media dealing spheroid formation of human liver cells.[385] This is driven by the need to develop liver cultures for pharmacological science and industry for studies of drug response and metabolism. The successful culture of undifferentiated HepaRG cell on CNF hydrogel produced canaliculi-like structures and is supported by the mRNA expression of hepatocyte markers. In wound healing, such as burn treatment, delayed healing can cause inflammation[386] and several materials have been applied for the wound dressings to tune the elasticity, to keep the moisture and pH levels, to prevent bacterial contaminations, to reduce pain, and to promote quick healing. The advantages of CNF also in wound healing have been shown recently even in clinical tests.[387,388] On the other hand, promoted wound healing after surgery is achieved by local application of human adipose mesenchymal stem cells (hASC) onto the wounds.[389–391] Therein hASC-loaded CNF-based surgery-threads could be feasible due to their biocompatibility, taken that the strength under moist conditions could be improved. Drastically improved wet strength was indeed achieved by glutaraldehyde crosslinking, still allowing hASC attachment on CNF in the undifferentiated state and preserved bioactivity, after glutaraldehyde was carefully removed (Figure 19b).[64] Also CNCs show potential in biomedical and pharmaceutical applications, e.g. as injectable gels in

combination with carboxymethyl cellulose and dextran.[392] The compositions were not cytotoxic as studied using NIH 3T3 fibroblast cells. CNC-based crosslinked hydrogel films rendered promoted adhesion or antifouling surfaces for C2C12 mouse myoblasts and MCF 10A premalignant human mammary epithelial cells.[393]

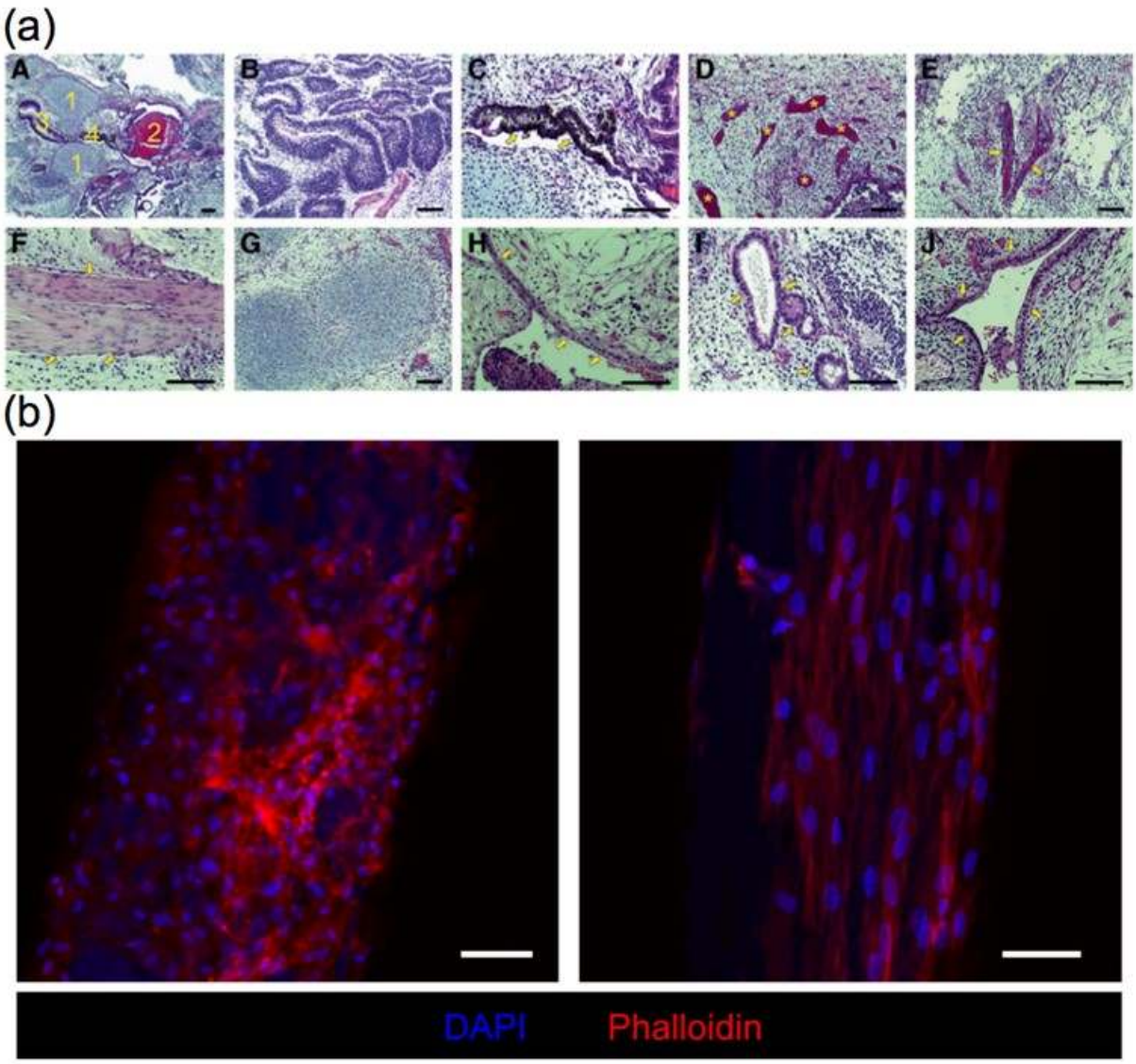

Figure 19. Scaffolding cells and viruses on nanocelluloses. a) Hematoxylin and eosin staining of 6-week-old teratoma sections (5 mm) of human embryonic stem cells (WA07/WiCell), cultured in CNF hydrogel for 26 days. (A) Cartilage (1), bone (2), epithelial tissue (3), and pigmented cells (4). (B) Neuronal rosettes. (C) Pigmented cells. (D) Blood vessels (indicated by asterisks). (E, F) Muscle (indicated by arrows). (G) Cartilage. (H–J) Endodermal epithelia (indicated by arrows). Scale bars 100 mm. Reproduced with permission.[384] Copyright 2014, Liebert Inc. b) Attachment of the human adipose cells on CNF surgery thread surface. Especially on crosslinked CNF, they exhibit elongated cytoplasmic intermediate filaments (stained red with phalloidin). Nuclei were counterstained in blue. Scale bars 50 mm. Reproduced with permission.[64] Copyright 2016, Elsevier.

3.9 Nanocellulose films, filtration membranes and waste water treatment

Variants of nanocellulose allow several interesting properties in films. The perhaps most spectacular property is the iridescence of CNC-based films which arises due to the cholesteric liquid crystallinity of CNCs in concentrated aqueous dispersions.[1,11,326,394] This leads the helically twisting patterns that are maintained also in dried films. These assemblies have also been used for templating of chirality to other components in hybrids, for example, to inorganics.[333,334,395]

In analogy with classic paper sheets, also CNF allows preparation of sheets or films, often termed "nanopapers". Such nanopapers have much better mechanical properties in comparison to classic paper sheets, for example the tensile strength in nanopapers is ca. 200-300 MPa compared to 20-50 MPa in classical papers.[126,437,396-401] Due to their smaller fibrils, the nanopapers have fundamentally different properties. The constituent nanoscale fibrils allow for example tunable transparency and haze which is useful for the future flexible devices.[8, 216, 339, 439, 402-412] Also their surfaces are smoother, which can be important e.g. for high definition of linewidths in printed devices. Nanopapers can be furnished also by a wealth of other functional properties, like barrier properties to reduce vapour permeation, fire-retardancy, magnetic properties, and electrical conductivity.[6, 175,193, 216, 296,298,314,316,413-434] Among the potential applications, we foresee that nanopaper device substrates for flexible transparent devices are particularly promising.

Another property inherent to nanopapers is the porosity due to the packing of nanofibrils.[126] Therefore, they may serve as nanofiltration membranes for organic solvents.[435] Organic solvent nanofiltration aims at separating particles or molecules of molecular weights from some hundreds of Da to some thousands Da from organic solvents with various polymeric and inorganic membrane materials used previously.[436] In comparison to them, CNF films could offer a simple and sustainable alternative based on the nanofiber packing.

Indeed, selective permeance is conceptually demonstrated using two types of CNF nanopapers for water, tetrahydrofuran and *n*-hexane. [435] The study was extended to ultrafiltration membranes, where nanopaper membranes were prepared using TEMPO-oxidized CNF, Masuko-ground CNF, bacterial cellulose and CNC. The ultrafiltration was explored by exploring rejection of aqueous dissolved PEG with molecular weights between 1 and 93 kDa (**Figure 20**a). TEMPO-oxidized CNF provides the smallest cut-off, corresponding to PEG molecular weight of 6 kDa and filter pore size 2.4 nm. The Masuko-ground CNF showed cut-off values of 25 kDa for PEG, which corresponds to a hydrodynamic radius of 5 nm. Bacterial cellulose provided less defined cut-offs due to its large pore size.

In waste water treatment, capture of metal ions on TEMPO-oxidized CNF was demonstrated already early.[437] Also, phosphorylated CNC had promoted heavy metal adsorption.[438] Toward practical constructs, layered membranes were prepared using a support layer based on cellulose sludge, containing CNF, but also cellulose microfibrils, hemicellulose and lignin (Figure 20b).[439] The surface layer was prepared from CNCs, which were additionally TEMPO-oxidized to promote charging. The layered membrane proved efficient in adsorption of Ag(I), Cu(II), and Fe(II)/Fe(III) from industrial effluents, still allowing high water permeability and promoted stability. The membranes were shown to be biodegradable. CNF films, like cellulose in general, can be grafted with different polymers.[72] By grafting CNF films with thermoresponsive polymers, thermoreversible membranes were achieved (Figure 20c). By surface-grafting poly(*N*-isopropylacrylamide), a temperature dependent water permeance is achieved, as the polymer forms hydrophobically collapsing coils upon heating.[440] In order to treat waste waters, various flocculants have been used to combine impurity particle into large aggregates, which can be removed by settling or flotation.[441-443] Anionically modified CNFs with tunable charge densities were explored as flocculants.[444] They are more stable under shear than conventional flocculants, i.e. cationic

polyacrylamide and ferric sulfate. In removing vanadium(V) from water, bisphosphonate functionalized CNF turned out to be particularly efficient.[445]

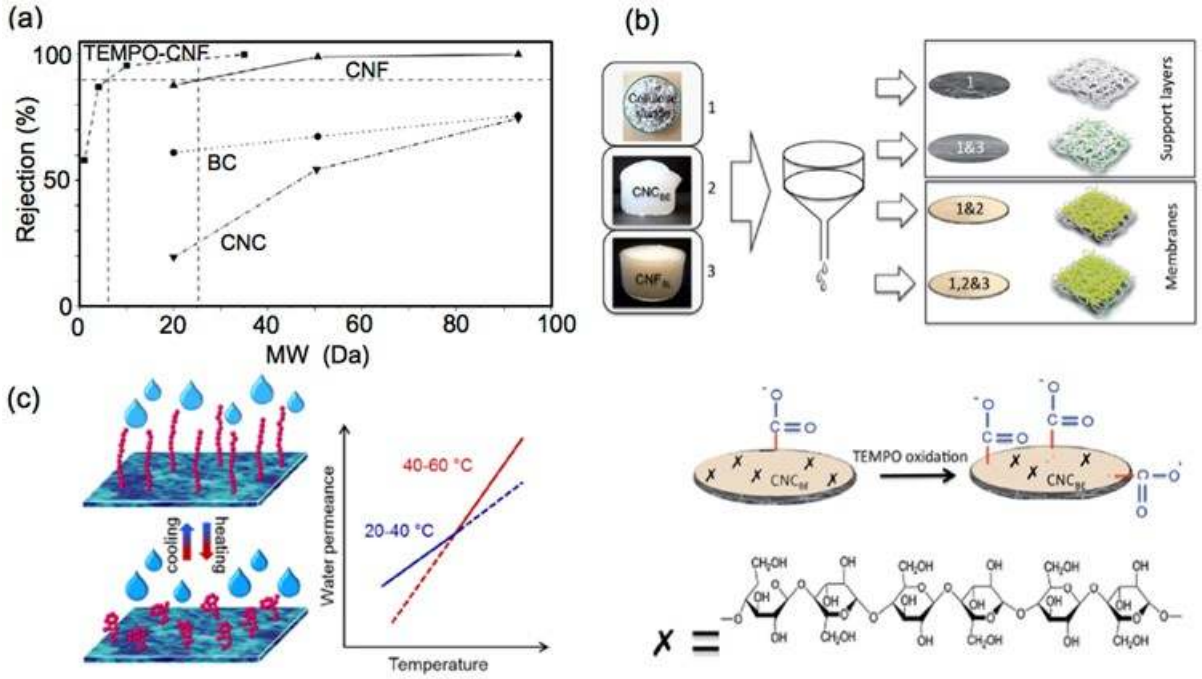

Figure 20. Waste-water treatment by nanocelluloses. a) Rejection of PEG by bacterial cellulose (BC), Masuko-ground CNF, tempo-oxidized CNF, and CNC membranes. Reproduced with permission.[446] Copyright 2015, Elsevier. b) TEMPO-oxidized films capture metal ions in nanocellulose layered film membranes. Reproduced under the terms of the CC-BY-X license.[439] Copyright 2017, Royal Society of Chemistry. c) Thermoresponsive membranes can be constructed by grafting nanocellulose films with poly(*N*-isopropylacrylamide). Reproduced with permission.[440] Copyright 2016, American Chemical Society.

Despite numerous literature accounts, use of nanocellulose in membrane technology is a nascent and relatively scattered field where quantitative comparison to the existing membrane materials like polypropylene, polysulfone and silicon is not straightforward. However, certain conceptual advantages can be pointed out, with bio-based origin and biodegradability being the most obvious. Furthermore, the use of organic solvents in membrane preparation, characteristic with most polymer membranes,[447] is not needed for nanocellulose-based membranes. Also fouling, prevalent with most hydrophobic membrane materials, is lower with the relatively hydrophilic nanocellulose. The hydrophilic nature, by contrast, may prove to be an obstacle for the perseverance of the membrane in water related applications.

3.10 Tribology

Investigations of the tribology of CNF have been carried out by different methods all the way from nanotribology to the macroscopic scale. A nanotribological study on polymer brush-decorated CNF surface under hydrated conditions was carried out by colloidal probe technique using atomic force microscopy (AFM).[448] The aim was to quantify how polyethylene glycol (PEG) chains attached on a cellulose surface lubricated the contact with unmodified cellulose surface. PEG was bound to the CNF through non-ionic adsorption of PEG-substituted carboxymethyl cellulose (CMC). The surface modification was suggested to serve as an efficient shear stress transferring interface in nanocomposite materials in order to increase the toughness. The normal adhesion between the PEG-modified CMC and the cellulose probe was measured, showing a clear electrosteric repulsion between the charged cellulose and PEG chains.[449] Interestingly, a low coefficient of friction (COF) was obtained with very low loads, whereas increasing the load led presumably to a decrease in the hydration in the contact, resulting in a tenfold increase of the friction (**Figure 21**a). This finding highlights the importance of hydration of the lubricated CNF surfaces.

Another exceptionally well-lubricated bio-inspired cellulose surface was obtained via conjugation of hyaluronic acid (HA) to the CNF.[450] Lubrication of the CNF was obtained by covalently bound hyaluronic acid which is a highly charged hydroscopic polysaccharide. Hyaluronic acid is nature's own lubricant that exists in many lubricated contacts in the body, including epithelial and contact tissues.[451] The reported friction coefficient measured between the hydrated hyaluronate-conjugated CNF and glass colloid was up to two decades lower than the friction at the CNF/glass contact (Figure 21b). The study proposes CNF as a possible biocompatible and sustainable material for joint prosthesis to replace damaged cartilage.

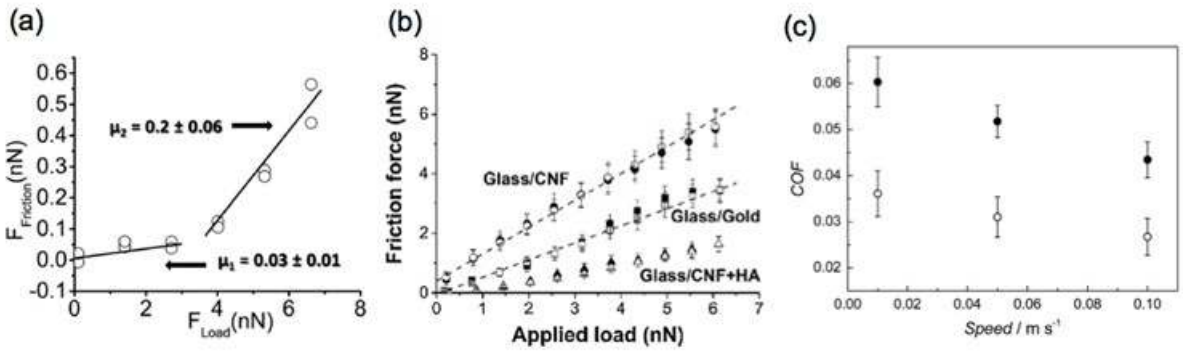

Figure 21. Tribology of nanocelluloses. a) Friction force as a function of load between the CMC-*g*-PEG-decorated CNF film and a cellulose sphere at pH 7.3. The slope of the solid lines represents the friction coefficients. Reproduced with permission.[448] Copyright 2013, Royal Society of Chemistry. b) Friction forces between a glass microsphere and a gold substrate (squares), a CNF film (circles), and a CNF film with HA attached (triangles) in PBS pH 7.4. Reproduced with permission.[450] Copyright 2015, Elsevier. c) Macroscopic friction coefficients of as-extracted quince mucilage as a function of sliding speed measured with pin-on-disc with a 50 N normal load. The concentration of the mucilage was1 g L^{-1} (closed circles) and 5 g L^{-1} (open circles). Reproduced with permission.[452] Copyright 2014, Royal Society of Chemistry.

The lubrication ability of a fruit-based quince nanocellulose was investigated by a macroscopic pin-on-disc method.[452] The tribology of the polyethylene and stainless steel contact, a typical material pair in joint prostheses, was studied. The CNF was readily extracted from the fruit seeds as a well-dispersed hydrogel, quince mucilage, containing more than 50 % of hemicelluloses, mainly heavily charged glucuronoxylans and very monodisperse 3 nm thick CNF. Due to the high content of the chiral hemicelluloses and the very high aspect ratio of the fibrils, the quince mucilage CNF assumes a helicoidal order, which makes it a special type of CNF, since the cholesteric assembly is typically observed only for CNC.[453] The viscosity as well as the friction were strongly dependent on the dry matter content of the mucilage showing much higher friction for diluted mucilage than the concentrated ones where the gel structure was stronger (Figure 21c). Lower friction forces between the polyethylene / stainless steel contact at higher shear rates were observed and it was suggested that this was due to the shear thinning behavior of the CNF.[454] Based on these studies the charged macromolecules associated with the CNF have a high impact on the tribological behavior of CNF and surfaces with very low friction can be built from the combination of nanocellulose

and charged molecules. These examples, including the as-extracted quince mucilage, demonstrate that the native hemicelluloses that are associated with the cellulose fibrils not only play an important role in CNF assembly but also strongly contribute to the tribology of the fibrillated nanocelluloses. Many other studies in the field of biolubrication employ mammalian glycoproteins as lubricants.[455] These systems function as oil-free lubrication systems and mimic the synovial systems and mucosa the closest, but they are currently unfeasable to produce. Plant-derived CNF that natively contains charged hemicellulose is thus a promising material due to its abundancy and high performance.

3.11 Superhydrophobicity

Superhydrophobicity refers to surfaces that are highly water repellant, i.e. where the water contact angle is in excess of 150^{o}, as originally found in the self-cleaning Lotus-leaves.[456,457] In more detail, superhydrophobicity refers to high contact angles both for advancing and receding water droplets, i.e., low contact angle hysteresis. Such properties emerge due to the balanced interplay between the surface topographies and low energy surface coatings. Corresponding synthetic biomimetic surface structures have been pursued in science and technology for self-cleaning and surface modification, also expanding to oil-repellent surfaces.[458,459] Cellulose papers, cotton fabrics and paperboards (or associated materials) are suitable for constructing superhydrophobic surfaces by low surface energy engineering while taking advantage of the natural roughness of the materials.[100,460] The concepts can be adapted also for the creation of superhydrophobic nanocelluloses. Materials with low surface energy include fluorocarbons, silicones, and some organic and inorganic materials. Among these, fluorocarbons are the most frequently used. For this purpose, partially fluorinated amphiphilic block or statistical polyelectrolytes were adsorbed from aqueous medium on cellulose. The formed surface layers consisted of polymeric nanoparticle aggregates that endowed the surfaces with varying surface coverage. After annealing, they

were rendered highly hydrophobic, with advancing contact angles of ~160 ° (**Figure 22**a).[461] Methods other than colloidal assembly to produce nano-roughness, as in the previous case, have included etching and lithography, sol-gel processing, layer-by-layer and electrochemical reactions. For example, chemical vapor deposition of nearly conformal TiO_2 coatings with thicknesses of ca. 7 nm were attached to nanocellulose aerogels, which displayed photo-switching between water-superabsorbent and water-repellent states.[219] In other efforts, also related to titanium dioxide, oleophilic coatings were made so that the nanocellulose structure selectively absorbed oil.[178] Fluorination of aerogel membranes by chemical vapor deposition using tridecafluoro-1,1,2,2-tetrahydrooctyl)trichlorosilane (FOTS) produced CNF-based materials displaying high water contact angle, as will be discussed later.[462] CNF itself, i.e., without topographies induced by the aerogels, can be used to produce surface features. For example, spray-dried CNF led to hierarchical surface roughness, closely resembling that of lotus leaves.[422] CNF was sprayed with an airbrush onto a surface followed by coating with (FOTS), via chemical vapor deposition, to render the system superhydrophobic. Alternatively, a toluene dispersion of CNF microparticles was allowed to react with FOTS and then sprayed onto the substrate, also resulting in superhydrophobicity, as determined by contact angle measurements and sliding angles of only a few degrees (Figure 22b).[463] These efforts, however, did not address the possibility of space-resolved superhydrophobicity, which could make nanocellulose materials (films and nanopapers) better suitable for applications requiring controlled wetting, such as in biomedical, biotechnological and diagnostics devices. Responding to this need, a facile process was adopted recently to tailor the surface wettability of CNF films by installing reactive nanoporous silicone nanofilaments by polycondensation of trichlorovinylsilane (TCVS). This afforded appropriate surface topologies while the vinyl groups in the nanofilaments formed with TCVS gave the reactivity necessary for UV-induced functionalization of thiol-containing molecules (photo “click” thiol-ene reaction). Thus, by using perfluoroalkyl thiols, superhydrophobic and slippery lubricant-infused CNF films were

demonstrated, with repellence against both aqueous and organic liquids with surface tensions as low as 18 $mN \cdot m^{-1}$. Furthermore, creation of patterned superhydrophobic-superhydrophilic domains was accomplished simply by using a photomask with given designs that allowed UV-activated click on the nanocellulose films, as illustrated in Figure 22c.[464]

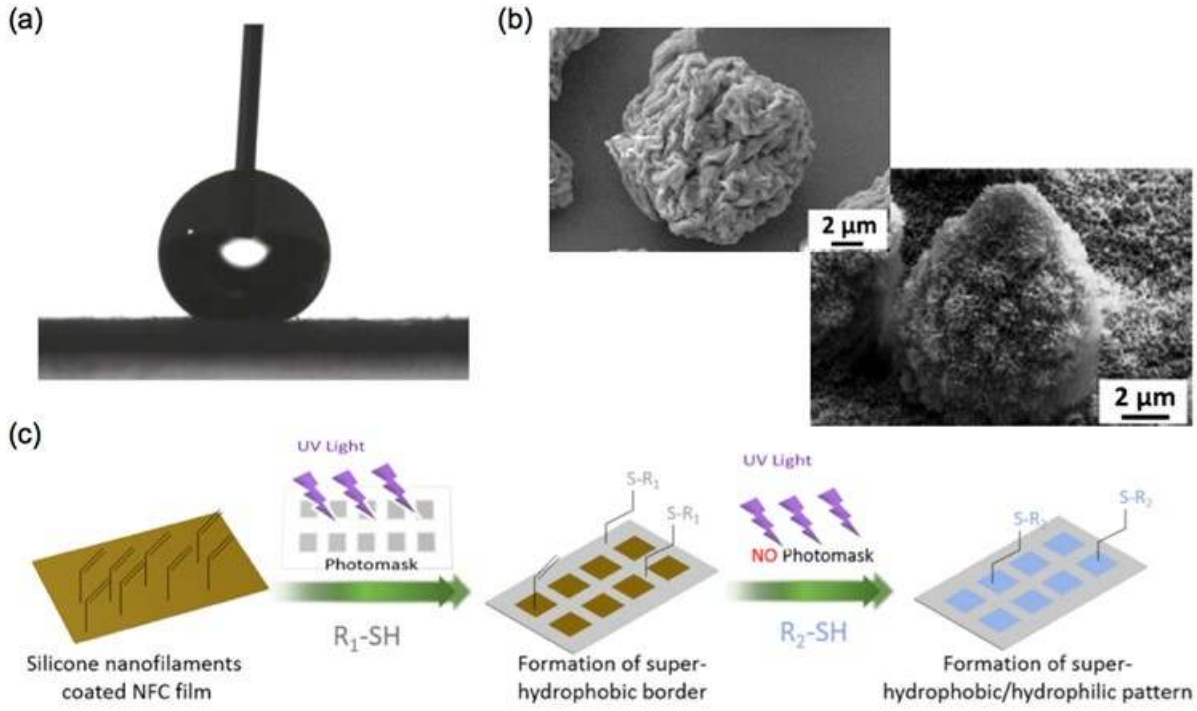

Figure 22. Superhydrophobic coatings based on CNFs. a) Adsorption of partly fluorinated statistical and block polyelectrolytes on CNF from aqueous medium with high water contact angles. Reproduced with permission.[461] Copyright 2010, American Chemical Society. b) Aerosol processing and fluorination of CNF (top image) mimics the lotus leaf through hierarchical surface topographies for superhydrophobicity (bottom image). Reproduced with permission. [463,465] Copyright 2009, 2012, Royal Society of Chemistry. c) Nanocellulose films can be modified to be superhydrophobic, slippery, and patterned. Reproduced with permission. [464] Copyright 2016, American Chemical Society.

3.12 Motility and actuation based on nanocelluloses

Nature demonstrates fascinating floating phenomena on water. The most remarkable ones are related to insects, as they can exploit the surface tension of water. Perhaps the most well-known example is given by water striders. [466] Their floating is due to a special structure of their legs, incorporating thin hair-like setae covered by secreted low surface energy wax. This leads to superhydrophobicity and floating. Perhaps a more striking phenomenon is seen

in fire ants, which upon water flooding connect to each other to form self-assembled mesh-like rafts, and thereby allowing them to float on water. [467] Not surprisingly, floating and load-bearing 2D or 3D meshes have been developed in engineering aiming at microdevices and environmental remedies. [468,469] CNF aerogels could be feasible to construct floating miniaturized objects for cargo carrying, as the aerogel skeletons form mesh-like structures and as the CNF surfaces can be chemically functionalized for superhydrophobicity. Indeed, upon freeze-drying CNF to aerogels and subsequent chemical vapor deposition of (tridecafluoro-1,1,2,2-tetrahydrooctyl)trichlorosilane gave a high water contact angle of 160°.[462] Perhaps surprisingly, also the contact angle for paraffin oil was high, i.e. 153°. Still, as there was a high contact angle hysteresis, the material may not be described as fully superhydrophobic. Still, they floated on both water and oil, and an aerogel raft with a mass of 3.0 mg and a diameter of 19 mm could carry a load of 1658 mg on water with a dimple of 3.7 mm (**Figure 23**a). On paraffin oil, it could carry a cargo of 960 mg and made a dimple of 2.7 mm depth. To provide motility, the Marangoni-effect [470] was exploited by generating an anisotropic surface tension. A classic example for Marangoni-based motility is given by the so-called "soap boat". Another example is provided by the so-called camphor boat. [471] They do not easily allow continuous movement as the water surface is modified due to the "fuel". In aerogels, the porosity allows liquids to evaporate through the rafts to modify the surface tension underneath the raft. If a chamber of volatile alcohol as a fuel is positioned on top of the raft leading to asymmetric surface tension underneath, locomotion follows (Figure 23b). [473] As the alcohol is volatile, the locomotion is continuous, lasting as long as the fuel in the chamber persists, unlike the soap-driven variant. In a typical experiment, evaporation of 25 ml of ethanol allows autonomous motion for 74 m during ca. 1 h hour for a centimeter-sized raft at a velocity of ca. 2 cm/s. The velocity can be tuned by the volatility of the fuel (Figure 23c).

Another example of CNF-based movements deals with actuation of a few micrometer thick CNF films. Qualitatively, upon posing such a film on uncovered skin, the film starts to

bend, see Figure 23d.[473] The bending is reversible, as the flat shape recovers by extending the distance from a skin. This bending is due to an asymmetric humidity penetration from skin and asymmetric humidity-driven swelling. More quantitatively, the bending was studied using controlled humidity and different film thicknesses, with the largest effects seen for thin films. Curiously, by exposing to a constant humidity, the bending reached a stable value, and it was reversible within recurring humidity cycles (Figure 23e). This is unlike a classic paper sheet on a liquid water surface, which leads to temporary bending due to initially anisotropic swelling of the opposite sides. [474] However, when the paper was wetted throughout, no anisotropy existed, and the default shape was observed. Obviously, the present water vapor dependent reversible actuation can be related to pine cone and wheat awn actuations. [475,476]

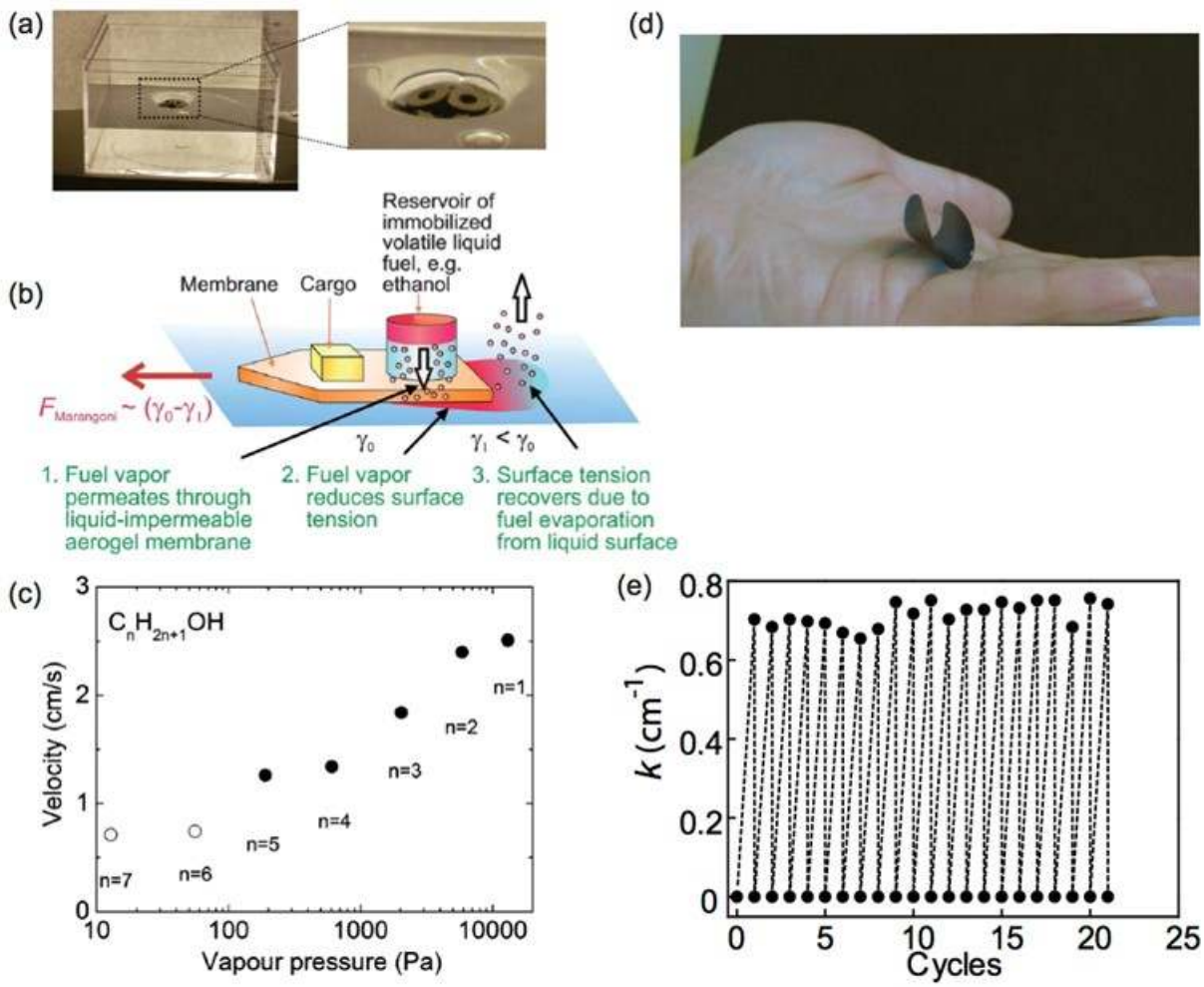

Figure 23. Motility and movement based on nanocelluloses. a) Fluorinated aerogels with high buoyancy display abilities to carry millimeter scale cargo. Reproduced with permission. [462] Copyright 2011, American Chemical Society. b) The buoyant fluorinated aerogel can

translocate efficiently with Marangoni effect on water surface by fuel vapor. c) The velocity of the aerogel can be tuned using linear alcohols with different vapor pressures. Reproduced with permission. [472] Copyright 2012, Royal Society of Chemistry. d) Thin CNF films allow reversible actuation by anisotropic humidity adsorption. e) The NFC film (thickness 8 μm) undergo repeated deflection upon cyclic humidity change. Reproduced with permission. [473] Copyright 2015, Wiley-VCH.

4. Concluding remarks

Here we have reviewed recent processes and a wealth of potential functionalizations of nanocelluloses to show different concepts and ways of applying them in materials. The work done so far shows that nanocelluloses offer a versatile platform for controlled structures and tailored properties for a range of applications. However, in order to allow a realistic materials platform, and not just a scientific curiosity, there are several subtle technical and economic issues to be considered in comparison to other materials options, which we next briefly address.

We will first summarize the most relevant properties of nanocelluloses, presented through the previous sections. As often reminded, cellulose is the most abundant source of polymeric raw material on Earth. In addition, it has the merit of being sustainable. Unlike molecular cellulose, nanocelluloses are colloidal level fibrillar objects, whose lateral dimensions depend on the source, and the length depends on the applied processing to cleave them from the plant or wood. The mechanical properties of individual fibrils are not yet known in detail, but they are likely to be remarkably good, i.e., with a modulus up to ca. 150 GPa and a tensile strength in the 2-6 GPa range. However, big challenges still exist to transfer such high mechanical properties into practical materials. An unfavorable property of nanocelluloses is that they suffer from a rather limited temperature window, i.e. they cannot be heated above ca. 200 °C without degradation. The nanocelluloses have a dense set of hydroxyls on their surface, thus allowing a rich variety of surface initiated chemistries to modify the colloids. Interestingly, the cellulose chains within nanocelluloses are in a parallel hydrogen bonded arrangement,

thus leading to a broken symmetry and piezoelectricity. The hydroxyl groups, however, result in high hygroscopicity of nanocellulose, meaning that most unmodified nanocellulose materials are susceptible to humidity and water. Finally, the celluloses are biologically compatible, which opens possibilities for biological scaffolding. Next, we place these properties into a perspective in relation to other materials.

The most obvious comparison of CNF relates to classic paper sheets, which comprise micronscale fibrils, i.e., of three orders of magnitude larger in lateral scale. As discussed before, the nanopapers have much better mechanical properties, and they can widely functionalized, to tune transparancy, haze, fire retardancy, magnetic and electric properties, tunable porosity, and tissue interactions. But perhaps the most exciting application potential of nanopapers is related to flexible devices,[8] which can directly benefit from the tunable optical properties, smooth surface, and smaller thermal expansion coefficient than many synthetic polymers. One can also foresee specific device applications in which degradability is required, for example in environmental monitoring or military applications, or more generally when aiming at sustainability. Such arguments have encouraged towards nanopapers as printable electronics substrates. On the other hand, the smaller fibrils in nanopapers pack more densely, thus leading to nanoscale porosity, allowing fundamentally different possibilities for functional membranes.

Another obvious comparison for nanocelluloses among organic materials are carbon nanotubes. [477] They both have nanoscale lateral dimensions and can show long and flexible variants (CNFs and single wall CNTs) and more rod like variants (CNCs and multi wall CNTs). However, there are several significant differences. Carbon nanotubes have orders of magnitude higher tensile elastic moduli (ca. 1000 GPa) and strengths (30-60 GPa) combined with a lower density 1.3 g/cm^3 versus the density of 1.5 g/cm^3 for nanocellulose. Even if both materials have high tensile properties, they easily bend under flexure. Both materilas require efficient alignment to transfer the mechanical properties to macroscopic materials, which is a

major challenge to achieve in a production-friendly fashion. Perhaps the most important difference is the tolerance towards elevated temperatures. Whereas nanocelluloses cannot be heated above ca. 200 ^{o}C, CNTs can be heated to substantially higher temperatures, thus allowing a wider range of processing options and widening the application potential. Finally regarding the availability, even if "semilarge" production capability of multiwall CNTs presently exists, the nanocelluloses ultimately suggest a much larger raw material source. At present, nanocelluloses are produced by specialized grinding methods and homogenizers, which are known from the food industry. One could foresee that new preparation techniques related to polymer composites can also become available, for example to prepare nanocelluloses by extruders in-situ in preparing nanocomposites, thus providing potentially economic preparation protocols. To reduce production costs further, various side streams for raw materials can be used to prepare nanocelluloses and one could foresee that economics in the scale of commodity plastics are reachable. This would be a landmark achievement, given the sustainability and the versatile properties of nanocelluloses.

Thus, one of the features that drives the wider appeal of the reviewed materials is obviously the cost of nanocellulose. According to the recent industrial economic surveys, the minimum product selling price (MPSP) of CNCs is estimated at ca. USD 7,000 /t. [478] The relatively high production costs stem mainly from the strong sulfuric acid hydrolysis resulting in complicated purification and recycling conditions. By contrast, the production of CNFs is significantly cheaper with the estimated MPSP in the range of USD 1500-2000/t.[478] Here, the major contributor to the cost is the price of raw material, generally chemical wood pulp that makes up ca. 60% of the total. These numbers can markedly change if conceptually new technologies are adapted, such as the afore described vapor HCl production for CNCs.[27] or utilization of very cheap agricultural waste as raw material.

For individuals who work with pulp and paper or inexpensive plastics, the nanocellulose price estimates appear rather high. However, a casual materials scientist may

view these as cost-efficient. For example, the price of CNF is in the same order of magnitude as the price of high molecular weight polyethylene. Compared to carbon nanotubes, on the other hand, also the CNCs are several decades cheaper. Obviously, when weighing the choices between materials, biodegradability and renewable nature of nanocellulose are particularly strong assets aside the price and ultimately, much of the eventual appeal will depend on future environmental legislation. Safety concerns raised for CNTs may also provide a significant incentive for rather choosing nanocellulose materials.

Considering next the potential applications, the first foreseen applications range from viscosity modifiers, packaging, and nanocomposites from renewable resources to tissue engineering scaffolds, where some of them are already in market, some pre-commercial, and some having a large commercial potential. We foresee that flexible devices and sensors on nanocellulose substrates are also likely, especially when transparency is needed. These applications do not require complete structural control and it is probable that additional similar applications will be identified. In materials science, there would be a great need to tune the materials properties *on-demand* and economically. Therein, molecular self-assembly and supramolecular chemistry have over the recent years progressed toward in-depth tunable properties by mastering structures at different length scales, size distributions, and supramolecular interactions. Also at the colloidal scale the need for structural control for tailored properties have become into the nodal point. Taken nanocelluloses as colloidal units, the lateral dimensions can already be controlled to some extent, whereas the length is yet poorly controlled. Therefore, well-defined 3D assemblies may not be seen in the near future. But one can foresee that aligned and 2D biomimetic assemblies with densely packed nanocelluloses with fracture energy dissipating media can become feasible to combine high strength, modulus, and toughness. Such materials could find their first applications in small scale specific applications, also incorporating the use of transparency. Furthermore, one could foresee the importance of topochemically positioned interaction sites, grafted polymers, or

inorganic domains at one or both ends of nanocelluloses, as well those laterally positioned along the nanocelluloses in defined blocks or sequences towards in-depth colloidal engineering of mechanical, thermal, electrical, iontronic, optical, magnetic, and biological functions. Even if some glimpses of such developments can be seen in this review, at large, such tunabilities remains still a huge challenge. We foresee that carefully engineered nanocelluloses and plant based materials could have major impact as components e.g. in sustainable energy sector, high tech clothing, and 3D printed materials. We hope that this review encourages novel explorations of nanocelluloses for novel fields as a branch of interdisciplinary sustainable high-tech engineering.

Acknowledgements
We gratefully acknowledge funding from Academy of Finland through Center of Excellence of Molecular Engineering of Biosynthetic Hybrid Materials Research, academy professorship, and several other grants, as well as European Research Council. The funding from National Technology Agency and UPM-Kymmene Ltd are also acknowledged at the earlier stages of the nanocellulose projects. Betulium Ltd is acknowledged for stimulating discussions related to future directions, especially economics of nanocelluloses. The authors have benefitted from numerous discussions with a very large number of colleagues. Their number is so large that we do not even try to give a list. Prof. André Gröschel acknowledges hospitality when spending post-doctoral period at Aalto University.

Received: ((will be filled in by the editorial staff))
Revised: ((will be filled in by the editorial staff))
Published online: ((will be filled in by the editorial staff))

References

[1] Y. Habibi, L. A. Lucia, O. J. Rojas, *Chem. Rev.* **2010***, 110*, 3479.

[2] R. J. Moon, A. Martini, J. Nairn, J. Simonsen, J. Youngblood, *Chem. Soc. Rev.,* **2011***, 40*, 3941.

[3] S. J. Eichhorn, *Soft Matter* **2011***, 7,* 303.

[4] D. Klemm, F. Kramer, S. Moritz, T. Lindström, M. Ankerfors, D. Gray, A. Dorris, *Angew. Chemie Int. Ed.* **2011***, 50*, 5438.

[5] N. Lin, J. Huang, A. Dufresne, *Nanoscale* **2012***, 4*, 3274.

[6] C. Salas, T. Nypelö, C. Rodriguez-Abreu, C. Carrillo, O. J. Rojas, *Curr. Opin. Colloid Interface Sci.* **2014***, 19*, 383.

[7] A. R. Lokanathan, A. H. Gröschel, M. B. Linder, O. J. Rojas, O. Ikkala, in *Handb. Nanocellulose Cellul. Nanocomposites* (Eds.: H. Kargarzadeh, I. Ahmad, S. Thomas, A. Dufresne), Wiley-VCH Verlag GmbH & Co. KGaA, Weinheim, 2017, pp. 123–174.

[8] H. Zhu, W. Luo, P. N. Ciesielski, Z. Fang, J. Y. Zhu, G. Henriksson, M. E. Himmel, L. Hu, *Chem. Rev.* **2016***, 116*, 9305.

[9] H. Kargarzadeh, I. Ahmad, S. Thomas, A. Dufresne, Eds., *Handbook of Nanocellulose and Cellulose Nanocomposites*, Wiley-VCH Verlag GmbH & Co. KGaA, Weinheim, 2017.

[10] T. Zimmermann, E. Pöhler, T. Geiger, *Adv. Eng. Mater.* **2004***, 6*, 754.

[11] K. Fleming, D. G. Gray, S. Matthews, *Chem. - A Eur. J.* **2001***, 7*, 1831.

[12] J. Majoinen, E. Kontturi, O. Ikkala, D. G. Gray, *Cellulose* **2012***, 19*, 1599.

[13] M. Pääkko, M. Ankerfors, H. Kosonen, A. Nykänen, S. Ahola, M. Österberg, J. Ruokolainen, J. Laine, P. T. Larsson, O. Ikkala, T. Lindström, *Biomacromolecules* **2007***, 8*, 1934.

[14] M. Bhattacharya, M. M. Malinen, P. Lauren, Y. R. Lou, S. W. Kuisma, L. Kanninen, M. Lille, A. Corlu, C. Guguen-Guillouzo, O. Ikkala, A. Laukkanen, A. Urtti, M. Yliperttula, *J. Control. Release* **2012***, 164*, 291.

[15] D. Trache, M. H. Hussin, M. K. M. Haafiz, V. K. Thakur, *Nanoscale* **2017***, 9*, 1763.

[16] E. Kontturi, *Nanocellulose and Sustainability: Production, Properties, Applications, and Case Studies*, Taylor And Francis Group, Boca Raton, 2017.

[17] H. P. S. Abdul Khalil, Y. Davoudpour, M. N. Islam, A. Mustapha, K. Sudesh, R. Dungani, M. Jawaid, *Carbohydr. Polym.* **2014***, 99*, 649.

[18] A. Isogai, T. Saito, H. Fukuzumi, *Nanoscale* **2011***, 3*, 71.

[19] L. Chen, J. Y. Zhu, C. Baez, P. Kitin, T. Elder, *Green Chem.* **2016***, 18*, 3835.

[20] A. C. W. Leung, S. Hrapovic, E. Lam, Y. Liu, K. B. Male, K. A. Mahmoud, J. H. T. Luong, *Small* **2011***, 7*, 302.

[21] M. Visanko, H. Liimatainen, J. A. Sirviö, J. P. Heiskanen, J. Niinimäki, O. Hormi, *Biomacromolecules* **2014***, 15*, 2769.

[22] H. Yang, D. Chen, T. G. M. van de Ven, *Cellulose* **2015***, 22*, 1743.

[23] J. Peyre, T. Paakkonen, M. Reza, E. Kontturi, *Green Chem.* **2015,** *17*, 808.

[24] R. Salminen, M. Reza, T. Pääkkönen, J. Peyre, E. Kontturi, *Cellulose* **2017,** *24*, 1657.

[25] S. Camarero Espinosa, T. Kuhnt, E. J. Foster, C. Weder, *Biomacromolecules* **2013***, 14*, 1223.

[26] Y. Liu, H. Wang, G. Yu, Q. Yu, B. Li, X. Mu, *Carbohydr. Polym.* **2014***, 110*, 415.

[27] E. Kontturi, A. Meriluoto, P. A. Penttilä, N. Baccile, J. M. Malho, A. Potthast, T. Rosenau, J. Ruokolainen, R. Serimaa, J. Laine, H. Sixta, *Angew. Chemie Int. Ed.* **2016***, 55*, 14455.

[28] W. Fang, S. Arola, J. M. Malho, E. Kontturi, M. B. Linder, P. Laaksonen, *Biomacromolecules* **2016***, 17*, 1458.

[29] M. Lorenz, S. Sattler, M. Reza, A. Bismarck, E. Kontturi, *Faraday Discuss.* **2017**, DOI 10.1039/C7FD00053G.

[30] A. N. Fernandes, L. H. Thomas, C. M. Altaner, P. Callow, V. T. Forsyth, D. C. Apperley, C. J. Kennedy, M. C. Jarvis, *Proc. Natl. Acad. Sci.* **2011***, 108*, E1195.

[31] B. Medronho, A. Romano, M. G. Miguel, L. Stigsson, B. Lindman, *Cellulose* **2012***, 19,* 581.

[32] Q. Li, S. Renneckar, *Biomacromolecules* **2011***, 12*, 650.

[33] R. Salminen, N. Baccile, M. Reza, E. Kontturi, *Biomacromolecules* **2017***, 18*, 1975.

[34] E. Niinivaara, M. Faustini, T. Tammelin, E. Kontturi, *Langmuir* **2015***, 31*, 12170.

[35] I. Filpponen, E. Kontturi, S. Nummelin, H. Rosilo, E. Kolehmainen, O. Ikkala, J. Laine, *Biomacromolecules 2012, 13*, 736.

[36] K. Mazeau, A. Rivet, *Biomacromolecules* **2008***, 9*, 1352.

[37] W. W. D. Klemm, B. Philipp, T. Heinze, U. Heinze, Comprehensive Cellulose Chemistry, Vol. 1, Wiley-VCH Verlag GmbH & Co. KGaA, Weinheim, 1998.

[38] K. J. De France, T. Hoare, E. D. Cranston, *Chem. Mater.* **2017***, 29*, 4609.

[39] S. Beck, J. Bouchard, R. Berry, *Biomacromolecules* **2011***, 12*, 167.

[40] L.-S. Johansson, T. Tammelin, J. M. Campbell, H. Setälä, M. Österberg, *Soft Matter* **2011***, 7*, 10917.

[41] D. Dax, M. S. C. Bastidas, C. Honorato, J. Liu, S. Spoljaric, J. Seppälä, R. T. Mendonça, C. Xu, S. Willför, J. Sánchez, *Nord. Pulp Pap. Res. J.* **2015***, 30*, 373.

[42] T. Saito, S. Kimura, Y. Nishiyama, A. Isogai, Biomacromolecules ***2007***, 8, 2485.

[43] E. Lasseuguette, D. Roux, Y. Nishiyama, *Cellulose* **2008***, 15*, 425.

[44] X. Zhang, J. Huang, P. R. Chang, J. Li, Y. Chen, D. Wang, J. Yu, J. Chen, *Polymer* **2010***, 51*, 4398.

[45] T. Saito, T. Uematsu, S. Kimura, T. Enomae, A. Isogai, *Soft Matter* **2011***, 7*, 8804.

[46] G. Gong, A. P. Mathew, K. Oksman, *Tappi J.* **2011***, 10*, 7.

[47] S. Arola, J. Malho, P. Laaksonen, M. Lille, M. B. Linder, *Soft Matter* **2013***, 9*, 1319.

[48] N. Lin, A. Dufresne, *Biomacromolecules* **2013***, 14*, 871.

[49] D. Klemm, H. Ahrem, F. Kramer, W. Fried, J. Wippermann, R. W. Kinne, in *Bacterial NanoCellulose* (Eds.: M. Gama, P. Gatenholm, D. Klemm), CRC Press, 2012, pp. 175–196.

[50] H. Dong, J. F. Snyder, K. S. Williams, J. W. Andzelm, Biomacromolecules **2013,** 14, 3338.

[51] A. Naderi, T. Lindström, *Cellulose* **2014,** *21*, 3507.

[52] A. Naderi, T. Lindström, T. Pettersson, *Cellulose* **2014,** *21*, 2357.

[53] J. R. McKee, S. Hietala, J. Seitsonen, J. Laine, E. Kontturi, O. Ikkala, *ACS Macro Lett.* **2014,** *3*, 266.

[54] Z. Hu, E. D. Cranston, R. Ng, R. Pelton, *Langmuir* **2014***, 30*, 2684.

[55] J. R. McKee, E. A. Appel, J. Seitsonen, E. Kontturi, O. A. Scherman, O. Ikkala, *Adv. Funct. Mater.* **2014***, 24*, 2706.

[56] G. Chinga-Carrasco, K. Syverud, *J. Biomater. Appl.* **2014***, 29*, 423.

[57] S. Rose, A. Prevoteau, P. Elzière, D. Hourdet, A. Marcellan, L. Leibler, *Nature* **2013***, 505*, 382.

[58] K. Dimic-Misic, K. Nieminen, P. Gane, T. Maloney, H. Sixta, J. Paltakari, *Appl. Rheol.* **2014***, 24*, 35616.

[59] J. Yang, J. J. Zhao, C. R. Han, J. F. Duan, F. Xu, R. C. Sun, *Cellulose* **2014,** *21*, 541.

[60] A. Chaker, S. Boufi, *Carbohydr. Polym.* **2015***, 131*, 224.

[61] L. Jowkarderis, T. G. M. Van De Ven, *Carbohydr. Polym.* **2015***, 123*, 416.

[62] E. R. Janeček, J. R. McKee, C. S. Y. Tan, A. Nykänen, M. Kettunen, J. Laine, O. Ikkala, O. A. Scherman, *Angew. Chemie Int. Ed.* **2015***, 54*, 5383.

[63] M. Chau, S. E. Sriskandha, D. Pichugin, H. Thérien-Aubin, D. Nykypanchuk, G. Chauve, M. Méthot, J. Bouchard, O. Gang, E. Kumacheva, *Biomacromolecules* **2015***, 16*, 2455.

[64] H. Mertaniemi, C. Escobedo-Lucea, A. Sanz-Garcia, C. Gandía, A. Mäkitie, J. Partanen, O. Ikkala, M. Yliperttula, *Biomaterials* **2016***, 82*, 208.

[65] N. Quennouz, S. M. Hashmi, H. S. Choi, J. W. Kim, C. O. Osuji, *Soft Matter* **2016***, 12*, 157.

[66] T. Pääkönen, K. Dimic-Misic, H. Orelma, R. Pönni, T. Vuorinen, T. Maloney, *Cellulose* **2016***, 23*, 277.

[67] C. Qiao, G. Chen, J. Zhang, J. Yao, *Food Hydrocoll.* **2016***, 55*, 19.

[68] V. Kuzmenko, T. Kalogeropoulos, J. Thunberg, S. Johannesson, D. Hägg, P. Enoksson, P. Gatenholm, *Mater. Sci. Eng. C* **2016***, 58*, 14.

[69] O. van der Berg, J. R. Capadona, C. Weder, *Biomacromolecules 2007, 8*, 1353.

[70] K. Missoum, M. Belgacem, J. Bras, *Materials (Basel)* **2013***, 6*, 1745.

[71] Y. Habibi, *Chem. Soc. Rev.* **2014***, 43*, 1519.

[72] A. Carlmark, E. Larsson, E. Malmström, *Eur. Polym. J.* **2012,** *48*, 1646.

[73] J. O. Zoppe, Y. Habibi, O. J. Rojas, R. A. Venditti, L. S. Johansson, K. Efimenko, M. Österberg, J. Laine, *Biomacromolecules* **2010***, 11*, 2683.

[74] S. Eyley, W. Thielemans, *Nanoscale* **2014***, 6*, 7764.

[75] M. Morits, J. R. McKee, J. Majoinen, J.-M. Malho, N. Houbenov, J. Seitsonen, J. Laine, A. H. Gröschel, O. Ikkala, *ACS Sustain. Chem. Eng.* **2017**, accepted.

[76] J. Majoinen, A. Walther, J. R. Mckee, E. Kontturi, J. M. Malho, J. Ruokolainen, O. Ikkala, *Biomacromolecules* **2011***, 12*, 2997.

[77] J. R. McKee, J. Huokuna, L. Martikainen, M. Karesoja, A. Nykänen, E. Kontturi, H. Tenhu, J. Ruokolainen, O. Ikkala, *Angew. Chemie Int. Ed.* **2014***, 53*, 5049.

[78] H. Rosilo, J. R. McKee, E. Kontturi, T. Koho, V. P. Hytönen, O. Ikkala, M. A. Kostiainen, *Nanoscale* **2014***, 6,* 11871.

[79] J. M. Malho, M. Morits, T. I. Löbling, Nonappa, J. Majoinen, F. H. Schacher, O. Ikkala, A. H. Gröschel, *ACS Macro Lett.* **2016***, 5*, 1185.

[80] J.-M. Malho, S. Arola, P. Laaksonen, G. R. Szilvay, O. Ikkala, M. B. Linder, *Angew. Chemie Int. Ed.* **2015***, 54*, 12025.

[81] M. Linder, T. T. Teeri, *J. Biotechnol.* **1997***, 57*, 15.

[82] D. Guillén, S. Sánchez, R. Rodríguez-Sanoja, *Appl. Microbiol. Biotechnol.* **2010***, 85*, 1241.

[83] P. Laaksonen, A. Walther, J.-M. Malho, M. Kainlauri, O. Ikkala, M. B. Linder, *Angew. Chemie Int. Ed.* **2011***, 50*, 8688.

[84] C. Xu, O. Spadiut, A. C. Araújo, A. Nakhai, H. Brumer, *ChemSusChem* **2012***, 5*, 661.

[85] K. S. Kontturi, K. Biegaj, A. Mautner, R. T. Woodward, B. P. Wilson, L.-S. Johansson, K.-Y. Lee, J. Y. Y. Heng, A. Bismarck, E. Kontturi, *Langmuir* **2017***, 33*, 5707.

[86] A. A. Domingues, F. V. Pereira, M. R. Sierakowski, O. J. Rojas, D. F. S. Petri, *Cellulose* **2016***, 23*, 2421.

[87] S. Varjonen, P. Laaksonen, A. Paananen, H. Valo, H. Haehl, T. Laaksonen, M. B. Linder, *Soft Matter* **2011***, 7*, 2402.

[88] Y. Habibi, I. Hoeger, S. S. Kelley, O. J. Rojas, *Langmuir* **2010***, 26*, 990.

[89] M. B. Linder, Curr. Opin. *Colloid Interface Sci.* **2009***, 14*, 356.

[90] H. Valo, M. Kovalainen, P. Laaksonen, M. Häkkinen, S. Auriola, L. Peltonen, M. Linder, K. Järvinen, J. Hirvonen, T. Laaksonen, *J. Control. Release* **2011***, 156*, 390.

[91] X. Jia, R. Xu, W. Shen, M. Xie, M. Abid, S. Jabbar, P. Wang, X. Zeng, T. Wu, *Food Hydrocoll.* **2015***, 43*, 275.

[92] J. Ruths, F. Essler, G. Decher, H. Riegler, *Langmuir* **2000,** *16,* 8871.

[93] D. J. Cosgrove, *Nat. Rev. Mol. Cell Biol.* **2005***, 6,* 850.

[94] R. Tanaka, T. Saito, T. Hänninen, Y. Ono, M. Hakalahti, T. Tammelin, A. Isogai, *Biomacromolecules* **2016,** *17*, 2104.

[95] K. S. Mikkonen, L. Pitkänen, V. Liljeström, E. Mabasa Bergström, R. Serimaa, L. Salmén, M. Tenkanen, *Cellulose* **2012***, 19*, 467.

[96] T. M. Tenhunen, M. S. Peresin, P. A. Penttilä, J. Pere, R. Serimaa, T. Tammelin, *React. Funct. Polym.* **2014,** *85*, 157.

[97] E. Rojo, M. S. Peresin, W. W. Sampson, I. C. Hoeger, J. Vartiainen, J. Laine, O. J. Rojas, *Green Chem.* **2015***, 17*, 1853.

[98] F. Jiang, Y. Lo Hsieh, *Biomacromolecules* **2015***, 16*, 1433.

[99] S. Galland, F. Berthold, K. Prakobna, L. A. Berglund, *Biomacromolecules* **2015,** *16,* 2427.

[100] M. A. Hubbe, O. J. Rojas, L. A. Lucia, *BioResources* **2015***, 10*, 6095.

[101] M. S. Toivonen, S. Kurki-Suonio, F. H. Schacher, S. Hietala, O. J. Rojas, O. Ikkala, *Biomacromolecules* **2015***, 16*, 1062.

[102] B. L. Tardy, S. Yokota, M. Ago, W. Xiang, T. Kondo, R. Bordes, O. J. Rojas, *Curr. Opin. Colloid Interface Sci.* **2017***, 29*, 57.

[103] Z. Emami, Q. Meng, G. Pircheraghi, I. Manas-Zloczower, *Cellulose* **2015***, 22*, 3161.

[104] B. Jean, L. Heux, F. Dubreuil, G. Chambat, F. Cousin, *Langmuir* **2009***, 25*, 3920.

[105] Q. Zhou, M. W. Rutland, T. T. Teeri, H. Brumer, *Cellulose* **2007***, 14*, 625.

[106] M. Lopez, H. Bizot, G. Chambat, M.-F. Marais, A. Zykwinska, M.-C. Ralet, H. Driguez, A. Buléon, *Biomacromolecules* **2010***, 11*, 1417.

[107] J. Hanus, K. Mazeau, *Biopolymers* **2006***, 82*, 59.

[108] S. Boye, D. Appelhans, V. Boyko, S. Zschoche, H. Komber, P. Friedel, P. Formanek, A. Janke, B. I. Voit, A. Lederer, *Biomacromolecules* **2012***, 13*, 4222.

[109] J. Majoinen, J. S. Haataja, D. Appelhans, A. Lederer, A. Olszewska, J. Seitsonen, V. Aseyev, E. Kontturi, H. Rosilo, M. Österberg, N. Houbenov, O. Ikkala, *J. Am. Chem. Soc.* **2014***, 136*, 866.

[110] K. J. De France, K. J. W. Chan, E. D. Cranston, T. Hoare, *Biomacromolecules* **2016***, 17*, 649.

[111] J. Lehtio, J. Sugiyama, M. Gustavsson, L. Fransson, M. Linder, T. T. Teeri, *Proc. Natl. Acad. Sci.* **2003***, 100*, 484.

[112] F. Jiang, J. D. Kittle, X. Tan, A. R. Esker, M. Roman, *Langmuir 2013, 29*, 3280.

[113] T. Weis-Fogh, *J. Exp. Biol.* **1960***, 4*, 889.

[114] W. Fang, A. Paananen, M. Vitikainen, S. Koskela, A. Westerholm-Parvinen, J. J. Joensuu, C. P. Landowski, M. Penttilä, M. B. Linder, P. Laaksonen, *Biomacromolecules* **2017***, 18*, 1866.

[115] R. Verker, A. Rivkin, G. Zilberman, O. Shoseyov, *Cellulose* **2014***, 21*, 4369.

[116] A. Rivkin, T. Abitbol, Y. Nevo, R. Verker, S. Lapidot, A. Komarov, S. C. Veldhuis, G. Zilberman, M. Reches, E. D. Cranston, O. Shoseyov, *Ind. Biotechnol.* **2015***, 11*, 44.

[117] N. Mittal, R. Jansson, M. Widhe, T. Benselfelt, K. M. O. Håkansson, F. Lundell, M. Hedhammar, L. D. Söderberg, *ACS Nano* **2017***, 11*, 5148.

[118] J. S. Haghpanah, R. Tu, S. Da Silva, D. Yan, S. Mueller, C. Weder, E. J. Foster, I. Sacui, J. W. Gilman, J. K. Montclare, *Biomacromolecules* **2013***, 14*, 4360.

[119] T. P. Knowles, A. W. Fitzpatrick, S. Meehan, H. R. Mott, M. Vendruscolo, C. M. Dobson, M. E. Welland, *Science* **2007***, 318,* 1900.

[120] E. Cudjoe, M. Younesi, E. Cudjoe, O. Akkus, S. J. Rowan, *Biomacromolecules* **2017***, 18*, 1259.

[121] Y. Wang, L. Chen, *ACS Appl. Mater. Interfaces* **2014***, 6*, 1709.

[122] A. Khakalo, I. Filpponen, O. J. Rojas, *Biomacromolecules* **2017***, 18*, 1426.

[123] A. Rising, J. Johansson, *Nat. Chem. Biol.* **2015***, 11*, 309.

[124] W. Huang, D. Ebrahimi, N. Dinjaski, A. Tarakanova, M. J. Buehler, J. Y. Wong, D. L. Kaplan, *Acc. Chem. Res.* **2017***, 50*, 866.

[125] C. Thamm, T. Scheibel, *Biomacromolecules* **2017***, 18*, 1365.

[126] M. Henriksson, L. A. Berglund, P. Isaksson, T. Lindström, T. Nishino, *Biomacromolecules* **2008***, 9,* 1579.

[127] L. Liu, X. Yang, H. Yu, C. Ma, J. Yao, *RSC Adv.* **2014***, 4,* 14304.

[128] Y. Feng, X. Li, M. Li, D. Ye, Q. Zhang, R. You, W. Xu, *ACS Sustain. Chem. Eng.* **2017***, 5*, 6227.

[129] J. Chen, A. Zhuang, H. Shao, X. Hu, Y. Zhang, *J. Mater. Chem. B* **2017***, 5*, 3640.

[130] J. Van Rie, W. Thielemans, *Nanoscale* **2017***, 9*, 8525.

[131] M. Kaushik, A. Moores, *Green Chem.* **2016***, 18*, 622.

[132] T. Nypelö, M. Österberg, J. Laine, *ACS Appl. Mater. Interfaces* **2011***, 3*, 3725.

[133] T. Nypelö, H. Pynnönen, M. Österberg, J. Paltakari, J. Laine, *Cellulose* **2012***, 19*, 779.

[134] J. Guo, I. Filpponen, P. Su, J. Laine, O. J. Rojas, *Cellulose* **2016***, 23*, 3065.

[135] D. Gebauer, V. Oliynyk, M. Salajkova, J. Sort, Q. Zhou, L. Bergström, G. Salazar-Alvarez, *Nanoscale* **2011***, 3*, 3563.

[136] A. R. Lokanathan, K. M. A. Uddin, O. J. Rojas, J. Laine, *Biomacromolecules* **2014***, 15*, 373.

[137] A. R. Lokanathan, M. Lundahl, O. J. Rojas, J. Laine, *Cellulose* **2014***, 21*, 4209.

[138] A. R. Lokanathan, A. Nykänen, J. Seitsonen, L. S. Johansson, J. Campbell, O. J. Rojas, O. Ikkala, J. Laine, *Biomacromolecules* **2013***, 14*, 2807.

[139] J. Majoinen, J. Hassinen, J. S. Haataja, H. T. Rekola, E. Kontturi, M. A. Kostiainen, R. H. A. Ras, P. Törmö, O. Ikkala, *Adv. Mater.* **2016***, 28*, 5262.

[140] M. Wang, A. Olszewska, A. Walther, J. M. Malho, F. H. Schacher, J. Ruokolainen, M. Ankerfors, J. Laine, L. A. Berglund, M. Österberg, O. Ikkala, *Biomacromolecules* **2011***, 12*, 2074.

[141] M. Vuoriluoto, H. Orelma, L. S. Johansson, B. Zhu, M. Poutanen, A. Walther, J. Laine, O. J. Rojas, *J. Phys. Chem. B* **2015***, 119*, 15275.

[142] A. J. Benítez, J. Torres-Rendon, M. Poutanen, A. Walther, *Biomacromolecules* **2013***, 14*, 4497.

[143] A. Boujemaoui, S. Mazières, E. Malmström, M. Destarac, A. Carlmark, *Polymer* **2016,** *99*, 240.

[144] K. Littunen, U. Hippi, L. S. Johansson, M. Österberg, T. Tammelin, J. Laine, J. Seppälä, *Carbohydr. Polym.* **2011***, 84*, 1039.

[145] J. O. Zoppe, X. Xu, C. Känel, P. Orsolini, G. Siqueira, P. Tingaut, T. Zimmermann, H. A. Klok, *Biomacromolecules* **2016***, 17*, 1404.

[146] G. Morandi, W. Thielemans, *Polym. Chem.* **2012***, 3*, 1402.

[147] E. Zeinali, V. Haddadi-Asl, H. Roghani-Mamaqani, *RSC Adv.* 2014, *4*, 31428.

[148] X. Qiu, S. Hu, *Materials (Basel)* **2013***, 6,* 738.

[149] L. Hou, H. Bian, Q. Wang, N. Zhang, Y. Liang, D. Dong, *RSC Adv.* **2016***, 6*, 53062.

[150] L. Hou, J. Fang, W. Wang, Z. Xie, D. Dong, N. Zhang, *J. Mater. Chem. B* **2017***, 5*, 3348.

[151] J. O. Zoppe, M. Österberg, R. A. Venditti, J. Laine, O. J. Rojas, *Biomacromolecules* **2011***, 12*, 2788.

[152] H. Hu, W. Yuan, F.-S. Liu, G. Cheng, F.-J. Xu, J. Ma, *ACS Appl. Mater. Interfaces* **2015***, 7*, 8942.

[153] G. Morandi, L. Heath, W. Thielemans, *Langmuir 2009,* **25**, 8280.

[154] K. H. M. Kan, J. Li, K. Wijesekera, E. D. Cranston, *Biomacromolecules* **2013***, 14*, 3130.

[155] U. D. Hemraz, K. a Campbell, J. S. Burdick, K. Ckless, Y. Boluk, R. Sunasee, *Biomacromolecules* **2015***, 16*, 319.

[156] J. Tang, M. F. X. Lee, W. Zhang, B. Zhao, R. M. Berry, K. C. Tam, *Biomacromolecules* **2014***, 15*, 3052.

[157] J. O. Zoppe, R. A. Venditti, O. J. Rojas, *J. Colloid Interface Sci.* **2012***, 369*, 202.

[158] R. Mincheva, L. Jasmani, T. Josse, Y. Paint, J. M. Raquez, P. Gerbaux, S. Eyley, W. Thielemans, P. Dubois, *Biomacromolecules* **2016***, 17*, 3048.

[159] T. Gegenhuber, M. Krekhova, J. Schöbel, A. H. Gröschel, H. Schmalz, *ACS Macro Lett.* **2016***, 5*, 306.

[160] R. Bahrami, T. I. Löbling, A. H. Gröschel, H. Schmalz, A. H. E. Müller, V. Altstädt, *ACS Nano* **2014***, 8*, 10048.

[161] A. Walther, M. Hoffmann, A. H. E. Müller, *Angew. Chemie Int. Ed.* **2008**, *47*, 711.

[162] D. V. Pergushov, A. H. E. Müller, F. H. Schacher, *Chem. Soc. Rev.* **2012**, *41*, 6888.

[163] T. I. Löbling, J. S. Haataja, C. V. Synatschke, F. H. Schacher, M. Müller, A. Hanisch, A. H. Gröschel, A. H. E. Müller, *ACS Nano* **2014**, *8,* 11330.

[164] X. Xu, F. Liu, L. Jiang, J. Y. Zhu, D. Haagenson, D. P. Wiesenborn, *ACS Appl. Mater. Interfaces* **2013**, *5*, 2999.

[165] C.-F. Huang, J.-K. Chen, T.-Y. Tsai, Y.-A. Hsieh, K.-Y. Andrew Lin, *Polymer* **2015**, *72*, 395.

[166] J. R. G. Navarro, U. Edlund, *Biomacromolecules* **2017**, *18*, 1947.

[167] S. M. George, *Chem. Rev.* **2010**, *110*, 111.

[168] T. Suntola, J. Hyvarinen, *Annu. Rev. Mater. Sci.* **1985**, *15,* 177.

[169] J. R. Capadona, O. Van Den Berg, L. A. Capadona, M. Schroeter, S. J. Rowan, D. J. Tyler, C. Weder, *Nat. Nanotechnol.* **2007**, *2*, 765.

[170] A. J. Svagan, M. A. S. A. Samir, L. A. Berglund, *Adv. Mater.* **2008**, *20*, 1263.

[171] M. Pääkkö, J. Vapaavuori, R. Silvennoinen, H. Kosonen, M. Ankerfors, T. Lindström, L. A. Berglund, O. Ikkala, *Soft Matter* **2008**, *4*, 2492.

[172] M. D. Gawryla, O. van den Berg, C. Weder, D. A. Schiraldi, *J. Mater. Chem.* **2009**, *19*, 2118.

[173] L. Heath, W. Thielemans, *Green Chem.* **2010**, *12,* 1448.

[174] H. Sehaqui, M. Salajková, Q. Zhou, L. A. Berglund, *Soft Matter* **2010**, *6*, 1824.

[175] R. T. Olsson, M. A. S. Azizi Samir, G. Salazar-Alvarez, L. Belova, V. Ström, L. A. Berglund, O. Ikkala, J. Nogués, U. W. Gedde, *Nat. Nanotechnol.* **2010**, *5*, 584.

[176] W. Chen, H. Yu, Q. Li, Y. Liu, J. Li, *Soft Matter* **2011**, *7*, 10360.

[177] C. Gebald, J. A. Wurzbacher, P. Tingaut, T. Zimmermann, A. Steinfeld, *Environ. Sci. Technol.* **2011**, *45*, 9101.

[178] J. T. Korhonen, M. Kettunen, R. H. A. Ras, O. Ikkala, *ACS Appl. Mater. Interfaces* **2011***, 3*, 1813.

[179] J. T. Korhonen, P. Hiekkataipale, J. Malm, M. Karppinen, O. Ikkala, R. H. A. Ras, *ACS Nano* **2011***, 5*, 1967.

[180] D. O. Carlsson, G. Nystrom, Q. Zhou, L. A. Berglund, L. Nyholm, M. Stromme, *J. Mater. Chem.* **2012***, 22*, 19014.

[181] S. Liu, Q. Yan, D. Tao, T. Yu, X. Liu, *Carbohydr. Polym.* **2012***, 89*, 551.

[182] L. Melone, L. Altomare, I. Alfieri, A. Lorenzi, L. De Nardo, C. Punta, *J. Photochem. Photobiol. A Chem.* **2013,** *261*, 53.

[183] W. Li, X. Zhao, S. Liu, *Carbohydr. Polym.* **2013***, 94*, 278.

[184] K. Gao, Z. Shao, X. Wang, Y. Zhang, W. Wang, F. Wang, *RSC Adv.* **2013***, 3*, 15058.

[185] Q. Zheng, A. Javadi, R. Sabo, Z. Cai, S. Gong, *RSC Adv.* **2013***, 3,* 20816.

[186] M. Hamedi, E. Karabulut, A. Marais, A. Herland, G. Nyström, L. Wågberg, *Angew. Chemie Int. Ed.* **2013***, 52,* 12038.

[187] M. Wang, I. V. Anoshkin, A. G. Nasibulin, J. T. Korhonen, J. Seitsonen, J. Pere, E. I. Kauppinen, R. H. A. Ras, O. Ikkala, *Adv. Mater.* **2013,** *25*, 2428.

[188] A. Javadi, Q. Zheng, F. Payen, A. Javadi, Y. Altin, Z. Cai, R. Sabo, S. Gong, *ACS Appl. Mater. Interfaces* **2013***, 5*, 5969.

[189] C. Y. Liu, G. J. Zhong, H. D. Huang, Z. M. Li, *Cellulose* **2014***, 21*, 383.

[190] J. C. Arboleda, M. Hughes, L. A. Lucia, J. Laine, K. Ekman, O. J. Rojas, *Cellulose* **2013***, 20*, 2417.

[191] S. Li, C. Li, C. Li, M. Yan, Y. Wu, J. Cao, S. He, *Polym. Degrad. Stab.* **2013***, 98,* 1940.

[192] J. Han, C. Zhou, Y. Wu, F. Liu, Q. Wu, Biomacromolecules 2013, 14, 1529.

[193] M. M. Hamedi, A. Hajian, A. B. Fall, K. Håkansson, M. Salajkova, F. Lundell, L. Wågberg, L. A. Berglund, *ACS Nano* **2014***, 8*, 2467.

[194] J. Lin, L. Yu, F. Tian, N. Zhao, X. Li, F. Bian, J. Wang, *Carbohydr. Polym.* **2014**, *109*, 35.

[195] N. Yildirim, S. M. Shaler, D. J. Gardner, R. Rice, D. W. Bousfield, *Cellulose* **2014,** *21*, 4337.

[196] T. Köhnke, T. Elder, H. Theliander, A. J. Ragauskas, *Carbohydr. Polym.* **2014**, *100,* 24.

[197] W. Chen, Q. Li, Y. Wang, X. Yi, J. Zeng, H. Yu, Y. Liu, J. Li, *ChemSusChem* **2014,** *7,* 154.

[198] S. Y. Cho, Y. S. Yun, H. J. Jin, *Macromol. Res.* **2014**, *22*, 753.

[199] F. Jiang, Y.-L. Hsieh, *J. Mater. Chem. A* **2014**, *2*, 350.

[200] P. Wang, J. Zhao, R. Xuan, Y. Wang, C. Zou, Z. Zhang, Y. Wan, Y. Xu, *Dalt. Trans.* **2014**, *43*, 6762.

[201] Z. Zhang, G. Sèbe, D. Rentsch, T. Zimmermann, P. Tingaut, *Chem. Mater.* **2014**, *26,* 2659.

[202] X. Yang, E. D. Cranston, *Chem. Mater.* **2014,** *26*, 6016.

[203] Y. Kobayashi, T. Saito, A. Isogai, *Angew. Chemie Int. Ed.* **2014**, *53*, 10394.

[204] D. Bendahou, A. Bendahou, B. Seantier, Y. Grohens, H. Kaddami, *Ind. Crops Prod.* **2015**, *65*, 374.

[205] Y. Wang, S. Yadav, T. Heinlein, V. Konjik, H. Breitzke, G. Buntkowsky, J. J. Schneider, K. Zhang, *RSC Adv.* **2014**, *4*, 21553.

[206] X. Yao, W. Yu, X. Xu, F. Chen, Q. Fu, *Nanoscale* **2015**, *7*, 3959.

[207] S. Zhao, Z. Zhang, G. Sèbe, R. Wu, R. V. Rivera Virtudazo, P. Tingaut, M. M. Koebel, *Adv. Funct. Mater.* **2015**, *25*, 2326.

[208] J. Nemoto, T. Saito, A. Isogai, *ACS Appl. Mater. Interfaces* **2015**, *7,* 19809.

[209] S. Zhou, M. Wang, X. Chen, F. Xu, *ACS Sustain. Chem. Eng.* **2015**, *3*, 3346.

[210] F. Zhang, W. Wu, S. Sharma, G. Tong, Y. Deng, *BioResources* **2015**, *10*, 7555.

[211] H.-D. Huang, C.-Y. Liu, D. Zhou, X. Jiang, G.-J. Zhong, D.-X. Yan, Z.-M. Li, J. *Mater. Chem. A* **2015***, 3*, 4983.

[212] B. Seantier, D. Bendahou, A. Bendahou, Y. Grohens, H. Kaddami, *Carbohydr. Polym.* **2016***, 138*, 335.

[213] N. Sobel, C. Hess, *Angew. Chemie Int. Ed.* **2015,** *54*, 15014.

[214] H. Sehaqui, M. E. Gálvez, V. Becatinni, Y. Cheng Ng, A. Steinfeld, T. Zimmermann, P. Tingaut, *Environ. Sci. Technol.* **2015***, 49*, 3167.

[215] G. Nyström, A. Marais, E. Karabulut, L. Wågberg, Y. Cui, M. M. Hamedi, *Nat. Commun.* **2015***, 6*, 7259.

[216] M. S. Toivonen, A. Kaskela, O. J. Rojas, E. I. Kauppinen, O. Ikkala, *Adv. Funct. Mater.* **2015***, 25*, 6618.

[217] B. Wicklein, A. Kocjan, G. Salazar-Alvarez, F. Carosio, G. Camino, M. Antonietti, L. Bergström, *Nat. Nanotechnol.* **2014***, 10*, 277.

[218] Z. Y. Wu, H. W. Liang, L. F. Chen, B. C. Hu, S. H. Yu, *Acc. Chem. Res.* **2016***, 49*, 96.

[219] M. Kettunen, R. J. Silvennoinen, N. Houbenov, A. Nykänen, J. Ruokolainen, J. Sainio, V. Pore, M. Kemell, M. Ankerfors, T. Lindström, M. Ritala, R. H. A. Ras, O. Ikkala, *Adv. Funct. Mater.* **2011***, 21*, 510.

[220] H. Jin, G. Marin, A. Giri, T. Tynell, M. Gestranius, B. P. Wilson, E. Kontturi, T. Tammelin, P. E. Hopkins, M. Karppinen, *J. Mater. Sci.* **2017***, 52*, 6093.

[221] J. Doshi, D. H. Reneker, *J. Electrostat.* **1995***, 35*, 151.

[222] M. Bognitzki, W. Czado, T. Frese, A. Schaper, M. Hellwig, M. Steinhart, A. Greiner, J. H. Wendorff, *Adv. Mater.* **2001***, 13*, 70.

[223] O. J. Rojas, G. A. Montero, Y. Habibi, *J. Appl. Polym. Sci.* **2009***, 113*, 927.

[224] J. O. Zoppe, M. S. Peresin, Y. Habibi, R. A. Venditti, O. J. Rojas, *ACS Appl. Mater. Interfaces* **2009***, 1*, 1996.

[225] M. S. Peresin, Y. Habibi, J. O. Zoppe, J. J. Pawlak, O. J. Rojas, *Biomacromolecules* **2010***, 11*, 674.

[226] M. S. Peresin, Y. Habibi, A. H. Vesterinen, O. J. Rojas, J. J. Pawlak, J. V. Seppälä, *Biomacromolecules* **2010***, 11*, 2471.

[227] M. E. Vallejos, M. S. Peresin, O. J. Rojas, *J. Polym. Environ.* **2012***, 20*, 1075.

[228] M. Ago, K. Okajima, J. E. Jakes, S. Park, O. J. Rojas, *Biomacromolecules* **2012,** *13*, 918.

[229] M. Ago, J. E. Jakes, L. Johansson, S. Park, O. J. Rojas, *Biomacromolecules* **2012***, 13*, 918.

[230] M. Ago, J. E. Jakes, O. J. Rojas, *ACS Appl. Mater. Interfaces **2013**, 5,* 11768.

[231] W. L. E. Magalhães, X. Cao, L. A. Lucia, *Langmuir* **2009***, 25*, 13250.

[232] A. Walther, J. V. I. Timonen, I. Díez, A. Laukkanen, O. Ikkala, *Adv. Mater.* **2011***, 23,* 2924.

[233] S. Iwamoto, A. Isogai, T. Iwata, *Biomacromolecules* **2011***, 12*, 831.

[234] E. E. Ureña-Benavides, C. L. Kitchens, *Mol. Cryst. Liq. Cryst.* **2012***, 556*, 275.

[235] D. Liu, J. Li, F. Sun, R. Xiao, Y. Guo, J. Song, *RSC Adv. 2014,* **4**, 30784.

[236] K. M. O. Håkansson, A. B. Fall, F. Lundell, S. Yu, C. Krywka, S. V. Roth, G. Santoro, M. Kvick, L. Prahl Wittberg, L. Wågberg, L. D. Söderberg, *Nat. Commun. 2014, **5***, 4018.

[237] N. Pugazhenthiran, S. Sen Gupta, A. Prabhath, M. Manikandan, J. R. Swathy, V. K. Raman, T. Pradeep, *ACS Appl. Mater. Interfaces* **2015***, 7*, 20156.

[238] H. Chang, A. T. Chien, H. C. Liu, P. H. Wang, B. A. Newcomb, S. Kumar, *ACS Biomater. Sci. Eng.* **2015***, 1*, 610.

[239] K. M. O. Håkansson, *RSC Adv.* **2015***, 5*, 18601.

[240] C. Clemons, *J. Renew. Mater.* **2016***, 4*, 327.

[241] M. J. Lundahl, V. Klar, L. Wang, M. Ago, O. J. Rojas, *Ind. Eng. Chem. Res.* **2017***, 56*, 8.

[242] J. G. Torres-Rendon, F. H. Schacher, S. Ifuku, A. Walther, *Biomacromolecules* **2014***, 15,* 2709.

[243] M. J. Lundahl, A. G. Cunha, E. Rojo, A. C. Papageorgiou, L. Rautkari, J. C. Arboleda, O. J. Rojas, *Sci. Rep.* **2016***, 6*, 30695.

[244] Y. Shen, H. Orelma, A. Sneck, K. Kataja, J. Salmela, P. Qvintus, A. Suurnäkki, A. Harlin, *Cellulose* **2016***, 23*, 3393.

[245] S. Hooshmand, Y. Aitomäki, N. Norberg, A. P. Mathew, K. Oksman, *ACS Appl. Mater. Interfaces* **2015,** *7,* 13022.

[246] W. J. Lee, A. J. Clancy, E. Kontturi, A. Bismarck, M. S. P. Shaffer, *ACS Appl. Mater. Interfaces* **2016***, 8*, 31500.

[247] M. S. Toivonen, S. Kurki-Suonio, W. Wagermaier, V. Hynninen, S. Hietala, O. Ikkala, *Biomacromolecules* **2017***, 18*, 1293.

[248] R. Grande, E. Trovatti, A. J. F. Carvalho, A. Gandini, *J. Mater. Chem. A* **2017***, 5*, 13098.

[249] M. G. Northolt, H. Boerstoel, H. Maatman, R. Huisman, J. Veurink, H. Elzerman, *Polymer* **2001***, 42*, 8249.

[250] H.-P. Fink, P. Weigel, H. . Purz, J. Ganster, *Prog. Polym. Sci.* **2001***, 26*, 1473.

[251] C. Woodings, in *Encyclopia of Polymer Science and Technology* (Ed.: H.F. Mark), John Wiley & Sons, Inc., Hoboken, NJ, USA, 2014, pp. 672–710.

[252] S. Asaadi, M. Hummel, S. Hellsten, T. Härkäsalmi, Y. Ma, A. Michud, H. Sixta, *ChemSusChem* **2016***, 9*, 3250.

[253] P. Mohammadi, M. S. Toivonen, O. Ikkala, W. Wagermaier, M. B. Linder, *Sci. Rep*. **2017**, accepted.

[254] P. J. Lemstra, C. W. M. Bastiaansen, S. Rastogi, in Struct. Form. Polym. Fibers (Ed.: D.R. Salem), Hanser Gardner Publications Inc, 2001, pp. 185–224.

[255] D. J. Sikkema, M. G. Northolt, B. Pourdeyhimi, *MRS Bull.* **2003***, 28*, 579.

[256] K. Kim, N. Selvapalam, Y. H. Ko, K. M. Park, D. Kim, J. Kim, *Chem. Soc. Rev.* **2007***, 36*, 267.

[257] S. A. Arvidson, J. R. Lott, J. W. McAllister, J. Zhang, F. S. Bates, T. P. Lodge, R. L. Sammler, Y. Li, M. Brackhagen, *Macromolecules* **2013***, 46*, 300.

[258] R. O. Ritchie, *Nat. Mater.* **2011***, 10*, 817.

[259] P. Y. Chen, J. McKittrick, M. A. Meyers, *Prog. Mater. Sci.* **2012***, 57*, 1492.

[260] B. J. F. Bruet, J. Song, M. C. Boyce, C. Ortiz, *Nat. Mater***. 2008***, 7*, 748.

[261] P. Fratzl, R. Weinkamer, *Prog. Mater. Sci.* **2007***, 52,* 1263.

[262] H.-B. Yao, H.-Y. Fang, X.-H. Wang, S.-H. Yu, *Chem. Soc. Rev.* **2011***, 40*, 3764.

[263] M. G. Willinger, A. G. Checa, J. T. Bonarski, M. Faryna, K. Berent, *Adv. Funct. Mater.* **2016***, 26*, 553.

[264] U. G. K. Wegst, H. Bai, E. Saiz, A. P. Tomsia, R. O. Ritchie, *Nat. Mater.* **2014***, 14*, 23.

[265] J. J. Blaker, K. Y. Lee, A. Bismarck, *J. Biobased Mater. Bioenergy* **2011***, 5*, 1.

[266] S. E. Naleway, M. M. Porter, J. McKittrick, M. A. Meyers, *Adv. Mater.* **2015***, 27*, 5455.

[267] A. R. Studart, *Chem. Soc. Rev.* **2016***, 45*, 359.

[268] O. Paris, G. Fritz-Popovski, D. Van Opdenbosch, C. Zollfrank, *Adv. Funct. Mater.* **2013***, 23*, 4408.

[269] F. Barthelat, Z. Yin, M. J. Buehler, *Nat. Rev. Mater.* **2016***, 1*, 16007.

[270] F. Bouville, E. Maire, S. Meille, B. Van de Moortèle, A. J. Stevenson, S. Deville, *Nat. Mater.* **2014***, 13*, 508.

[271] M. Mirkhalaf, A. K. Dastjerdi, F. Barthelat, Nat. Commun. 2014, 5, 1.

[272] M. A. Meyers, J. McKittrick, P.-Y. Chen, *Science* **2013***, 339*, 773.

[273] G. E. Fantner, E. Oroudjev, G. Schitter, L. S. Golde, P. Thurner, M. M. Finch, P. Turner, T. Gutsmann, D. E. Morse, H. Hansma, P. K. Hansma, *Biophys. J.* **2006***, 90*, 1411.

[274] N. Pan, *Appl. Phys. Rev.* **2014,** *1*, 21302.

[275] L. Li, J. C. Weaver, C. Ortiz, *Nat. Commun.* **2015***, 6*, 6216.

[276] Y. A. Shin, S. Yin, X. Li, S. Lee, S. Moon, J. Jeong, M. Kwon, S. J. Yoo, Y.-M. Kim, T. Zhang, H. Gao, S. H. Oh, *Nat. Commun.* **2016***, 7*, 10772.

[277] J. Aizenberg, P. Fratzl, *Adv. Mater.* **2009***, 21*, 187.

[278] M. Sarikaya, C. Tamerler, A. K.-Y. Jen, K. Schulten, F. Baneyx, *Nat. Mater.* **2003***, 2*, 577.

[279] J. H. E. Cartwright, A. G. Checa, *J. R. Soc. Interface* **2007***, 4*, 491.

[280] M. Suzuki, K. Saruwatari, T. Kogure, Y. Yamamoto, T. Nishimura, T. Kato, H. Nagasawa, *Science* **2009***, 325*, 1388.

[281] R. Z. Wang, Z. Suo, A. G. Evans, N. Yao, I. A. Aksay, *J. Mater. Res.* **2001***, 16*, 2485.

[282] F. Barthelat, H. Tang, P. D. Zavattieri, C. M. Li, H. D. Espinosa, *J. Mech. Phys. Solids* **2007***, 55*, 306.

[283] A. P. Jackson, J. F. V. Vincent, R. M. Turner, *Proc. R. Soc. B Biol. Sci.* **1988***, 234*, 415.

[284] A. Y. M. Lin, P. Y. Chen, M. A. Meyers, *Acta Biomater.* **2008***, 4*, 131.

[285] L. J. Bonderer, A. R. Studart, L. J. Gauckler, *Science* **2008***, 319,* 1069.

[286] A. Finnemore, P. Cunha, T. Shean, S. Vignolini, S. Guldin, M. Oyen, U. Steiner, *Nat. Commun.* **2012***, 3*, 966.

[287] X. Q. Li, H. C. Zeng, *Adv. Mater.* **2012***, 24*, 6277.

[288] Z. Tang, N. A. Kotov, S. Magonov, B. Ozturk, *Nat. Mater.* **2003***, 2*, 413.

[289] S. Deville, E. Saiz, R. K. Nalla, A. P. Tomsia, *Science* **2006***, 311*, 515.

[290] E. Munch, M. E. Launey, D. H. Alsem, E. Saiz, A. P. Tomsia, R. O. Ritchie, *Science* **2008***, 322*, 1516.

[291] M. E. Launey, E. Munch, D. H. Alsem, E. Saiz, A. P. Tomsia, R. O. Ritchie, *J. R. Soc. Interface* **2010***, 7*, 741.

[292] L.-B. Mao, H.-L. Gao, H.-B. Yao, L. Liu, H. Colfen, G. Liu, S.-M. Chen, S.-K. Li, Y.-X. Yan, Y.-Y. Liu, S.-H. Yu, *Science* **2016***, 354*, 107.

[293] A. Walther, I. Bjurhager, J. M. Malho, J. Pere, J. Ruokolainen, L. A. Berglund, O. Ikkala, *Nano Lett.* **2010***, 10*, 2742.

[294] A. Walther, I. Bjurhager, J.-M. Malho, J. Ruokolainen, L. Berglund, O. Ikkala, *Angew. Chemie Int. Ed.* **2010***, 49,* 6448.

[295] M. Morits, T. Verho, J. Sorvari, V. Liljeström, M. A. Kostiainen, A. H. Gröschel, O. Ikkala, *Adv. Funct. Mater.* **2017***, 27*, 1605378.

[296] A. Liu, A. Walther, O. Ikkala, L. Belova, L. A. Berglund, *Biomacromolecules* **2011***, 12,* 633.

[297] A. Liu, L. A. Berglund, *Eur. Polym. J.* **2013***, 49*, 940.

[298] F. Carosio, J. Kochumalayil, F. Cuttica, G. Camino, L. Berglund, *ACS Appl. Mater. Interfaces* **2015***, 7*, 5847.

[299] T. Furuhashi, C. Schwarzinger, I. Miksik, M. Smrz, A. Beran, *Comp. Biochem. Physiol. Part B Biochem. Mol. Biol.* **2009***, 154*, 351.

[300] M. A. Meyers, A. Y. M. Lin, P. Y. Chen, J. Muyco, *J. Mech. Behav. Biomed. Mater.* **2008***, 1*, 76.

[301] H. Liimatainen, N. Ezekiel, R. Sliz, K. Ohenoja, J. A. Sirviö, L. Berglund, O. Hormi, J. Niinimäki, *ACS Appl. Mater. Interfaces* **2013***, 5*, 13412.

[302] Y. Zhang, S. Gong, Q. Zhang, P. Ming, S. Wan, J. Peng, L. Jiang, Q. Cheng, *Chem. Soc. Rev.* **2016,** *45*, 2378.

[303] J. Duan, S. Gong, Y. Gao, X. Xie, L. Jiang, Q. Cheng, *ACS Appl. Mater. Interfaces* **2016***, 8*, 10545.

[304] H. Jin, A. Cao, E. Shi, J. Seitsonen, L. Zhang, R. H. A. Ras, L. A. Berglund, M. Ankerfors, A. Walther, O. Ikkala, *J. Mater. Chem. B* **2013***, 1*, 835.

[305] J.-M. Malho, P. Laaksonen, A. Walther, O. Ikkala, M. B. Linder, *Biomacromolecules* **2012,** *13*, 1093.

[306] G. E. Fantner, T. Hassenkam, J. H. Kindt, J. C. Weaver, H. Birkedal, L. Pechenik, J. A. Cutroni, G. A. G. Cidade, G. D. Stucky, D. E. Morse, P. K. Hansma, *Nat. Mater.* **2005,** *4*, 612.

[307] A. J. Benítez, F. Lossada, B. Zhu, T. Rudolph, A. Walther, *Biomacromolecules* **2016***, 17*, 2417.

[308] A. Olszewska, J. J. Valle-Delgado, M. Nikinmaa, J. Laine, M. Österberg, *Nanoscale* **2013***, 5,* 11837.

[309] D. Berman, A. Erdemir, A. V. Sumant, *Mater. Today* **2014***, 17*, 31.

[310] S. Spoljaric, A. Salminen, N. D. Luong, J. Seppälä, *RSC Adv.* **2015***, 5*, 107992.

[311] T. Nypelö, C. Rodriguez-Abreu, J. Rivas, M. D. Dickey, O. J. Rojas, *Cellulose* **2014***, 21*, 2557.

[312] J. Guo, I. Filpponen, L.-S. Johansson, P. Mohammadi, M. Latikka, M. B. Linder, R. H. A. Ras, O. J. Rojas, *Biomacromolecules* **2017***, 18*, 898.

[313] A. S. Leppänen, C. Xu, J. Liu, X. Wang, M. Pesonen, S. Willför, *Macromol. Rapid Commun.* **2013***, 34*, 1056.

[314] N. D. Luong, J. T. Korhonen, A. J. Soininen, J. Ruokolainen, L. S. Johansson, J. Seppälä, *Eur. Polym. J.* **2013***, 49*, 335.

[315] N. D. Luong, N. Pahimanolis, U. Hippi, J. T. Korhonen, J. Ruokolainen, L.-S. Johansson, J.-D. Nam, J. Seppälä, *J. Mater. Chem.* **2011***, 21*, 13991.

[316] Y. Song, Y. Jiang, L. Shi, S. Cao, X. Feng, M. Miao, J. Fang, *Nanoscale* **2015***, 7*, 13694.

[317] S. S. Prakash, C. J. Brinker, A. J. Hurd, S. M. Rao, *Nature* **1995***, 374*, 439.

[318] M. Wang, I. V. Anoshkin, A. G. Nasibulin, R. H. A. Ras, N. Nonappa, J. Laine, E. I. Kauppinen, O. Ikkala, *RSC Adv.* **2016***, 6*, 89051.

[319] J. Biener, M. Stadermann, M. Suss, M. A. Worsley, M. M. Biener, K. A. Rose, T. F. Baumann, *Energy Environ. Sci.* **2011***, 4*, 656.

[320] H. Sun, Z. Xu, C. Gao, *Adv. Mater.* **2013***, 25*, 2554.

[321] S. Nardecchia, D. Carriazo, M. L. Ferrer, M. C. Gutiérrez, F. del Monte, *Chem. Soc. Rev.* **2013***, 42*, 794.

[322] R. J. White, N. Brun, V. L. Budarin, J. H. Clark, M.-M. Titirici, *ChemSusChem* **2014***, 7*, 670.

[323] Z. Xu, Y. Zhang, P. Li, C. Gao, *ACS Nano* **2012***, 6*, 7103.

[324] S. Araby, A. Qiu, R. Wang, Z. Zhao, C.-H. Wang, J. Ma, *J. Mater. Sci.* **2016***, 51*, 9157.

[325] C. F. Castro-Guerrero, D. G. Gray, *Cellulose* **2014***, 21*, 2567.

[326] J. P. F. Lagerwall, C. Schütz, M. Salajkova, J. Noh, J. Hyun Park, G. Scalia, L. Bergström, *NPG Asia Mater.* **2014***, 6*, e80.

[327] A. G. Dumanli, G. Kamita, J. Landman, H. van der Kooij, B. J. Glover, J. J. Baumberg, U. Steiner, S. Vignolini, *Adv. Opt. Mater.* **2014***, 2*, 646.

[328] D. Gray, *Nanomaterials* **2016***, 6*, 213.

[329] B. Frka-Petesic, G. Guidetti, G. Kamita, S. Vignolini, *Adv. Mater.* **2017***, 109*, 1701469.

[330] M. Giese, J. C. De Witt, K. E. Shopsowitz, A. P. Manning, R. Y. Dong, C. A. Michal, W. Y. Hamad, M. J. Maclachlan, *ACS Appl. Mater. Interfaces* **2013***, 5*, 6854.

[331] C. C. Y. Cheung, M. Giese, J. A. Kelly, W. Y. Hamad, M. J. Maclachlan, *ACS Macro Lett.* **2013**, *2,* 1016.

[332] M. Giese, M. K. Khan, W. Y. Hamad, M. J. MacLachlan, *ACS Macro Lett.* **2013**, *2*, 818.

[333] J. A. Kelly, M. Giese, K. E. Shopsowitz, W. Y. Hamad, M. J. MacLachlan, *Acc. Chem. Res.* **2014**, *47*, 1088.

[334] M. Giese, L. K. Blusch, M. K. Khan, M. J. MacLachlan, *Angew. Chemie Int. Ed.* **2015**, *54*, 2888.

[335] S. Vignolini, P. J. Rudall, A. V. Rowland, A. Reed, E. Moyroud, R. B. Faden, J. J. Baumberg, B. J. Glover, U. Steiner, *Proc. Natl. Acad. Sci.* **2012**, *109,* 15712.

[336] P. X. Wang, W. Y. Hamad, M. J. MacLachlan, *Angew. Chemie Int. Ed.* **2016**, *55*, 12460.

[337] R. M. Parker, B. Frka-Petesic, G. Guidetti, G. Kamita, G. Consani, C. Abell, S. Vignolini, *ACS Nano* **2016**, *10*, 8443.

[338] Y. Li, J. Jun-Yan Suen, E. Prince, E. M. Larin, A. Klinkova, H. Thérien-Aubin, S. Zhu, B. Yang, A. S. Helmy, O. D. Lavrentovich, E. Kumacheva, *Nat. Commun.* **2016**, *7*, 12520.

[339] M. Nogi, S. Iwamoto, A. N. Nakagaito, H. Yano, *Adv. Mater.* **2009**, *21*, 1595.

[340] M. Zhu, J. Song, T. Li, A. Gong, Y. Wang, J. Dai, Y. Yao, W. Luo, D. Henderson, L. Hu, *Adv. Mater.* **2016**, *28*, 5181.

[341] M. Zhu, Y. Wang, S. Zhu, L. Xu, C. Jia, J. Dai, J. Song, Y. Yao, Y. Wang, Y. Li, D. Henderson, W. Luo, H. Li, M. L. Minus, T. Li, L. Hu, *Adv. Mater.* **2017**, *29*, 1606284.

[342] K. Yao, S. Huang, H. Tang, Y. Xu, G. Buntkowsky, L. A. Berglund, Q. Zhou, *ACS Appl. Mater. Interfaces* **2017**, *9,* 20169.

[343] X. Xu, R. Ray, Y. Gu, H. J. Ploehn, L. Gearheart, K. Raker, W. A. Scrivens, *J. Am. Chem. Soc.* **2004**, *126*, 12736.

[344] K. Junka, J. Guo, I. Filpponen, J. Laine, O. J. Rojas, *Biomacromolecules* **2014***, 15*, 876.

[345] J. Guo, D. Liu, I. Filpponen, L. Johansson, J.-M. Malho, S. Quraishi, F. Liebner, H. A. Santos, O. J. Rojas, *Biomacromolecules* **2017***, 18*, 2045.

[346] M. I. Stockman, *Opt. Express* **2011***, 19*, 22029.

[347] V. K. Valev, J. J. Baumberg, C. Sibilia, T. Verbiest, Adv. Mater. 2013, 25, 2517.

[348] L. M. Liz-Marzán, *Langmuir* **2006***, 22*, 32.

[349] O. Neumann, C. Feronti, A. D. Neumann, A. Dong, K. Schell, B. Lu, E. Kim, M. Quinn, S. Thompson, N. Grady, P. Nordlander, M. Oden, N. J. Halas, *Proc. Natl. Acad. Sci.* **2013***, 110*, 11677.

[350] K. Saha, S. S. Agasti, C. Kim, X. Li, V. M. Rotello, *Chem. Rev.* **2012***, 112*, 2739.

[351] A. Querejeta-Fernández, B. Kopera, K. S. Prado, A. Klinkova, M. Methot, G. Chauve, J. Bouchard, A. S. Helmy, E. Kumacheva, *ACS Nano* **2015***, 9*, 10377.

[352] M. Kaushik, K. Basu, C. Benoit, C. M. Cirtiu, H. Vali, A. Moores, *J. Am. Chem. Soc.* **2015***, 137*, 6124.

[353] R. Wang, K. Hashimoto, A. Fujishima, M. Chikuni, E. Kojima, A. Kitamura, M. Shimohigoshi, T. Watanabe, *Nature* **1997***, 388*, 431.

[354] B. Frka-Petesic, B. Jean, L. Heux, *Europhys. Lett.* **2014,** *107*, 28006.

[355] L. Csoka, I. C. Hoeger, P. Peralta, I. Peszlen, O. J. Rojas, *J. Colloid Interface Sci.* **2011***, 363*, 206.

[356] L. Csoka, I. C. Hoeger, O. J. Rojas, I. Peszlen, J. J. Pawlak, P. N. Peralta, *ACS Macro Lett.* **2012***, 1*, 867.

[357] S. Rajala, T. Siponkoski, E. Sarlin, M. Mettänen, M. Vuoriluoto, A. Pammo, J. Juuti, O. J. Rojas, S. Franssila, S. Tuukkanen, *ACS Appl. Mater. Interfaces* **2016***, 8,* 15607.

[358] A. Hänninen, S. Rajala, T. Salpavaara, M. Kellomäki, S. Tuukkanen, *Procedia Eng.* **2016***, 168*, 1176.

[359] S. Arola, T. Tammelin, A. Tullila, M. B. Linder, Biomacromolecules 2012, 13, 594.

[360] R. Weishaupt, G. Siqueira, M. Schubert, M. M. Kämpf, T. Zimmermann, K. Maniura-Weber, G. Faccio, *Adv. Funct. Mater.* **2017***,* 27, 1604291.

[361] R. Weishaupt, G. Siqueira, M. Schubert, P. Tingaut, K. Maniura-Weber, T. Zimmermann, L. Thöny-Meyer, G. Faccio, J. Ihssen, *Biomacromolecules* **2015***, 16,* 3640.

[362] M. Vuoriluoto, H. Orelma, M. Lundahl, M. Borghei, O. J. Rojas, *Biomacromolecules* **2017***, 18*, 1803.

[363] H. Orelma, L. Johansson, I. Filpponen, O. J. Rojas, J. Laine, *Biomacromolecules* **2012,** *13*, 2802.

[364] C. Uth, S. Zielonka, S. Hörner, N. Rasche, A. Plog, H. Orelma, O. Avrutina, K. Zhang, H. Kolmar, *Angew. Chemie Int. Ed.* **2014***, 53*, 12618.

[365] H. Orelma, I. Filpponen, L.-S. Johansson, M. Österberg, O. J. Rojas, J. Laine, *Biointerphases* **2012***, 7*, 61.

[366] Y. Zhang, R. G. Carbonell, O. J. Rojas, *Biomacromolecules* **2013***, 14*, 4161.

[367] Y. Zhang, O. J. Rojas, *Biomacromolecules* **2017***, 18*, 526.

[368] D. Khatayevich, T. Page, C. Gresswell, Y. Hayamizu, W. Grady, M. Sarikaya, *Small 2014,* **10**, 1505.

[369] M. C. Cushing, K. S. Anseth, *Science* **2007***, 316*, 1133.

[370] O. W. Petersen, L. Rønnov-Jessen, A. R. Howlett, M. J. Bissell, *Proc. Natl. Acad. Sci. U. S. A.* **1992***, 89*, 9064.

[371] B. M. Baker, C. S. Chen, *J. Cell Sci.* **2012***, 125*, 3015.

[372] S. R. Caliari, J. A. Burdick, *Nat. Methods* **2016***, 13*, 405.

[373] E. S. Place, N. D. Evans, M. M. Stevens*, Nat. Mater.* **2009***, 8*, 457.

[374] C. M. Magin, D. L. Alge, K. S. Anseth, *Biomed. Mater.* **2016,** *11*, 22001.

[375] D. E. Discher, *Science* **2005***, 310*, 1139.

[376] C. Storm, J. J. Pastore, F. C. MacKintosh, T. C. Lubensky, P. A. Janmey, *Nature* **2005***, 435*, 191.

[377] A. M. van Buul, E. Schwartz, P. Brocorens, M. Koepf, D. Beljonne, J. C. Maan, P. C. M. Christianen, P. H. J. Kouwer, R. J. M. Nolte, H. Engelkamp, K. Blank, A. E. Rowan, *Chem. Sci.* **2013***, 4*, 2357.

[378] M. Jaspers, M. Dennison, M. F. J. Mabesoone, F. C. MacKintosh, A. E. Rowan, P. H. J. Kouwer, *Nat. Commun.* **2014***, 5*, 5808.

[379] R. H. Pritchard, Y. Y. Shery Huang, E. M. Terentjev, *Soft Matter* **2014***, 10,* 1864.

[380] M. Jaspers, S. L. Vaessen, P. van Schayik, D. Voerman, A. E. Rowan, P. H. J. Kouwer, *Nat. Commun.* **2017***, 8*, 15478.

[381] N. Petersen, P. Gatenholm, *Appl. Microbiol. Biotechnol.* **2011***, 91*, 1277.

[382] P. Krontiras, P. Gatenholm, D. A. Hägg, *J. Biomed. Mater. Res. Part B Appl. Biomater.* ***2015****, 103*, 195.

[383] G. F. Picheth, C. L. Pirich, M. R. Sierakowski, M. A. Woehl, C. N. Sakakibara, C. F. de Souza, A. A. Martin, R. da Silva, R. A. de Freitas, *Int. J. Biol. Macromol.* **2017***, 104*, 97.

[384] Y.-R. Lou, L. Kanninen, T. Kuisma, J. Niklander, L. A. Noon, D. Burks, A. Urtti, M. Yliperttula, *Stem Cells Dev.* **2014***, 23*, 380.

[385] M. M. Malinen, L. K. Kanninen, A. Corlu, H. M. Isoniemi, Y. R. Lou, M. L. Yliperttula, A. O. Urtti, *Biomaterials* **2014***, 35*, 5110.

[386] M. P. Rowan, L. C. Cancio, E. A. Elster, D. M. Burmeister, L. F. Rose, S. Natesan, R. K. Chan, R. J. Christy, K. K. Chung, *Crit. Care* **2015***, 19*, 243.

[387] T. Hakkarainen, R. Koivuniemi, M. Kosonen, C. Escobedo-Lucea, A. Sanz-Garcia, J. Vuola, J. Valtonen, P. Tammela, A. Mäkitie, K. Luukko, M. Yliperttula, H. Kavola, *J. Control. Release* **2016***, 244*, 292.

[388] J. Liu, G. Chinga-Carrasco, F. Cheng, W. Xu, S. Willför, K. Syverud, C. Xu, *Cellulose 2016,* **23**, 3129.

[389] A. K. Reckhenrich, B. M. Kirsch, E. A. Wahl, T. L. Schenck, F. Rezaeian, Y. Harder, P. Foehr, H.-G. Machens, J. T. Egaña, *PLoS One* **2014***, 9*, e91169.

[390] T. Georgiev-Hristov, M. García-Arranz, I. García-Gómez, M. A. García-Cabezas, J. Trébol, L. Vega-Clemente, P. Díaz-Agero, D. García-Olmo, *Eur. J. Cardio-thoracic Surg.* **2012***, 42*, 40.

[391] M. Teng, Y. Huang, H. Zhang, *Wound Repair Regen.* **2014***, 22*, 151.

[392] L. Wu, H. Zhou, H.-J. Sun, Y. Zhao, X. Yang, S. Z. D. Cheng, G. Yang, *Biomacromolecules* **2013***, 14*, 1078.

[393] L. J. Goujon, S. Hariharan, B. Sayyar, N. A. D. Burke, E. D. Cranston, D. W. Andrews, H. D. H. Stöver, *Langmuir 2015,* **31**, 5623.

[394] J.-F. Revol, H. Bradford, J. Giasson, R. H. Marchessault, D. G. Gray, *Int. J. Biol. Macromol.* **1992***, 14*, 170.

[395] K. E. Shopsowitz, H. Qi, W. Y. Hamad, M. J. MacLachlan, *Nature* **2010***, 468*, 422.

[396] H. Sehaqui, Q. Zhou, O. Ikkala, L. A. Berglund, *Biomacromolecules* **2011***, 12*, 3638.

[397] H. Sehaqui, N. Ezekiel Mushi, S. Morimune, M. Salajkova, T. Nishino, L. A. Berglund, *ACS Appl. Mater. Interfaces* **2012***, 4*, 1043.

[398] R. Mao, S. Goutianos, W. Tu, N. Meng, G. Yang, L. A. Berglund, T. Peijs, *J. Mater. Sci* **2017***, 52*, 9508.

[399] L. A. Berglund, T. Peijs, *MRS Bull. **2010**, 35*, 201.

[400] A. J. Benítez, A. Walther, *J. Mater. Chem. A* **2017***, 5*, 16003.

[401] Michael Ashby, Ed., Materials and the Environment, Eco-Informed Material Choice, Butterworth-Heineman, Amsterdam, 2012.

[402] H. Zhu, Z. Fang, C. Preston, Y. Li, L. Hu, Energy Environ. Sci. 2014, 7, 269.

[403] H. Yagyu, T. Saito, A. Isogai, H. Koga, M. Nogi, *ACS Appl. Mater. Interfaces* **2015***, 7*, 22012.

[404] M.-C. Hsieh, H. Koga, K. Suganuma, M. Nogi, *Sci. Rep.* **2017***, 7*, 41590.

[405] H. Zhu, Z. Xiao, D. Liu, Y. Li, N. J. Weadock, Z. Fang, J. Huang, L. Hu, *Energy Environ. Sci* **2013***, 67*, 2105.

[406] J. Huang, H. Zhu, Y. Chen, C. Preston, K. Rohrbach, J. Cumings, L. Hu, *ACS Nano* **2013***, 7*, 2106.

[407] Z. Fang, H. Zhu, Y. Yuan, D. Ha, S. Zhu, C. Preston, Q. Chen, Y. Li, Xiaogang Han, S. Lee, G. Chen, T. Li, J. Munday, J. Huang, L. Hu, *Nano Letters* **2014***, 14*, 765.

[408] J. Zhong, H. Zhu, Q. Zhong, J. Dai, W. Li, S.-H. Jang, Y. Yao, D. Henderson, Q. Hu, L. Hu, J. Zhou, *ACS Nano* **2015***, 9*, 7399.

[409] W. Luo, F. Shen, C. Bommier, H. Zhu, X. Ji, L. Hu, *Acc. Chem. Res.* ***2016****, 49*, 231.

[410] F. Hoeng, A. Denneulin, J. Bras, *Nanoscale* **2016***, 8*, 13131.

[411] J. Tao, Z. Fang, Q. Zhang, W. Bao, M. Zhu, Y. Yao, Y. Wang, J. Dai, A. Zhang, C. Leng, D. Henderson, Z. Wang, L. Hu, *Adv. Electron. Mater.* **2017**, *3*, 1600539.

[412] X. Gao, L. Huang, B. Wang, D. Xu, J. Zhong, Z. Hu, L. Zhang, J. Zhou, *ACS Appl. Mater. Interfaces* **2016***, 8*, 35587.

[413] S. S. Nair, J. Y. Zhu, Y. Deng, A. J. Ragauskas, *Sustain. Chem. Process* **2014***, 2*, 23.

[414] A. Ferrer, L. Pal, M. Hubbe, *Ind. Crops Prod.* **2017***, 95*, 574.

[415] H. M. C. Azeredo, M. F. Rosa, Morsyleide F.; L. H. C. Mattoso, *Ind. Crops Prod.* **2017**, 97, 664.

[416] M. Salajkova, L. Valentini, Q. Zhou, L. A. Berglund, *Compos. Sci Technol.* **2013***, 87*, 103.

[417] L. Valentini, S. Bittolo Bon, E. Fortunati, J. M. Kenny, *J. Mater. Sci* **2014***, 49*, 1009.

[418] P. Bober, J. Liu, K. S. Mikkonen, P. Ihalainen, M. Pesonen, C. Plumed-Ferrer, A. von Wright, T. Lindfors, C. Xu, R.-M. Latonen, *Biomacromolecules* **2014***, 15,* 3655.

[419] S. Cao, X. Feng, Y. Song, X. Xue, H. Liu, M. Miao, J. Fang, L. Shi, *ACS Applied Mater. Interfaces* **2015***, 7*, 10695.

[420] Y. Lu, J. E. Poole II, T. Aytug, H. M. Meyer III, S. Ozcan, *RSC Adv.* **2015**, *5*, 103680.

[421] S. Liu, H. Liu, Z. Huang, M. Fang, Y.-G. Liu, X. Wu, C. He, *Mater. Res. Express* **2016**, *3*, 115022.

[422] Y. Beeran P. T., V. Bobnar, S. Gorgieva, Y. Grohens, M. Finšgar, S. Thomas V. Kokol, *RSC Advances* **2016**, *6*, 49138.

[423] M. Lay, J. A. Mendez, M. Delgado-Aguilar, K. N. Bun, F. Vilaseca, *Carbohydr. Polym.* **2016**, *152*, 361.

[424] F. Hoeng, A. Denneulin, G. Krosnicki, J. Bras, *J. Mater. Chem. C* **2016**, *4*, 10945.

[425] W. Yang, Z. Zhao, K. Wu, R. Huang, T. Liu, H. Jiang, F. Chen, Q. Fu, *J. Mater. Chem. C* **2017**, *5*, 3748.

[426] A. Yamakawa, S. Suzuki, T. Oku, K. Enomoto, M. Ikeda, J. Rodrigue, K. Tateiwa, Y. Terada, H. Yano, S. Kitamura, *Carbohydr. Polym.* **2017**, *171*, 129.

[427] Y. Ko, D. Kim, U.-J. Kim, J. You, *Carbohydr. Polym* **2017**, *173*, 383.

[428] Y. Su, Y. Zhao, H. Zhang, X. Feng, L. Shi, J. Fang, *J. Mater. Chem. C* **2017**, *5*, 573.

[429] C. Sasso, N. Bruyant, D. Beneventi, J. Faure-Vincent, E. Zeno, M. Petit-Conil, D. Chaussy, M. N. Belgacem, *Cellulose* **2011**, *18*, 1455.

[430] D. Valtakari, V. Kumar, M. Toivakka, J. J. Saarinen, J. Liu, C. Xu, *Nanoscale Res. Letters* **2015**, *10*, 386.

[431] L. H. C. Mattoso, E. S. Medeiros, D. A. Baker, J. Avloni, D. F. Wood, W. J. Orts, *J. Nanosci. Nanotechnol.* **2009**, *9*, 2917.

[432] F. Carosio, F. Cuttica, L. Medina, L. A. Berglund, *Mater. Des.* **2016**, *93*, 357.

[433] W. Y. Hamad, *Adv. Polym. Sci* **2016**, *271*, 287.

[434] R. M. A. Domingues, M. E. Gomes, R. L. Reis, *Biomacromolecules* **2014**, *15,* 2327.

[435] A. Mautner, K.-Y. Lee, P. Lahtinen, M. Hakalahti, T. Tammelin, K. Li, A. Bismarck, *Chem. Commun. 2014,* **50**, 5778.

[436] P. Vandezande, L. E. M. Gevers, I. F. J. Vankelecom, *Chem. Soc. Rev. 2008,* **37**, 365.

[437] T. Saito, A. Isogai, *Carbohydr. Polym.* **2005**, *61*, 183.

[438] P. Liu, P. F. Borrell, M. Božič, V. Kokol, K. Oksman, A. P. Mathew, *J. Hazard. Mater.* **2015***, 294*, 177.

[439] Z. Karim, M. Hakalahti, T. Tammelin, A. P. Mathew, *RSC Adv.* **2017***, 7*, 5232.

[440] M. Hakalahti, A. Mautner, L. S. Johansson, T. Hänninen, H. Setälä, E. Kontturi, A. Bismarck, T. Tammelin, *ACS Appl. Mater. Interfaces* **2016***, 8*, 2923.

[441] Y. C. Ho, I. Norli, A. F. M. Alkarkhi, N. Morad, *Bioresour. Technol.* **2010***, 101*, 1166.

[442] B. Bolto, J. Gregory, *Water Res.* **2007***, 41*, 2301.

[443] N. K. Shammas, *Handbook of Environmental Engineering, Physicochemical Treatment Processes*, Humana Press Inc., Totowa, USA, 2005.

[444] T. Suopajärvi, E. Koivuranta, H. Liimatainen, J. Niinimäki, *J. Environ. Chem. Eng.* **2014***, 2*, 2005.

[445] J. A. Sirviö, T. Hasa, T. Leiviskä, H. Liimatainen, O. Hormi, *Cellulose* **2016***, 23*, 689.

[446] A. Mautner, K. Y. Lee, T. Tammelin, A. P. Mathew, A. J. Nedoma, K. Li, A. Bismarck, *React. Funct. Polym.* **2015***, 86*, 209.

[447] D. J. Miller, D. R. Dreyer, C. W. Bielawski, D. R. Paul, B. D. Freeman, *Angew. Chemie Int. Ed.* **2017***, 56*, 4662.

[448] A. Olszewska, K. Junka, N. Nordgren, J. Laine, M. W. Rutland, M. Österberg, *Soft Matter 2013, **9***, 7448.

[449] C. Schneider, A. Jusufi, R. Farina, F. Li, P. Pincus, M. Tirrell, M. Ballauff, *Langmuir* **2008***, 24*, 10612.

[450] J. J. Valle-Delgado, L.-S. Johansson, M. Österberg, *Colloids Surfaces B Biointerfaces* **2016***, 138*, 86.

[451] M. Benz, N. Chen, J. Israelachvili, *J. Biomed. Mater. Res.* **2004***, 71A*, 6.

[452] T. J. Hakala, V. Saikko, S. Arola, T. Ahlroos, A. Helle, P. Kuosmanen, K. Holmberg, M. B. Linder, P. Laaksonen, *Tribol. Int.* **2014***, 77*, 24.

[453] D. Reis, B. Vian, H. Chanzy, J.-C. Roland, *Biol. Cell* **1991***, 73*, 173.

[454] J. Li, Y. Liu, J. Luo, P. Liu, C. Zhang, *Langmuir* **2012***, 28*, 7797.

[455] J. M. Coles, D. P. Chang, S. Zauscher, *Curr. Opin. Colloid Interface Sci.* **2010***, 15*, 406.

[456] W. Barthlott, C. Neinhuis, *Planta* **1997***, 202*, 1.

[457] K. Koch, B. Bhushan, W. Barthlott, *Prog. Mater. Sci.* **2009***, 54*, 137.

[458] R. Blossey, *Nat. Mater.* **2003***, 2*, 301.

[459] A. Tuteja, W. Choi, G. H. McKinley, R. E. Cohen, M. F. Rubner, *MRS Bull.* **2008***, 33*, 752.

[460] J. Song, O. J. Rojas, *Pap. Chem.* **2013***, 28*, 216.

[461] L. Nurmi, K. Kontturi, N. Houbenov, J. Laine, J. Ruokolainen, J. Seppälä, *Langmuir* **2010***, 26*, 15325.

[462] H. Jin, M. Kettunen, A. Laiho, H. Pynnönen, J. Paltakari, A. Marmur, O. Ikkala, R. H. A. Ras, *Langmuir* **2011***, 27*, 1930.

[463] H. Mertaniemi, A. Laukkanen, J.-E. Teirfolk, O. Ikkala, R. H. A. Ras, *RSC Adv.* **2012***, 2*, 2882.

[464] J. Guo, W. Fang, A. Welle, W. Feng, I. Filpponen, O. J. Rojas, P. A. Levkin, *ACS Appl. Mater. Interfaces* **2016***, 8*, 34115.

[465] K. Koch, B. Bhushan, Y. C. Jung, W. Barthlott, *Soft Matter* **2009***, 5*, 1386.

[466] X. Gao, L. Jiang, *Nature* **2004***, 432*, 36.

[467] C. Anderson, G. Theraulaz, J.-L. Deneubourg, *Insectes Soc.* **2002***, 49*, 99.

[468] Q. Pan, M. Wang, *ACS Appl. Mater. Interfaces* **2009***, 1*, 420.

[469] J. Li, P. Guan, M. Li, Y. Zhang, P. Cheng, R. Jia, X. Y. Zhou, Q. J. Xue, T. Ren, Q. Xue, *New J. Chem***. 2017***, 41*, 4862.

[470] L. E. Scriven, C. V. Sternling, *Nature* **1960***, 187*, 186.

[471] S. Nakata, M. I. Kohira, Y. Hayashima, *Chem. Phys. Lett.* **2000***, 322*, 419.

[472] H. Jin, A. Marmur, O. Ikkala, R. H. A. Ras, *Chem. Sci.* **2012***, 3*, 2526.

[473] M. Wang, X. Tian, R. H. A. Ras, O. Ikkala, *Adv. Mater. Interfaces* **2015***, 2*, 1.

[474] E. Reyssat, L. Mahadevan, *Europhys. Lett.* **2011***, 93*, 54001.

[475] E. Reyssat, L. Mahadevan, *J. R. Soc. Interface* **2009***, 6*, 951.

[476] R. Elbaum, L. Zaltzman, I. Burgert, P. Fratzl, *Science* **2007***, 316*, 884.

[477] J. Li, G. P. Pandey, *Annu. Rev. Phys. Chem.* **2015***, 66*, 331.

[478] C. A. de Assis, C. Houtman, R. Phillips, E. M. T. Bilek, O. J. Rojas, L. Pal, M. S. Peresin, H. Jameel, R. Gonzalez, *Biofuels, Bioprod. Biorefining* **2017***, 11*, 682.

The table of contents entry

Nanocelluloses with their hydrogen bonded internal structures are colloidal fibrillar materials with attractive mechanical properties, functionalizability, and most recently also economics for sustainable nanoconstruction. Beyond the already emerging main stream applications, here we review potential novel concepts for nanocellulose-based advanced materials exploiting self-assembly, directed self-assembly, supramolecular and supracolloidal chemistry and protein engineering.

Keywords: Nanocellulose, cellulose nanofiber, nanofibrillated cellulose, cellulose nanocrystal, functional

E. Kontturi, P. Laaksonen, M. Linder, Nonappa, A.H. Gröschel, O. Rojas, O. Ikkala*

Novel materials through assembly of nanocelluloses

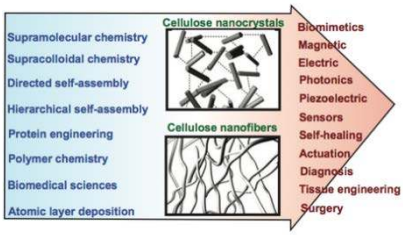

Prof. Eero Kontturi is heading a research group Materials Chemistry of Cellulose at Aalto University (Finland). He has a PhD degree from Eindhoven University of Technology (the Netherlands) and he has worked as an academic visitor in UPMC Paris (France), University of Vienna (Austria), and Imperial College London (UK). He was appointed as associate professor at the Department of Bioproducts and Biosystems at Aalto University in 2014.

Dr. Päivi Laaksonen is an Assistant Professor at the department of Bioproducts and Biosystems at Aalto University. Laaksonen obtained her PhD in physical chemistry in the Helsinki University of Technology on 2008 and has worked since in the research of novel biomolecular material. Between 2008 and 201,3 Laaksonen worked as senior scientist at the Technical Research Centre of Finland VTT. Laaksonen has published 46 research papers and her group of Nanomaterials and Structures focuses on biophysics, chemistry and materials science of biomolecules and materials consisting of them.

Prof. Markus Linder is at Aalto University Department of Bioproducts and Biosystems. He earned PhD from Helsinki University of Technology 1993. Thereafter he has been at VTT Technical Research Centre of Finland Ltd first as a researcher and later as the Protein Engineering Group leader, Academy of Finland Research fellow, and VTT research professor. Since 2012, prof Linder has been in his present affiliation at Aalto University leading the Biomolecular Research Group. He is a member in Academy of Finland Centre of Excellence in Molecular Engineering of Biosynthetic Hybrid Materials Research. His research interests are in protein engineering for materials science.

Dr. Nonappa received PhD in 2008 under the guidance of Prof. Uday Maitra from IISc, Bangalore, India on the synthesis of rare bile acids and supramolecular gels. After postdoctoral research at the University of Jyväskylä, Finland, on soft matter solid state NMR with Prof. Erkki Kolehmainen, he joined the group of Prof. Olli Ikkala at the Department of Applied Physics, Aalto University, where he is now an Adjunct Professor (Docent) in soft

matter microscopy and Research Fellow at the Department of Bioproducts and Biosystems. His current research interests are colloidal self-assembly and soft matter electron tomography.

Jun.-Prof. André Gröschel received his PhD 2012 in Macromolecular Chemistry (University Bayreuth) dealing with hierarchical self-assembly and multicompartment nanostructures. From 2013-2015 he did his postdoc in the group of Prof. Olli Ikkala in the Department of Applied Physics (Aalto University) on bio- and biomimetic materials. In 2016, he received an endowed Evonik-Juniorprofessorship at the University Duisburg-Essen and in 2017 he was awarded an Emmy Noether Research Group. He is currently moving into a new research facility (NETZ, Duisburg) focusing on topographic nano- and microparticles, and renewable resources for energy conversion.

Professor Orlando Rojas is chair of the Materials Platform of Aalto University where he holds double affiliation with the departments of Bioproducts and Biosystems and Applied Physics.

He is also Adjunct Professor in North Carolina State University. Prof. Rojas is elected Fellow of the American Chemical Society, the Finnish Academy of Science and Letters and is the recipient of the 2015 Tappi Nanotechnology Award. He has published over 260 peer-reviewed papers related to the core research of his group, “Bio-based Colloids and Materials”, which mainly deals with nanostructures from renewable materials and their utilization in multiphase systems.

Prof. Olli Ikkala heads Molecular Materials laboratory of Aalto University and Centre of Excellence of Academy of Finland. After PhD 1983 in materials physics at Helsinki University of Technology, he worked 10 years in chemical industry developing conducting polymers, thereafter returning to Helsinki University of Technology (now Aalto University). He has been awarded twice ERC Advanced Grant, twice Academy Professorship of Academy of Finland, and is elected in Finnish Academy of Science and Letters and Technology Academy of Finland. Presently he has part time position at Université Grandes Alpes, Grenoble. His interests cover functional materials by hierarchical self-assemblies and biomimetics.